THE TRANSPORT PROPERTIES OF CATION EXCHANGE MEMBRANES IN BI-IONIC FORMS

A thesis submitted to
The University of Glasgow
for the degree of Ph.D

by

HUSSEIN A. AL-ZUBAIDI

FACULTY OF SCIENCE
CHEMISTRY DEPARTMENT

November 1986

ProQuest LLC.
789 East Eisenhower Parkway
P.O. Box 1346
Ann Arbor, MI 48106 – 1346

This work is dedicated

to

my Mother

and

to the memory of

my Father who

made all this possible

CONTENTS

Page

APPENDICES

ACKNOWLEDGEMENTS

I would like to take this opportunity to express my thanks and deep appreciation to all the people who contributed to the work described in this thesis. In particular, Dr. Russell Paterson for all his advice and encouragement shown over the years. He has constantly kept me with an open mind to new ideas, especially in stimulating discussions on the problems encountered in obtaining the results which follow.

I should also like to thank my fellows in electrochemistry for their assistance, especially Dr. Paul Doran for the valuable discussions and collaboration, and also Mr. Sam McFadean for all his help in maintenance of the equipment in the electrochemistry section.

My thanks also are extended to all the staff in the mechanical, the electronic workshops and glass-blowing for their excellent work.

I should like to thank The University of Salahaldeen, Iraq, for the scholarship awarded to me.

I am very grateful for the help and kindness I received from the following people, without which this work would not be possible: Professor S.J. Thomson, Head of the Chemistry Department, The University of Glasgow, Dr. Ahmad N. Mahmood, and Mr. Naji M. Ali.

In this regard I wish to acknowledge the kindness of Miss Betty Forbes for her assistance on many occasions and in addition I wish to thank everyone in the Chemistry Department who offered me aid.

LIST OF SYMBOLS

Symbol	Name
A	Exposed membrane area (cm^2)
a_i	Activity of ionic species i
a'	Area multiplied by the distribution coefficient, α
$a_{\pm}$	Mean ionic activity of salt
c	Concentration in solution
$\bar{c}$	Concentration in membrane
c^o	Initial concentration
C	Capitance
D_i	Diffusion coefficient of species i
e	Effort in bond graph
f	Flow in bond graph
F	Faraday's constant
J_i	Flow of species i (mol cm^2 s^{-1})
J_3	Water flow (mol cm^2 s^{-1}
J_i^*	Flow of species i on arbitrary frame of reference
K	Wave number $[(\omega/2D)^{\frac{1}{2}}]$
K	Constant equal RT/F
K_H^K	Selectivity coefficient for potassium over hydrogen eqn. (4-2)
$K_{H_{(th)}}^K$	Thermodynamic coefficient eqn. (4-3)
i	Electric current A
I	Electric current density (A cm^{-2})
ℓ	Membrane thickness (cm)

Symbol	Name
L_{ii}	Direct mobility coefficient
L_{ik}	Coupling coefficient
M	Molarity of solution
m	Internal molality of the exchanger phase
n	Number of lumps into which a membrane is divided in an R-C model
n_i	Number of mole of species i
n_3	Number of mole of water
P	Permeability (cm s^{-1})
Q	Charge on a capacitor
$Q_{(t)}$	Quantity of permeated solute eqn. (7-1)
Q	Flow rate (mL min^{-1})
q	Charge on a chemical capacitor, (mole)
R	Resistor in a circuit
R	Gas constant (J K^{-1} mol^{-1})
s	Second
t	Time (s)
T	Period of a wave(s)
T	Thermodynamic temperature (K)
$\bar{T}_i$	Integral transport number of an ion, i
$\bar{T}_3$	Integral transference number of water, 3
$\bar{t}_i$	Differential transport number of species i (counterion or coion)
$\bar{t}_3$	Differential transference number of water, 3
U_i	Electrochemical mobility of species i
$\bar{U}_3$	Mobility of pore liquid

Symbol	Name
V_i^*	Velocity (cm s^{-1})
$\bar{V}_w$	Fractional pore volume
V	Collecting volume (cm^3)
X	Concentration of fixed charge (mol cm^{-3})
X_i	Thermodynamic force (J mol^{-1} cm^{-1})
x	Distance (cm)
z_i	Valency including sign of ion i

Greek Letter

α	Parameter defined in Chapter 2
α_i	Distribution coefficient $\bar{c}_i/c_i$
β	Slip-term, Chapter 6
β_n	Root of transcendental equation
γ	Activity coefficient
κ	Electrical conductivity
Θ	Tortuosity factor defined in Chapter 5
Θ	A function defined in Chapter 8
λ_i	Root of eqn. (A.7-6)
μ_i	Chemical potential of species i, (J mol^{-1})
ϕ	Osmotic coefficient
ϕ	Phase shift angle defined in eqn. (8-5)
Φ	Dissipation function eqn. (2-1)
τ	Time-lag for diffusion (s) eqn. (7-2)
ψ	Electrical potential

Subscripts/ Superscripts	Name
+	Cation
-	Anion
±	Mean value of thermodynamic quantity of cations and anions
i,k	Components i and k
',''	Left and right of a membrane surface
–	The overbar to indicate the membrane phase

CHAPTER 1

Introduction

1.1 INTRODUCTION

Membrane technology has only recently become of great practical importance to the chemical and pharmaceutical theories of membrane processes that are well-developed. This has come from a proper understanding of relationships between molecular and ionic flows and the 'forces' which generate them. This understanding has come from the theory of irreversible processes created by Onsager and developed by Prigogine, DeGroot, Mazur, Fitts and many others, as a branch of thermodynamics concerned with spontaneous processes. Onsager showed that, close to equilibrium, there is a linear relationship between the flows and applied forces. He also showed that these thermodynamic 'forces' included concentration, pressure and electrical potential gradients, similar to those developed by the experimental laws of Fick, Poiseuille and Ohm. Irreversible thermodynamics, however, besides including all these as part of generalised force on molecules (the gradient of electrochemical potential) also predicted that coupling between flows was a natural consequence of the theory and these may be estimated by analysis of results of properly constructed experiments. Coupling phenomena are of great importance in membrane processes. For example, electro-osmotic flows of water, where an electrical force (proportional to the voltage gradient) causes water to flow, not directly, since it has no effect on water molecules, but indirectly, by its effect upon ions in the pore solutions.

Measurement and interpretation of coupling coefficients in homo-ionic membrane systems, particularly ion exchange (electro-dialysis) and reverse osmosis membranes was performed and advanced

by Katchalsky, Kedem, Spiegler, Scatchard, Meares and Paterson. As a result of considerable experimental effort on a few selected membranes, an overall picture of transport of ions and water in such membranes was obtained.

Such experimental work had to be to the highest possible standards. For these workers, it required several years to obtain sufficient experimental data for irreversible thermodynamics analysis of a single membrane. With existing methods such detailed assessment of new membranes, however useful for practical applications, could not be contemplated as a routine matter.

The advancement of membrane applications in industry and the laboratory requires that such experimental transport measurements by irreversible thermodynamics (or for other less complete assessments) should be improved and speeded by new techniques which will facilitate screening, but without introducing significant (or any) loss of precision.

At the start of this work a major research programme was in hand in this laboratory to model transport and diffusion processes, using Network Thermodynamics and also to devise new methods for characterising membranes, using computer controlled experiments.[1-3]

In particular, two methods for determining diffusion coefficients and selectivity coefficients were under consideration.[2,3] One of the major successes of membrane science and technology has been the development of perfluorosulphonic acid membranes, Fig. (1-1) and their application to the chlor-alkali industry[4-6]. They act as selective transporters of sodium ion between two halves of the cell, separating brine saturated with chlorine gas, from 40% sodium hydroxide at 80-90°C.

The performance of these membranes is remarkable both as regards their chemical stability and their efficient exclusion of coion (OH^- and $C\ell^-$) in various concentrated solutions. These membranes are now being used for a variety of new processes, but many questions regarding their transport remain unanswered. To investigate these membranes further, it was decided to investigate the transport behaviour of mixed ionic forms, in particular, bi-ionic systems. This was partly to investigate the little understood mechanisms of coupling between two counterions (in this case, cations) within a charged membrane. It was hoped that this coupling would be observable and might be compared with other data on the more traditional polystyrene sulphonic acid membranes, on which much work had been published from this laboratory.[7,8]

The current interpretation of single ion transport data on these Nafion membranes suggested that their unique properties are due to an 'island' or micelle-type of structure for the charged sites, counterions and water, separated by regions of hydrophobic uncharged (or sparsely charged) matrix polymers.[9-11]

It was of interest to see if such an interpretation was also compatible with bi-ionic measurements as a confirmation of these structural features. The particular choice of bi-ionic systems was, however, of great general significance as in practical applications most membranes will contain several counterions. Proposals for applications of membranes for new processes which involve such conditions might be inserious error, if no conception of the degree of counterion coupling is available. Although the methodology for characterising homo-ionic

membranes is more demanding experimentally and less well-defined.

In this research therefore, it was a secondary aim to develop new methods for determining inter-ionic diffusion coefficients for cation exchange across bi-ionic membrane systems. Two new methods were devised for determining diffusion coefficients by Doran and Paterson[2,3] and had been tested for electrolyte diffusion across uncharged membranes as a demonstration.

It was a major aim in this research to develop and refine these methods to deal with interionic diffusion across bi-ionic membranes, which is technically much more difficult. During this research, computer controlled equipment was designed and constructed to perform these experiments on mixed ionic forms for the first time (Chapters 7 and 8).

A similar problem arose with the measurements of bi-ionic membrane potentials. The problem here was to correct the measurement for the undesired effects of unstirred layers of solution at both membrane surfaces. These are particularly important in bi-ionic systems, where there is a rapid exchange of ions between solutions in this work. Once more, a completely new membrane experiment was designed and tested (successfully). The experimental data was treated using a theoretical method devised by Professor J.W. Lorimer (University of Western Ontario) who spent six months of study leave in this laboratory during this period and took an active interest in this part of the work. (A joint paper is now being prepared). The methods were tested in a number of experiments on several membranes in homo-ionic forms - as before, being applied to bi-ionic systems.

The main research was on mixed H^+/K^+ forms of Nafion 125 and Nafion 117 perfluorosulphonic acid membranes. The corrected data were used to calculate the two counterion transport numbers in mixed forms: 50% in H^+ and 50% in K^+ forms. The theoretical equations were derived using irreversible thermodynamics.

The experimental measurements made on Nafion membranes included, electrical conductivities and water contents of homo-ionic membranes. For bi-ionic systems, measurements included exchange isotherms, water contents, electrical conductivities of mixed ionic forms, transport numbers of the exchanging ions and interionic diffusion coefficients, using two new methods.

These data were interpreted using irreversible thermodynamics developed specifically for bi-ionic systems. The results showed the value of the new computer controlled experiments and the interpretation of data, although incomplete, showed that the perfluorosulphonic acid membranes are unique in their bi-ionic properties. The data on bi-ionic potentials was quite unlike that polystyrene sulphonic acid or any other membranes, but was entirely compatible with the micelle or 'island' structure, now widely accepted from spectral and diffraction interpretations on single-ion forms.

Fig.(1-1)

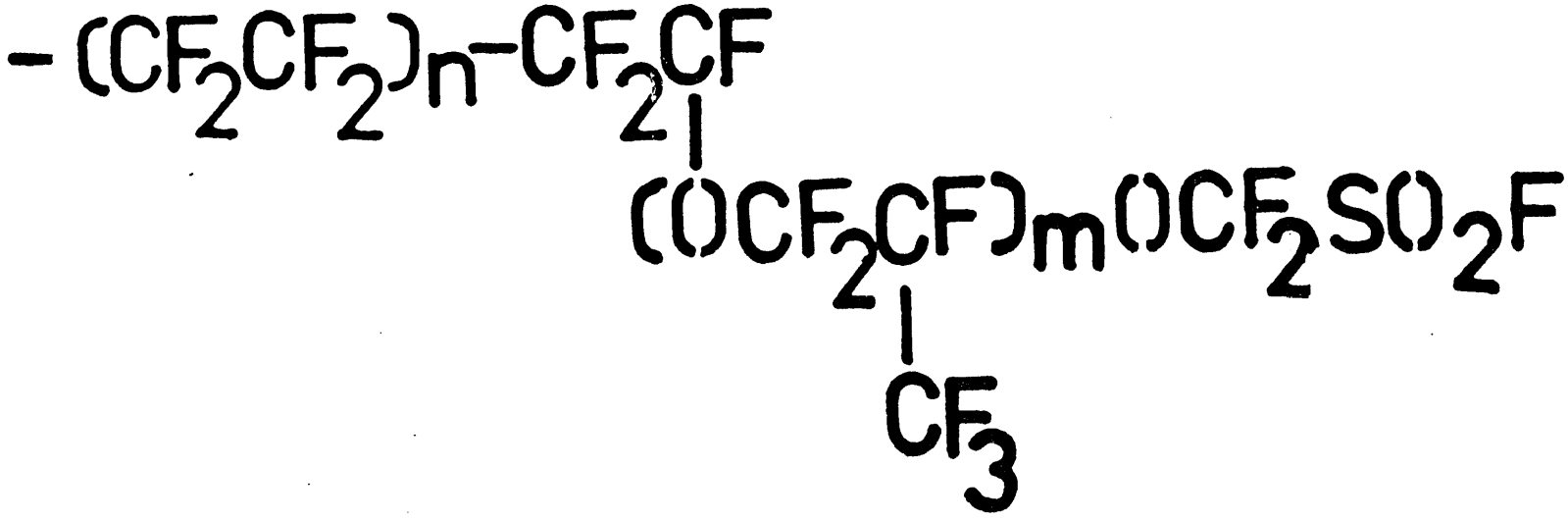

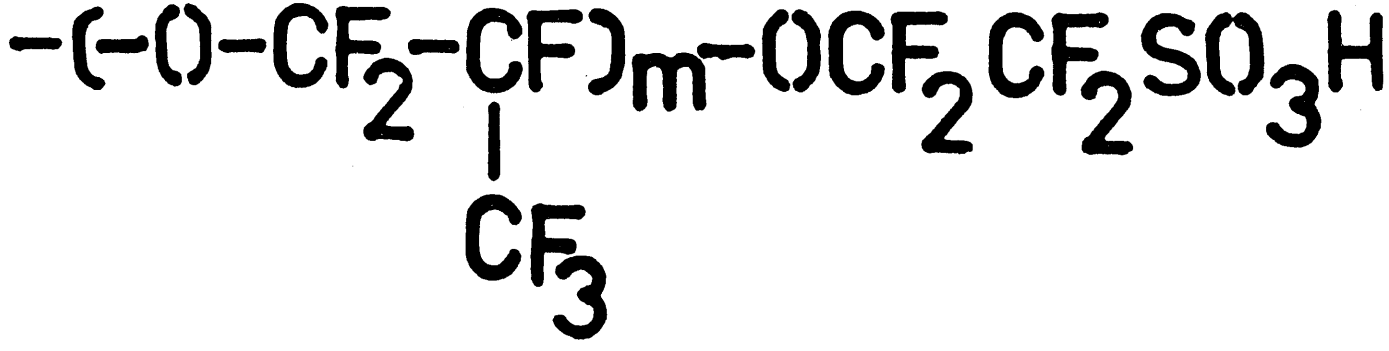

References

1. R. Paterson and Lutfullah, in: Ion Exchange Technology, (Eds. D. Naden and N. Streat), Ellis Horwood, Chichester, p.242 (1984).
2. R. Paterson and P. Doran, J. Membrane Sci., 26, 289 (1986).
3. R. Paterson and P. Doran, J. Membrane Sci., 27 105, (1986).
4. T. Berzins, The Electrochemical Society Meeting, Atlanta, Georgia, Oct. 1977.
5. T.D. Gierke, The Electrochemical Society Meeting, Atlanta, Georgia, Oct. 1977.
6. C.J. Hora and D.E. Maloney, The Electrochemical Society Meeting, Atlanta, Georgia, 1977.
7. R. Paterson and C.R. Gardner, J. Chem. Soc. A, 2254 (1971).
8. R. Paterson, Pontificae Academiae Scientiarum Scripta Varia, 40 517 (1976).
9. R.S. Yeo and A. Eisenberg, Polym. Prepr., 16, 104 (1975).
10. R.S. Yeo, J. Electrochem. Soc., 130, 533 (1983).
11. A. Eisenberg and H.L. Yeager, Eds., Perfluorinated Ionomer Membranes, Am Chem. Soc. Symposium Series No. 180, 1982.

CHAPTER 2

Irreversible Thermodynamic Descriptions of Transport Properties of Charged Membranes

2.1 INTRODUCTION

The transport properties of charged membranes are infinitely variable since they depend upon the composition and concentration of the electrolyte solutions with which they are in contact and upon the type, magnitude and direction of the driving forces selected.

They are used to characterise a particular membrane system with a series of experiments performed under controlled conditions, which are suitable for the interested application, whether it is theoretical or practical.

Basic measurements such as electrical conductivity, membrane potential, ionic diffusion rates and similar are of obvious practical value when assessing a membrane for a particular process. A full appreciation of membrane processes however requires a comprehensive theory.

The most rigorous of the theories available and the most useful for our purposes is irreversible thermodynamics.

The present chapter summarises the basic application of irreversible thermodynamics to the transport processes which are selected in this thesis. The application of these theories, although well-established, is not universal and following the thermodynamic analysis there is a short discussion on the correlation of this theory with the more commonly applied (and less precise) Nernst-Planck treatment.

2,2 The Dissipation Function and Frame of Reference

For spontaneous (irreversible) processes the rate of dissipation of free energy, Φ, can be shown to equal the sum of products of local flows and 'forces'.[1,2] The dissipation function, Φ, is shown below for isothermal transport processes, in the absence of chemical reaction, eqn. (2-1). The thermodynamic 'force' is defined here as the negative gradient of electrochemical potential, $\tilde{\mu}_i$

$$\Phi = \sum_{i=1}^{P} J_i^* \text{ grad } (-\tilde{\mu}_i) \geqslant 0 \qquad (2\text{-}1)$$

where J_i^* is the flow of species i on an arbitrary frame of reference, see below.

It is usual to represent the thermodynamic force on species i as X_i, eqn. (2-2)

$$X_i = \text{grad } (-\tilde{\mu}_i) \qquad (2\text{-}2)$$

Eqn. (2-1) therefore becomes

$$\Phi = \sum_{i=1}^{p} J_i^* X_i \geqslant 0 \qquad (2\text{-}3)$$

It is necessary to define practical frames of reference for the flows J_i of species i.

If the system under study is in a state of mechanical equilibrium, eqn. (2-3) will apply for any frame of reference.[1] In the study of

membrane transport processes, flows are most conveniently measured relative to the membrane itself and so this apparatus-fixed frame of reference is desirable.

In the application of this research, the membrane consists of a counterion 1, coion 2 (or counterion 2, in bi-ionic systems where coion is negligible), solvent 3 and matrix 4, so that eqn. (2-3) becomes

$$\Phi = J_1^* X_1 + J_2^* X_2 + J_3^* X_3 + J_4^* X_4 \geqslant 0 \qquad (2\text{-}4)$$

For one dimensional isothermal isobaric diffusion, the thermodynamic force X_i, eqn. (2-2) may be written as

$$X_i = -\frac{d\tilde{\mu}_i}{dx} = -\frac{d\mu_i}{dx} + z_i F \left(-\frac{d\psi}{dx}\right) \qquad (2\text{-}5)$$

where μ_i is the concentration dependent part of the chemical potential, z_i is the signed valency, F is the Faraday constant, ψ the internal electrical potential of the membrane phase, and x the distance parameter in cm.

From the Gibbs-Duhem equation, eqn. (2-6) is easily obtained and so in a system with p forces only p-1 forces are independent.

$$\sum_{i=1}^{4} n_i X_i = 0 \qquad (2\text{-}6)$$

or equivalently

$$\sum_{i=1}^{4} c_i X_i = 0$$

where n_i is the number of moles of species i or concentration units c_i may be used by considering a local volume (e.g. unit of c_i mole L^{-1} may be employed).

Eliminating X_4 (the force on the fixed charge), using eqns. (2-5) and (2-6), eqn. (2-4) becomes

$$\Phi = (J_1^* - \frac{c_1}{c_4} J_4^*) X_1 + (J_2^* - \frac{c_2}{c_4} J_4^*) X_2 + (J_3^* - \frac{c_3}{c_4} J_4^*) X_3 \geqslant 0 \qquad (2\text{-}7)$$

Since J_i^* is defined by $c_i V_i^*$, where V_i^* is the velocity of species i relative to any arbitrary frame of reference, then $(J_i^* - \frac{c_i}{c_4} J_4^*) = c_i(V_i^* - V_4^*)$ (where i = 1,2,3).

Since $(V_i^* - V_4^*)$ is the velocity of species i relative to 4, eqn. (2-7) may be simplified to

$$\Phi = J_1^4 X_1 + J_2^4 X_2 + J_3^4 X_3 = \sum_{i=1}^{3} J_i^4 X_i \geqslant 0 \qquad (2\text{-}8)$$

where J_i^4 are the flows of species i(=1,2,3), relative to the charge 4 fixed on the polymer.

2.3 Linear Phenomenological Equations

Onsager showed[3,4] that, for systems close to thermodynamic equilibrium and in a steady state, flows and forces (as defined by the dissipation function, eqn. (2-8)), are linearly related by phenomenological equations, which may be written as eqn. (2-9). Membrane fixed flows, J_i^4, will be used exclusively for the remainder of this thesis, and so the

superscript 4 will be omitted for convenience, in eqn. (2-9) and subsequently: for J_i^4 we will now simply write J_i

$$J_i = \sum_{k=1}^{p-1} L_{ik} X_k \qquad (i=1,2,.....p-1) \qquad (2\text{-}9)$$

where the mobility coefficients, L_{ik} are generalised as 'conductance' or 'permeability' coefficients. Eqn. (2-9) may be represented in matrix form (eqn. (2-10))

$$\begin{vmatrix} J_1 \\ J_2 \\ J_3 \\ \vdots \\ J_{(p-1)} \end{vmatrix} \begin{vmatrix} L_{11} & L_{12} & L_{13} & L_{1(p-1)} \\ L_{21} & L_{22} & L_{23} & L_{2(p-1)} \\ L_{31} & L_{32} & L_{33} & L_{3(p-1)} \\ \vdots & \vdots & \vdots & \vdots \\ L_{(p-1)1} & L_{(p-1)2} & L_{(p-1)3} & L_{(p-1)(p-1)} \end{vmatrix} \begin{vmatrix} X_1 \\ X_2 \\ X_3 \\ \vdots \\ X_{(p-1)} \end{vmatrix} \qquad (2\text{-}10)$$

There are two sorts of mobility coefficients, direct coefficients L_{ii} which, via the contribution $L_{ii}X_i$, of eqns. (2-9) or (2-10), define the contribution of the force X_i or its (own) conjugate flow J_i.

The other coefficients L_{ik} ($i \neq k$) are the coupling or cross-coefficients which show that a non-conjugate force X_k will contribute to a flow J_i through terms of the sort $L_{ik}X_k$ ($i \neq k$), eqn. (2-10).

It is clear that the flow J_i is no longer solely a function of its conjugate force X_i as in the laws of Fick and Ohm, for example.

Applying the principle of microscopic reversibility, Onsager[3] showed that L-coefficient matrices are symmetrical for conditions 'close to equilibrium', and so,

$$L_{ik} = L_{ki} \qquad (i \neq k) \tag{2-11}$$

This is formally known as the Onsager Reciprocal Relations (O.R.R.). These relationships reduce the number of coefficients required to characterise a system which contains p independent forces from p^2 to $\frac{p(p+1)}{2}$.

Application of condition for overall positive entropy production the eqns. (2-1) and (2-10) causes the cross-coefficients to be limited by the inequalities

$$L_{ii}\, L_{kk} \geqslant L_{ik}\, L_{ki} \tag{2-12}$$

or using O.R.R.

$$L_{ii}\, L_{kk} \geqslant (L_{ik})^2$$

The direct coefficients must be positive but cross-coefficients L_{ik} can be either positive or negative, as shown by eqn. (2-12).

2.4 Mobility Coefficients

The mobility coefficient approach has been used, Miller[5], to describe transport processes in binary solutions (solvent-fixed frame of reference) and Paterson for membranes.[6] It is very useful when applied to membranes since it produces relatively simple equations for observed transport properties (e.g. electrical conductivity and transport number). For a system with three mobile components, p=3, it can be seen that six phenomenological coefficients are required to characterise the system, (p(p+1)/2), as defined above. The L_{ik} coefficient matrix may therefore be solved from the results of six independent experiments. A full solution was not attempted here for any membrane.

When isobaric and isothermal conditions are observed, only electrical and chemical potential forces may be used. A theoretical treatment of experiments available using these two forces under steady state conditions will now be considered. The phenomenological equations for this system are eqn. (2-13)

$$\begin{aligned} J_1 &= L_{11}X_1 + L_{12}X_2 + L_{13}X_3 \\ J_2 &= L_{21}X_1 + L_{22}X_2 + L_{23}X_3 \\ J_3 &= L_{31}X_1 + L_{32}X_2 + L_{33}X_3 \end{aligned} \qquad (2\text{-}13)$$

Here the flows J_1, J_2 and J_3 on the membrane or 4-fixed flows as defined previously in eqn. (2-8).

Since we now consider only membrane fixed flows, these superscripts will be omitted for convenience, as previously stated.

2.5 Measured Transport Properties of Membranes in Terms of Mobility Coefficients

2.5.1 Electrical conductivity and transport number

If an electrical force is applied to an isothermal isobaric system containing ions, species 1 and 2, and water, species 3, in the absence of chemical potential gradients, X_1 and X_2 are determined solely by electrical potential gradients and X_3 (for water) is zero. Therefore from eqn. (2-5)

$$X_i = z_i F \left(-\frac{d\psi}{dx}\right) \qquad i=1,2 \tag{2-14}$$

$$X_3 = 0 \tag{2-15}$$

It is under these conditions that electrical conductivity and transport number experiments are carried out.

The current density I (A cm^{-2}) is defined by eqn. (2-16),

$$I = (z_1 J_1 + z_2 J_2) F \tag{2-16}$$

From eqns. (2-14) and (2-15) the phenomenological eqns. (2-13) now become,

$$J_1 = L_{11} X_1 + L_{12} X_2$$

$$J_2 = L_{21} X_1 + L_{22} X_2 \qquad (2\text{-}17)$$

$$J_3 = L_{31} X_1 + L_{32} X_2$$

Using eqns. (2-14) and (2-17), eqn. (2-16) becomes

$$I = (z_1^2 L_{11} + 2z_1 z_2 L_{12} + z_2^2 L_{22}) F^2 (-\frac{d\psi}{dx}) \qquad (2\text{-}18)$$

Since the mobility coefficients are constants independent of the force, eqn. (2-18) shows that the membrane will obey Ohm's law, usually written in the form

$$I = \bar{\kappa} (-\frac{d\psi}{dx}) \qquad (2\text{-}19)$$

or $$\bar{\kappa} = \alpha F^2$$

where

$$\alpha = (z_1^2 L_{11} + 2z_1 z_2 L_{12} + z_2^2 L_{22})$$

The transport number of an ion is defined for a membrane in the same manner as electrolyte solution. The transport number of an ion, i, in the membrane $\bar{t}_i$, is defined as the fraction of total current carried by that ion, eqn. (2-20)

$$\bar{t}_i = \frac{z_i F J_i}{I} \qquad i=1,2 \qquad (2\text{-}20)$$

For an exchanger membrane containing two ions, 1 and 2, it is easily shown that transport numbers $\bar{t}_1$ and $\bar{t}_2$ may be obtained, eqns. (2-21) and (2-22) using eqns. (2-17), (2-18) and (2-14) in eqn. (2-20).

$$\bar{t}_1 = (z_1^2 L_{11} + z_1 z_2 L_{12})/\alpha \qquad (2\text{-}21)$$

$$\bar{t}_2 = (z_2^2 L_{22} + z_1 z_2 L_{12})/\alpha \qquad (2\text{-}22)$$

The water transference number, $\bar{t}_3$, is defined by

$$\bar{t}_3 = \frac{J_3 F}{I} \qquad (2\text{-}23)$$

From eqns. (2-17), (2-18) and (2-14), we obtain

$$\bar{t}_3 = (z_1 L_{13} + z_2 L_{23})/\alpha \qquad (2\text{-}24)$$

The same equations apply equally to homoionic membranes in which 1 is counterion, 2, coion, or to bi-ionic membranes (with negligible coion uptake) in which both ions 1 and 2 are counterions. Both conditions are encountered in later experiments in Chapter 6 of this thesis.

2.5.2 The diffusion potential across a membrane exposed to ionic concentration gradients

When a chemical potential gradient is set up across the membrane, due to concentration differences, it causes diffusion of ions, osmotic flow and creates membrane potential. In the steady state situation there is no electric current.

$$I = (z_1 J_1 + z_2 J_2) F = 0 \qquad (2\text{-}25)$$

In this case the forces acting on the species are again given by negative gradients of their electrochemical potentials, eqn. (2-5)

$$X_i = (-\frac{d\tilde{\mu}_i}{dx}) = (-\frac{d\mu_i}{dx}) + z_i F (-\frac{d\psi}{dx}) \qquad (2\text{-}5)$$

Substituting in eqn. (2-13), eqn. (2-25) becomes

$$(z_1 L_{11} + z_2 L_{21}) X_1 + (z_1 L_{12} + z_2 L_{22}) X_2 + (z_1 L_{13} + z_2 L_{23}) X_3 = 0 \qquad (2\text{-}26)$$

Comparison of the bracketed terms with eqns. (2-21), (2-22) and (2-24) shows that eqn. (2-26) may be rewritten, if the O.R.R. are obeyed

$$\frac{\bar{t}_1}{z_1} X_1 + \frac{\bar{t}_2}{z_2} X_2 + \bar{t}_3 X_3 = 0 \qquad (2\text{-}27)$$

This relationship may be used to define the electrical potential gradient in the membrane since

$$X_i = (-\frac{d\bar{\tilde{\mu}}}{dx}) + z_i F (-\frac{d\bar{\psi}}{dx}) \quad \text{then}$$

$$-F\, d\bar{\psi} = \frac{\bar{t}_1}{z_1} d\bar{\mu}_1 + \frac{\bar{t}_2}{z_2} d\bar{\mu}_2 + \bar{t}_3 d\bar{\mu}_3$$

which is the 'Henderson' equation for the membrane phase. It is to be used in order that the osmotic gradient contributes to the electrical potential explicitly.

Derivation of equivalent expressions for diffusion coefficients in terms of L_{ik} coefficients are well-known but since they do not enter later discussions, they are omitted here.

2.6 Nernst-Planck Equations

Commonly, the Nernst-Planck equations are used in the analysis of membrane transport. It will be shown here how this application is related to the more rigorous irreversible thermodynamic analysis (using L_{ik} coefficients (given above).

In a situation where a system deviates only slightly from equilibrium, linear phenomenological equations may be written relating to the flow of species, i, to all other forces so that for a p-1 component system

$$J_i = \sum_{k=1}^{p-1} L_{ik} X_k \qquad (i=1,2,3....p-1) \qquad (2\text{-}9)$$

The terms L_{ik} are the phenomenological coefficients and are independent of the forces. The L_{ik} coefficients measure the degree to which a flow of species i, affected by a forces on species k, if $i \neq k$.

If there is no coupling all $L_{ik}=0$ $(i \neq k)$ and each flow may be written as proportional and its conjugate force as in Ohm's law and Fick's law.

$$J_i = L_{ii} X_i \qquad (2\text{-}28)$$

For an ionic system, the electrochemical force, X_i, is given by eqn. (2-5)

$$X_i = \frac{RT}{a_i}\left(-\frac{da_i}{dx}\right) + z_i F \left(-\frac{d\psi}{dx}\right) \qquad (2\text{-}5)$$

Substituting in eqn. (2-28) and if activity a_i may be approximated by concentration c_i, we obtain eqn. (2-29) for the flow of an ion under electrochemical force, if no coupling exists with other species

$$J_i = L_{ii}\frac{RT}{c_i}\left(-\frac{dc_i}{dx}\right) + L_{ii}\, z_i F \left(-\frac{d\psi}{dx}\right) \qquad (2\text{-}29)$$

We may compare this expression with the equivalent Nernst-Planck equation, eqn. (2-30)

$$J_i = D_i\left(-\frac{dc_i}{dx}\right) + c_i U_i \left(-\frac{d\psi}{dx}\right) \qquad (2\text{-}30)$$

This describes the total flow as the sum of the diffusional flow (the first term on the right hand side of eqn. (2-30)) and electrical flow, (the second term), where D_i and U_i are respectively the ionic diffusion coefficients and the electrical mobility.

If we compare coefficients in eqns. (2-29) and (2-30) we may express D_i and U_i in terms of L_{ii}, the direct mobility coefficient, eqns. (2-31) and (2-32)

$$D_i = L_{ii}\frac{RT}{c_i} \qquad (2\text{-}31)$$

and

$$D_i = \frac{RT}{z_i F} U_i \qquad (2\text{-}33)$$

It is clear therefore that the Nernst-Planck equations and the Nernst-Einstein relationship are simple examples of reduced irreversible thermodynamic treatment in which coupling is omitted.

Failure to understand that the Nernst-Planck equations are simple approximations to a more complex coupled system, often causes incorrect interpretation. This is particularly so for ion exchange membranes where interionic coupling is large and counterion-solvent causes large electro-osmotic flows, under a simple applied electrical field, with no concentration gradients. The Nernst-Planck needs the arbitrary assumption of convection effects. The irreversible thermodynamic treatment however recognises coupling between ions and water measured by the coupling coefficients, L_{13} and L_{23} (above), so that for electrical forces only a flow of water, J_3, is defined

$$J_3 = (z_1 L_{13} + z_2 L_{23}) F (- \frac{d\psi}{dx})$$

if the coupling coefficients are zero.

This phenomena, electro-osmosis, is measured by the transference numbers, $\bar{t}_3$, defined by eqn. (2-24).

References

1. S.R. DeGroot and P. Mazur, Non-equilibrium Thermodynamics, North-Holland, Amsterdam, 1962.

2. A. Katchalsky and P. Curran', Non-equilibrium Thermodynamics in Biophysics', Harvard University Press, Cambridge, Mass., U.S.A., P.8, 1965.

3. L. Onsager, Phys. Rev., 37, 405 (1931).

4. L. Onsager, 'ibid', 38, 2265 (1931).

5. D.G. Miller, J. Phys. Chem., 70, 2639 (1966).

6. R. Paterson, in Pontificae Academiae Scientiarum Scripta Varia, 40, 517 (1976).

CHAPTER 3

Physical Properties of Nafion 125 and 117 Membranes in Different Ionic Forms

3.1 INTRODUCTION

It is important to characterize the ion exchange membranes before use. Nafion 125 and 117 membranes (1200 and 1100 EW respectively were used in different ionic (H^+, Li^+, Na^+, K^+ and Ca^{2+}) forms. Their physical parameters, such as water content, internal molalities, thicknesses and diameters have been determined for salt chloride solutions at 0.05 and 0.1M.

An interesting and important practical property of Nafion perfluorosulphonic acid membranes is their ability to sorb relatively large amounts of water and other solvents. The polymers typically sorb water to 10-50% of their dry weight, depending upon polymer equivalent weight, counterion form and temperature of equilibration. Counterions with large hydration energies increase water uptake, as does low equivalent weight.

For exchange diffusion (Chapters 7 and 8) and bi-ionic potential (Chapter 6) measurements, the two ions chosen were H^+ and K^+, due to their large differences in mobility.

Consequently, a detailed study of mixed K^+/H^+ forms were made over a complete range of ionic compositions. In Chapter 4 the selectivity coefficients for their exchange are reported.

3.2 Solutions

The salts were of analytical grade, obtained from Koch-Light Laboratories or Hopkin and Williams. Solutions were prepared using conductivity water without recrystallisation or further purification.

Sodium hydroxide solutions were prepared using standard volumetric concentrated solutions (vial) supplied by May and Baker. The solutions were prepared under carbon dioxide free conditions. The vial was diluted in carbon dioxide free distilled water contained in the glass reservoir of an automatic burette.

The solution was made while nitrogen was being bubbled through the water in the reservoir. The burette itself was flushed with nitrogen during the process and was protected from subsequent carbon dioxide uptake by "Sofnolite" guard tubes. Solutions of sodium hydroxide prepared in this way were standardised by titration against weighed samples of potassium hydrogen phthalate.

The solution was prepared by dissolving a weighed quantity of Analar potassium hydrogen phthalate (BDH grade). The indicator used was phenolphthalein.

3.3 Membrane Conditioning Process

Discs approximately 4.2 cm in diameter were cut from sheets of ion exchange membrane, using a machined brass dye. These discs were conditioned (1) by a cycle of equilibrations with, in turn, methanol; 1M HCℓ; distilled water; 1M NaOH and finally, distilled water. Each treatment lasted several hours.

This cycle of treatment was repeated a number of times. The methanol was used to remove residual monomer or other alcohol-soluble materials remaining in the membranes. The treatments with HCℓ and NaOH removed any base or acid-soluble impurities, such as iron or other heavy metal ions accumulated in the course of preparation.

The cycling process was continued for several treatments. The weights of leached (potassium, sodium, lithium, calcium and hydrogen) forms of the membrane were determined, as described below. The discs were equilibrated in each (potassium, sodium, lithium, calcium and hydrogen chlorides) for several days with repeated changes of solution to ensure that they were completely converted to the required ionic form, i.e. only the chosen counterion would be present "associated" with the sulphonate fixed sites. The membranes were washed with distilled water for several hours to leach out any sorbed electrolyte.

For succeeding experiments, the membranes were equilibrated in chloride solutions of particular concentrations. The equilibration solutions were frequently changed.

3.4 Wet Weights

A kinetic method of weighing was used to determine the wet weights of each membrane after equilibration with water or potassium, sodium, lithium, calcium and hydrogen chloride solutions.

The membrane was removed from the solution with which it had equilibrated and its surface blotted between two pads of hardened filter paper. The membrane was taken from the filter pads and the stopwatch

started. It was quickly placed on a weighed watch glass. The combined weight of watch glass and membrane was then noted every fifteen seconds for the next two minutes. The total time taken for this procedure was approximately two and a half minutes. Weights were plotted against time and extrapolated back to zero time to estimate the true wet weight of the membrane. A weight loss of about 1 mg every fifteen seconds was typical. This procedure was carried out several times for each membrane in equilibrating solution. The wet weight thus obtained was reproducible to ± 0.1%.

This procedure was carried out for each membrane of the required (potassium, sodium, lithium, calcium and hydrogen chloride) concentrations. The complete process was then repeated after cycling in various ionic forms (potassium, sodium, lithium, calcium and hydrogen) to determine if any weight change had occurred during the cycle. No such changes were observed.

3.5 Dry Weights

The leached membrane in potassium form was placed in a weighing bottle inside a desiccator containing phosphorous pentaoxide. The desiccator was then evacuated using a water pump. It was then placed in an oven at 80°C for several days.

The membranes were then weighed to determine their dry weight. This process was repeated until a constant weight was obtained. At no time in the course of subsequent experiments was any of the membranes allowed to dry again. The dry weights obtained were reproducible to ± 0.3%.

3.6 Physical Dimensions

3.6.1 Diameter

The membrane was removed from its equilibrating solution and placed, still wet, between two optically flat glass plates. It was then under 10X-A lens of Nikon Profile Projector (Model 6C) and its diameter measured using the micrometer stage of this microscope. The average of six determinations was taken as the diameter.

3.6.2 Thickness

The membrane thickness was measured using a micrometer accurate to ± 0.01 mm. The membrane was clamped between two microscope cover plates, the thickness of which was known. The thickness of glass plates plus membrane was then measured. The average differences of ten such determinations was taken as a thickness of the membrane and were reproducible to ± 0.1%.

3.6.3 Membrane volume

Two methods were used to determine the volume of the membrane: The direct method, by using specific gravity bottles. The ion exchange was equilibrated with the solution of interest. The specific gravity bottle was filled with solution and put in a water bath maintained at 25 ± 0.01°C. After thermal equilibrium was attained the bottle was weighed (after careful drying of its surface). The process was repeated with the test membrane placed in the bottle and the bottle plus solution plus membrane weighed as before. The volume of the membrane was found from the

change in weight between the two systems ($W_2 - W_1$) and the previously determined weight of the wet membrane, W_m.

$$W_2 = W_m + W'_s + W_b$$

$$W_1 = W^\circ_s + W_b$$

where

$$\Delta W = W_2 - W_1 = W_m + W'_s - W^\circ_s$$

The weight of solution which is equal to the volume of the membrane is given by

$$\Delta W - W_m = W'_s - W^\circ_s$$

Therefore the volume of the membrane is obtained

$$V_m = \frac{W'_s - W^\circ_s}{d}$$

where

W_m = wt. of the membrane (gm)

W'_s = wt. of the solution in the presence of a membrane (gm)

W_b = wt. of the bottle (gm)

W°_s = wt. of the solution in the absence of a membrane (gm)

d = density of the solution (gm/cm^3)

In the other method the membrane volume was determined from the radius and the thickness of the membrane by using $\pi r^2 \ell$. This method was not accurate because although the original disc of dry membrane

was circular, in swelling the circular shape was distorted towards elliptical in most cases, indicating some anisotropy in the sheet membrane, as received, and is no doubt due to the techniques of manufacture.

3.7 Capacity Determination

The ion exchange capacity of membranes was determined by first converting them completely to the H-form by successive equilibrations with hydrochloric acid (1M). They were then removed from the acid and rinsed thoroughly with distilled water to remove the sorbed electrolyte. After blotting between filter papers, the membrane was equilibrated with 25 ml of 1M sodium chloride for several hours. The following exchange

$$\bar{H}^{+} + Na^{+} \rightleftharpoons \bar{N}a^{+} + H^{+}$$

takes place. The sodium ions in solution are exchanged for hydrogen ions of the membrane. The H^{+} released was titrated with standard sodium hydroxide solution. This procedure was repeated until $> 99.9\%$ of H^{+} was removed and so exchange was in effect complete.

The combined equilibration solutions were then titrated with sodium hydroxide and a glass electrode assembly. An Orion Digital pH/mV meter, model 801A was used. The amount of H^{+} released by the membrane is stoichiometrically equivalent to the amount of NaOH added at the end point. The end point of the titration was calculated from pH data using a linear titration plot method based upon the Gran plot method.

3.8 RESULTS AND DISCUSSION

The ion exchange capacity, water content, internal molalities and water exchange sites mole ratio for Nafion 125 and 117 (1200 and 1100 EW) are listed in Tables (3-1) and (3-2) at two different external solution concentrations (0.05 and 0.1M) of K^+, Na^+, Li^+, H^+ and Ca^{2+} chlorides. The physical properties of Nafion 125 membrane in mixed K^+/H^+ were given in Table (3-3). These are a major topic of much discussion in the following chapters.

A striking feature of Tables (3-1) and (3-2) is the massive drop in water content when the counterion is changed from hydrogen to potassium. This would be expected on the basis of different hydration ionic size of the counter ions.

With increasing counterion weight, the relative water molecules number per exchange site ($n_{H_2O}/n_{SO_3^-}$) decrease, Tables (3-1) and (3-2) while the number of sulphonic groups ($-SO_3^-$) increases. The water-fixed charged site mole ratio reflects the dynamic character of ion cluster morphology compared to cross-linked ion exchange (2) (see Chapter 4, Table (4-3)).

As the external solution concentration increased from 0.05 to 0.1M, the wet weight, water content and the thickness decreased, while co-ion uptake increased as might be expected from general theory. Nafion 125 membranes equilibrated in comparable concentrations of NaCℓ, the concentration (m) of uptake increase (3) from 1.5×10^{-2} to 3.2×10^{-2}.

Tables (3-1) and (3-2)

Physical characteristics of Nafion membranes at different external solutions - concentration in variety of homoionic forms.

Table (3-1). Nafion 125 membrane disc with ion exchange capacity = 0.2368 mmole/disc used here

Physical Parameters \ Ionic Forms	a - At 0.05M external solution				
	K^+	Na^+	Ca^{2+}	Li^+	H^+
Dry weight (gm)	0.3063	0.3025	0.3018	0.2987	0.2973
Wet wt. (gm)	0.3475	0.3540	0.3580	0.3611	0.3633
Wt. of H_2O/ disc (gm)	0.0412	0.0515	0.6562	0.0624	0.0660
% of H_2O content w.r.t. * Dry matrix	13.87	17.33	18.91	21.00	22.21
Eq. mol kg^{-1} of pore water	5.7475	4.5980	4.2135	3.7948	3.5875
$nH_2O/n\text{-}SO_3^-$	9.66	12.07	13.17	14.63	15.47
Diameter (cm)	4.1596	4.2289	4.2249	4.2769	4.2911
Thickness (cm)	0.0137	0.0142	0.0138	0.0143	0.0143
Volume (cm^3) **	0.194	0.1990	0.1989	0.205	0.206
Volume (cm^3) ***	0.1636	0.1612	0.1639	0.1594	0.1580

* The weight of polymer sulphonate backbone present in the disc, but excluding the weight of counterion

** $(\pi r^2 \ell)$: *** (Direct)

Nafion 125 membrane disc with ion exchange capacity = 0.2368 mmole/disc used here

Physical Parameters \ Ionic Forms	b - At 0.1M external solution				
	K^+	Na^+	Ca^{2+}	Li^+	H^+
Wet wt. (gm)	0.3456	0.3510	0.3559	0.3602	0.3625
Wt. of H_2O/ disc (gm)	0.0393	0.0485	0.0541	0.0615	0.0652
% of H_2O content w.r.t. Dry matrix	13.23	16.32	18.21	20.73	21.94
Eq. molal kg^{-1} of pore water	6.0254	4.8824	4.3771	3.8504	3.6319
$nH_2O/n\text{-}SO_3^-$	9.21	11.37	12.68	14.41	15.28
Diameter (cm)	4.1322	4.1734	4.3155	4.2648	4.2791
Thickness (cm)	0.0135	0.0140	0.0136	0.0141	0.0142
Volume (cm^3) **	0.189	0.1925	0.1989	0.2014	0.1999
Volume (cm^3) ***	0.1627	0.1600	0.1635	0.1554	0.1580

** ($\pi r^2 \ell$: *** (Direct)

Table (3-2). Nafion 117 membrane disc with ion exchange capacity = 0.3523 mmole/disc

Physical parameters \ Ionic Forms	a - At 0.05M external solution				
	K^+	Na^+	Ca^{2+}	Li^+	H^+
Dr. wt. (gm)	0.4161	0.4104	0.4094	0.4047	0.4026
Wet wt. (gm)	0.4868	0.5037	0.5126	0.5164	0.5206
Wt. of H_2O/ disc (gm)	0.0707	0.0933	0.1032	0.1117	0.1180
% of H_2O content w.r.t. Dry matrix	17.57	23.19	25.65	27.76	29.33
Eq. molal kg^{-1} of pore water	4.9830	3.7760	3.4137	3.1539	2.9855
$nH_2O/n\text{-}SO_3^-$	11.1378	14.6980	16.2580	17.5972	18.5898
Diameter (cm)	4.2347	4.2612	4.3155	4.3961	4.3918
Thickness (cm)	0.0193	0.0195	0.0138	0.0195	0.0199
Volume (cm^3) **	0.2656	0.2860	0.2019	0.2970	0.306
Volume (cm^3) ***	0.2156	0.2127	0.2161	0.2090	0.2077

** ($\pi r^2 \ell$): *** (Direct)

Nafion 117 membrane disc with ion exchange capacity = 0.3523 mmole/disc

Physical Parameters \ Ionic Forms	b - At 0.1M external solution				
	K^+	Na^+	Ca^{2+}	Li^+	H^+
Wet wt. (gm)	0.4853	0.5010	0.5063	0.5107	0.5165
Wt. of H_2O/ Disc (gm)	0.0692	0.0906	0.0969	0.1060	0.1139
% of H_2O content w.r.t. Dry matrix	17.20	22.52	24.08	26.34	28.31
Eq. molal kg^{-1} of pore water	5.0910	3.8885	3.6357	3.3235	3.0930
$nH_2O/n\text{-}SO_3^-$	10.9015	14.2728	15.2652	16.6992	17.9437
Diameter (cm)	4.1346	4.2304	4.3072	4.3641	4.3856
Thickness (cm)	0.0191	0.0194	0.0137	0.0198	0.0197
Volume (cm^3) **	0.256	0.272	0.1996	0.2961	0.297
Volume (cm^3) ***	0.2211	0.2182	0.2204	0.2137	0.2152

** ($\pi r^2 \ell$): *** (Direct)

Table (3-3). Physical properties of Nafion 125 membrane in mixed K^+/H^+ form at complete range of loading.

Nafion 125 membrane disc with ion-exchange capacity = 0.2364 mmole/disc. Dry weight = 0.3045

Physical parameters \ X_{H^+}	0	0.10	0.30	0.50	0.70	0.90	1.00
Wet wt. of the disc (gm)	0.3369	0.3387	0.3411	0.3429	0.3454	0.3457	0.3548
Wt. of H_2O/disc (gm)	0.0323	0.0342	0.0366	0.0384	0.0409	0.0412	0.0503
$\bar{d}$ (gm/cm^3)	1.0014	1.0022	1.0019	1.0016	1.0013	1.0010	0.9987
$\bar{V}$ (cm^3)	0.1623	0.1609	0.1605	0.1584	0.1586	0.1564	0.1589
$\bar{V}_w$	0.1991	0.2125	0.2279	0.2423	0.2577	0.2634	0.3165
m (molal kg^{-1} of pore (H_2O)	7.3189	6.9122	6.4590	6.1563	5.7799	5.7378	4.6998
$\frac{n_{H_2O}}{n_{SO_3}}$	7.58	8.03	8.59	9.01	9.60	9.67	11.81

REFERENCES

1. F. Helfferich. "Ion Exchange", McGraw-Hill, New York, 1962, p.230.

2. O.D. Bonner, J. Phys. Chem., 59 719 (1955).

3. L. Bimibi, C. Fabiani, M. De Francesco and B. Scuppa, Comitato Nazionale Energia Nucleare, Rome, Italy, CNEN-RT/CHI 11, 1981.

(2)
The water absorption decrease with increasing EW.
This can be expected because the higher the equivalent weight, the lower conc. of ionic group per unit polymer wt.

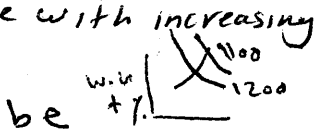

CHAPTER 4

Selectivity Coefficients of Perfluorosulphonic Acid Membranes (Nafion) in Mixed K^+/H^+ Forms

4.1 INTRODUCTION

Ion exchangers can distinguish between different counterions. When counterions are exchanged, the ion exchanger usually takes up certain counterions in preference to others. This selectivity arises from one of several physical causes. It depends upon the counterion charge which, via the Donnan potential, causes ions of higher charge to be selected. Within a specific group of ions with equal charge, specific interaction between counterions and the fixed ionic groups results in preference.

In these studies K^+/H^+ selectivity is examined. These ions were chosen partly because they are ions which have vastly differing swelling tendencies in the exchanger and partly because they are ideally suited for tests of new diffusion techniques due to their large differences in ionic mobility. This was particularly useful for tests of the oscillatory method (Chapter 8) where these two ions were exchanged across the membrane. The degree of exchange was then measurable in terms of conductivity in the closed collecting vessel, (Chapter 7).

The study of selectivity of perfluorinated ionomer membranes (Nafion) provided the necessary basic information which was necessary to evaluate diffusion coefficient, flux and electrical conductivity and depend upon membrane composition.

It was interesting in this respect to make a comparison between Nafion and conventional cross-linked Dowex 50 (1) membranes in terms of selectivity coefficients and water content.

4.2 Membrane Isotherm-Selectivity Coefficient

Ion exchange equilibria are characterized by the ion exchange isotherm. This isotherm is a graphical representation which, in principle, covers all possible experimental conditions at a given temperature. In a simple ion exchange process involving two counterions, it is a plot of the ionic fractions of the exchanged ions in the resin or membrane as a function of the corresponding solution composition. Their rates define the selectivity coefficient.

When a cation exchange membrane is placed in a solution containing a mixture of electrolyte, in this case, potassium chloride and hydrochloric acid, an equilibrium is quickly set up at the solution membrane interface so that

$$\bar{K}^+ + H^+ \rightleftharpoons \bar{H}^+ + K^+ \qquad (4\text{-}1)$$

(The exchanger is assumed to exclude coion (chloride) completely.*

The position of this equilbrium defines the selectivity of the exchanger for one cation over the other. The selectivity coefficient K_H^K is usually as given in eqn. (4-2)

$$K_H^K = \frac{\bar{X}_K}{\bar{X}_H} \cdot \frac{c_H . f_H}{c_K . f_K} \qquad (4\text{-}2)$$

where c_H and c_K, the solution molarities and $\bar{X}_H$, $\bar{X}_K$ represent the equivalent ionic fraction of these ions in the membrane phase and f_H, f_K the single-ion activity coefficients in solution. These latter approximat-

* Footnote: With external electrolyte concentrations of HCℓ + KCℓ 0.05M, (as here) the uptake of chloride is << 0.5% of the ionic composition in the membrane phase.

ely cancel for univalent ion exchange in dilute solution.

If the membrane phase molar activity coefficients $\bar{f}_K$ and $\bar{f}_H$ are defined in the same manner as the solution molar activity coefficients, that is, if the same standard states are used for the membrane and solution, then the thermodynamic equilibrium constant $K^K_{H(th)}$ is defined as unity.

$$\frac{\bar{X}_K}{\bar{X}_H}\,\frac{c_H}{c_K}\,\frac{\bar{f}_K}{\bar{f}_H}\cdot\frac{f_H}{f_K} \equiv 1 = K^K_{H(th)} \qquad (4\text{-}3)$$

Thus the selectivity coefficient, K^K_H is the inverse of the ratio of membrane phase activity coefficients, $(\bar{f}_K/\bar{f}_H)$.

Selectivity coefficients, K^K_H are not constant in general, but change with membrane or resin composition. This variation of selectivity with composition has been the subject of much discussion and the matter will be raised again at the end of this chapter.

For diffusion studies, however, it is essential to know the composition of the membrane phase in contact with each solution. In later studies conditions were chosen (from these measurements) such that the membrane phase was 50% loaded with each. $\bar{X}_H = \bar{X}_K = 0.5$, so that the concentration effects on fluxes were, as near as possible, equal, and the measurements provided information on the relative mobilities of the two ions.

4.3 EXPERIMENTAL

Each disc in K or H-form was usually equilibrated with 10 ml of a mixed HCℓ + KCℓ solution of total composition 0.05M at 25°C. Previous studies showed that, under such conditions, the uptake of chloride (coion) was negligible (< 1%). After equilibrium (sometimes taking several days but at least 24 hours in the most favourable case K^+ exchange on to H-form) the equilibrated disc was removed from solution. Adherent solution was washed from the disc which was set aside for analysis if needed. The change in composition of the equilibrated solution was determined by titration of H^+ ions. In selected cases the potassium ion was measured also. In all cases the total ionic strength of the solution was measured at 0.05M.

The disc or membrane composition was also determined by conversion to the K-form and titration of the released H^+ ion. In all cases mass balance was confirmed.

The ion exchange membrane isotherms can be determined from a series of equilibrium measurements with solutions of different compositions covering the whole range of ionic loading from 0 to 1. The test of equilibrium was to approach the same equilibrium conditions from both sides, i.e., by using membranes initially in the H-form and then repeating with a similar set of experiments, but starting with the K-form.

Consider that we began with the membrane disc in K-form. The ionic composition of the membranes and the selectivity coefficients can be determined as follows:

To determine the ionic composition in the solution, suppose that the equilibrating (mixed solution of HCℓ + KCℓ, total concentration 0.05M) has a volume, V cm^3, a concentration c^o_K and c^o_H (the initial concentration of KCℓ and HCℓ in mixed solution) mmoles/cm^3.

The concentration of HCℓ after equilibřium is

$$c_H = \frac{MT}{V}$$

where M = the molarity of sodium hydroxide, M

T = the volume of the titre, cm^3

V = the total volume of the solution, cm^3.

The concentration of K^+ ion is given by

$$c_K = c^o_K + c^o_H - c_H$$

Therefore, the ionic fraction of H^+ and K^+ ions in solution after equilibrium are:

$$X_H = \frac{c_H}{c^o_K + c^o_H} \quad \text{and} \quad X_K = \frac{c_K}{c^o_K + c^o_H}$$

where $c^o_K + c^o_H = 0.05M$.

The ionic compositions in the exchanger membrane were determined as follows:

The number of mmoles of potassium, $\bar{K}$ in the disc is equal to the capacity of the disc, $\bar{X}$ mmoles, while in the solution, c^o_K became c_K and after equilibrium gain in potassium ion K^+ by the solution is equal to $(c_K - c^o_K)$ V mmoles which is equivalent to loss of H^+ by the solution.

Therefore, the ionic fraction of $\bar{K}$ and $\bar{H}$ in the exchanger are equal to

$$\bar{X}_K = \frac{\bar{X}-(c_K - c_K^o)V}{\bar{X}}$$

and

$$\bar{X}_H = \frac{(c_K - c_K^o)V}{\bar{X}}$$

The selectivity coefficient,

$$K_H^K = \frac{\bar{X}_K}{\bar{X}_H} \cdot \frac{c_H}{c_K}$$

4.4 RESULTS AND DISCUSSION

Potassium-hydrogen exchange on Nafion 125 and Nafion 117 perfluorosulphonic acid membranes (1200 and 1100 EW respectively) are characterized by the ion exchange isotherms, Figs. (4-1a,b). Alternatively the selectivity coefficient, K_H^K can be used for describing these ion exchange equilibria, eqn. (4-1), and defined by eqn. (4-2). Selectivity coefficients of Nafion 125 and Nafion 117 for potassium-hydrogen ion exchange are shown as a function of equivalent fraction of K^+ ion in solution of (HCℓ + KCℓ) of 0.05M in Fig. (4-2).

The K_H^K is greater than unity for all compositions, so that for all conditions, the K^+ ion is selected over the H^+ ion. This is also clearly seen in Figs. (4-1a,b), where the isotherms are convex towards the $\bar{X}_K$ axis, indicating that the membranes are always richer in

potassium than the equilibrating solution. Examination of selectivity coefficients, Tables (4-1 and 4-2) and Fig. (4-2) show, however, that the selectivity coefficient is not constant but varies with loading and is higher for Nafion 125 (1200 EW) than for Nafion 117 (1100 EW). In common with almost all other systems in the literature (1,2) the preferred ion (here K^+) is more selective when the exchanger is largely in the H-form, i.e., at low loading of K^+ in the membrane phase.

The explanations given for such (common) selectivities in the literature are many and varied (2,3). A common one is that the resin/membrane has sulphonic acid groups with a large range of intrinsic selectivities, dependent upon their locations within the amorphous polymeric skeleton of the membrane. For this reason it is supposed that the first sites to be loaded by the K^+ ion are the most preferred. The overall selectivity coefficient would then be expected to fall as these sites were occupied by K^+ ion and the loading of this ion was increased.

The concept of sites with variable selectivity may not apply here. In some ionomer membranes, such as Dupont's Nafion, the membrane fixed charge is not randomly distributed, but occurs in clusters (4-9). Thus, the membrane solution is phase-separated, with ion clusters acting as inverted micelles in a polymer solvent (in which the acid groups line the water-polymer interface shielding the exterior fluorocarbons from the interlay aqueous phase (10)).

It is not immediately obvious how such structures might effect selectivity, but an interesting parallel from work on selectivities of liquid ion exchangers, (11), suggests that the selectivity patterns

observed here, Fig. (4-2) (and quite commonly elsewhere (2)) may be due to micelle formation.

Hogfeldt et al., (11,12,13) using dinonylnaphthalene sulphonic acid groups which are very similar to those in strong acid polystyrene cation exchangers like Dowex 50. The study of this liquid membrane system is of interest because it permits a comparison of solid and liquid exchangers. In many cases the aggregation in the latter is supposed to be extensive enough for micelles to be formed (12).

Such studies of fluid systems with no predetermined structures show qualitatively the same selectivity variations as here with Nafion for K^+/H^+ exchange. It is therefore reasonable to consider that the micelle formation in the Nafion membrane is similar to that in large liquid ion exchangers (12). The causes for these selectivity coefficient variations for sulphonate ion exchange resins have been investigated by several workers. As noted above it is generally concluded that the cause is non-uniformity of exchange site environments. This non-uniformity is attributed to local exchange site concentration in the resin.

To understand the causes of the selectivity properties of Nafion, it is useful to compare (2) the isotherms of those conventional cross-linked ion exchangers containing sulphonate groups (3). There is a much greater dependence of selectivity coefficient on ionic fraction of metal ion for these systems compared to Nafion. The selectivity coefficients (metal ion/hydrogen ion) in Dowex 50 change from 1.61 for Na^+ to 3.06 for K^+ and 3.17 for Cs^+. In comparison with Nafion (2), these coefficients are spread over a much wider range (Na^+ 1.22, K^+ 3.97 and Cs^+ 9.11) . This is the most interesting feature about

the selectivity coefficients for the alkali metal ions in Nafion compared to conventional sulphonate resins. In particular, the relative change in selectivity from potassium ion to caesium ion is much greater than for Dowex 50 resins of 4, 8 or 16% cross-linking (3). The water content (mol H_2O/mol SO_3^-) as a function of counterion form is listed in Table (4-3) for Nafion and Dowex 50. These values indicate that there are significantly larger changes in water content for exchange of alkali metal ions in Nafion (decreasing from 14.3 for Li^+ to 6.6 for Cs^+) than for Dowex 50 (decreasing from 11.1 for Li^+ to 8.8 for Cs^+). These differences between the conventional resins and Nafion are due to the lesser hydration for K^+ and Cs^+ in Nafion which causes a stronger interaction of the cation with the sulphonic group. From infra-red measurements made on Nafion by Lowry and Mauritz (14) it may be deduced that in the case of Cs^+ or even Rb^+, outer or even inner sphere complexes are formed with sulphonic group even in the hydrated membrane, while in the case of Na^+ or K^+, completely dissociated hydrated ion pairs are formed (due to their much larger hydration shell).

Tables (4-1) and (4-2)

The selectivity coefficient (K_H^K) and ionic fraction of the two competing ions of H^+ and K^+ in the solution and membrane are given for Nafion 125 (Table (4-1)) and Nafion 117 (Table (4-2)) over a complete range of loadings.

Table (4-1)

Ionic Fraction in Solution		Ionic Fraction in Membrane		Selectivity Coefficient
X_H	X_K	$\bar{X}_H$	$\bar{X}_K$	K_H^K
0	1.0	0	1.0	-
0.085	0.915	0.032	0.968	2.810
0.166	0.834	0.073	0.927	2.528
0.245	0.755	0.117	0.883	2.449
0.414	0.586	0.182	0.818	3.175
0.566	0.434	0.283	0.717	3.302
0.642	0.358	0.334	0.666	3.576
0.698	0.302	0.427	0.573	3.102
0.758	0.242	0.454	0.546	3.767
0.864	0.136	0.652	0.348	3.391
0.921	0.079	0.745	0.255	3.990
0.973	0.027	0.846	0.154	6.560
1.0	0	1.0	0	-

Barred Symbols in the membrane phase

H = hydrogen : K = potassium

Table (4-2)

Ionic Fraction in Solution		Ionic Fraction in Membrane		Selectivity Coefficient
X_H	X_K	$\bar{X}_H$	$\bar{X}_K$	K_H^K
0	1.0	0	1.0	-
0.800	0.920	0.029	0.971	2.912
0.158	0.842	0.060	0.940	2.946
0.241	0.759	0.084	0.916	3.463
0.390	0.610	0.157	0.843	3.433
0.537	0.463	0.232	0.768	3.839
0.597	0.403	0.289	0.711	3.639
0.656	0.344	0.347	0.653	3.588
0.719	0.281	0.400	0.600	3.838
0.798	0.202	0.575	0.425	2.920
0.895	0.105	0.722	0.278	3.282
0.934	0.066	0.809	0.191	3.341
0.976	0.024	0.892	0.108	3.918
1.0	0	1.0	0	-

Table (4-3). Water content of Nafion and Dowex 50 (mol H_2O/mol SO_3^-)

Ion	Nafion			Dowex 50 (3)		
	117	125	120[2]	4% DVB	8% DVB	16% DVB
H^+	17.94	15.28	16.7	-	-	-
Li^+	16.70	14.41	14.3	23.2	11.7	7.2
Na^+	14.27	11.37	11.9	20.6	10.2	6.5
K^+	10.90	9.21	8.8	18.9	9.0	5.9
Rb^+	-	-	7.7	19.0	8.8	5.9
Cs^+	-	-	6.6	19.0	8.8	5.7
Ca^{2+}	15.27	12.68	12.9	-	-	-

Figure (4-1)

K^+/H^+ exchange isotherms for Nafion membranes equilibrated with mixed potassium chloride and hydrochloric acid solutions of total molarity 0.05M.

(a) For Nafion 125 : EW 1200

(b) For Nafion 117 : EW 100

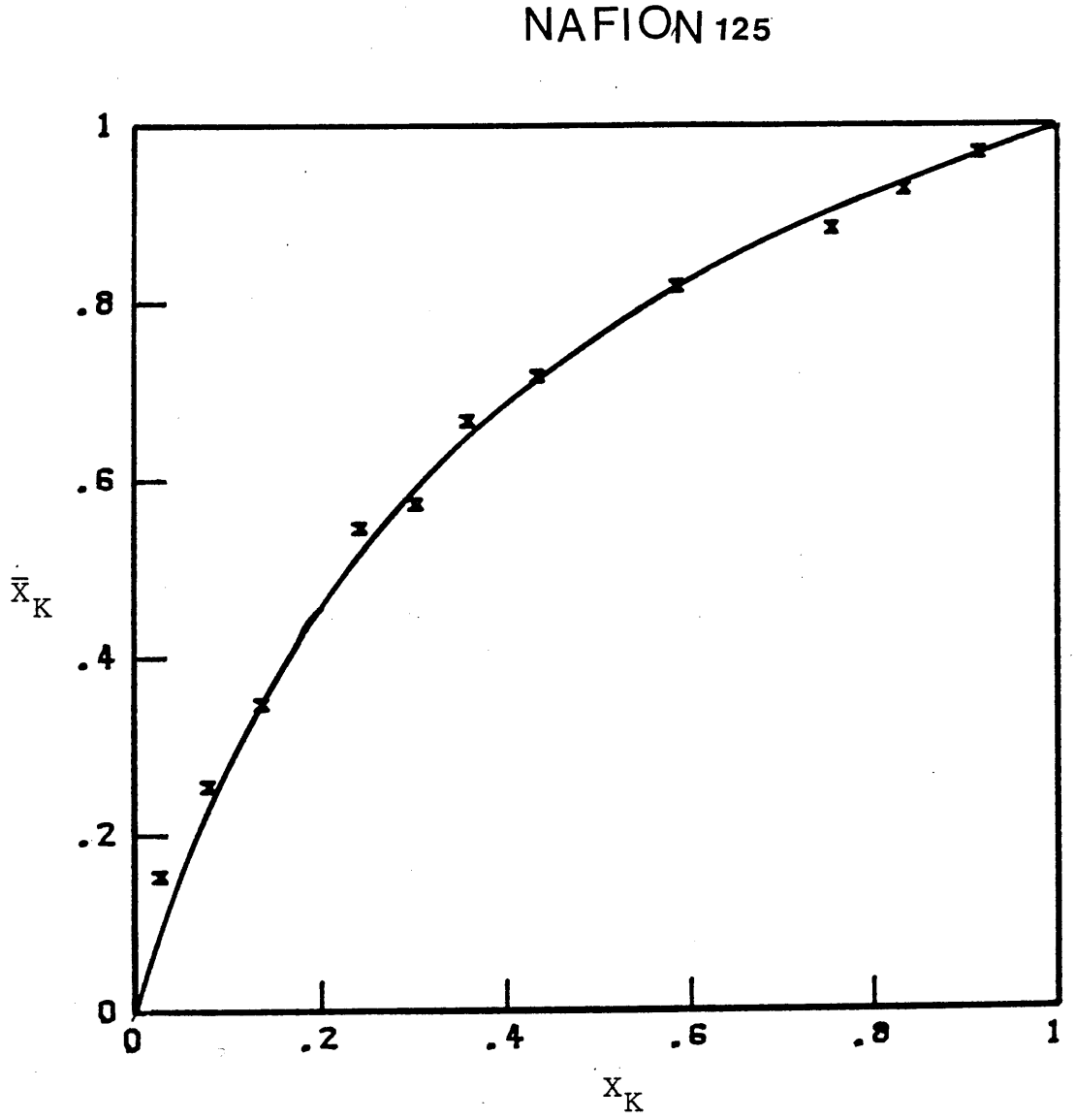
NAFION 125
1
.8
.6
.4
.2
0
$\bar{X}_K$
0
.2
.4
.6
.8
1
X_K

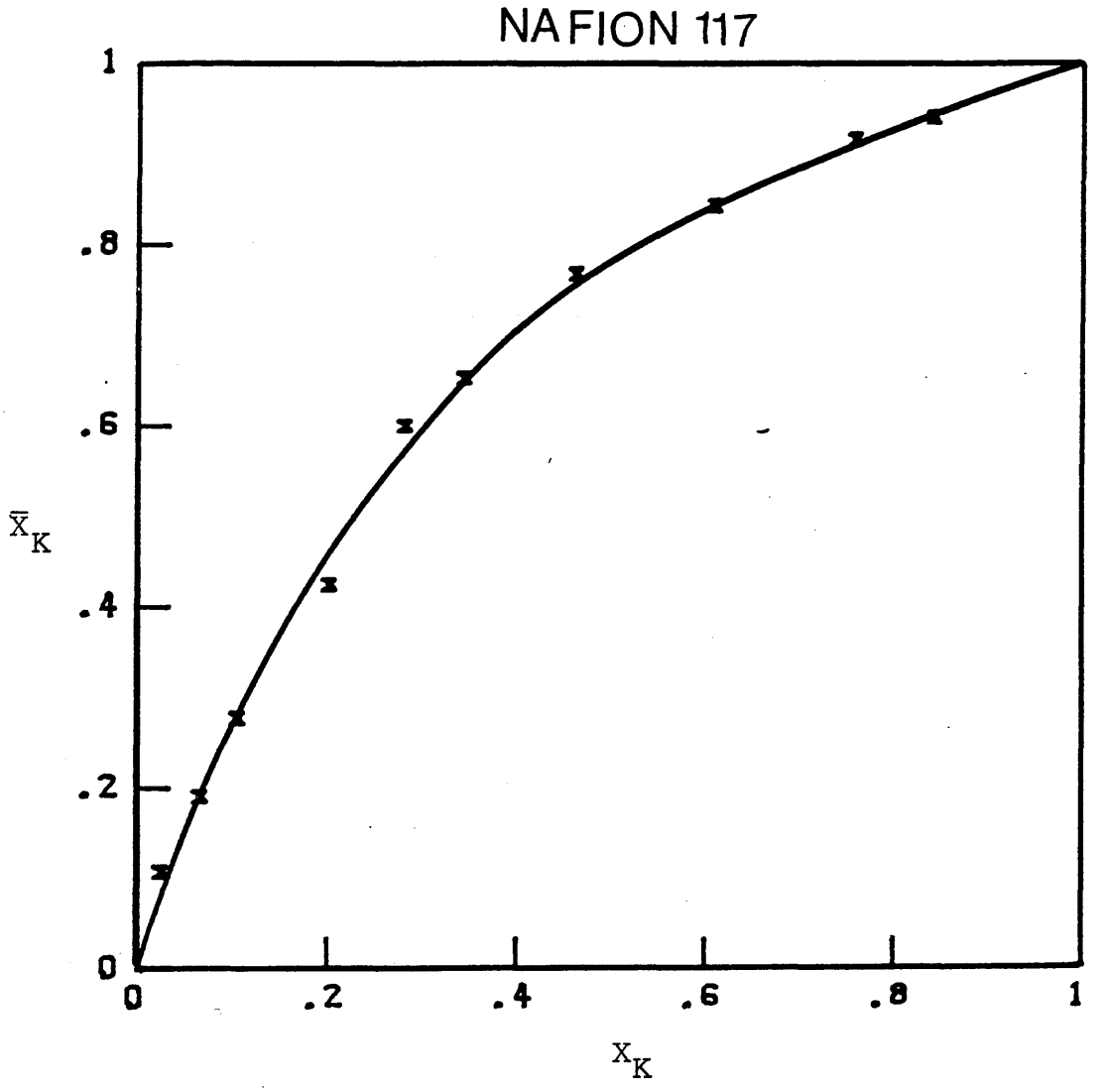
NAFION 117
1
.8
.6
.4
.2
0
$\bar{X}_K$
0
.2
.4
.6
.8
1
X_K

Figure (4-2)

Selectivity coefficients, K_H^K (eqn. 4-2) for Nafion membranes, as a function of the equivalent fraction of K^+ in solution of ($HC\ell$ + $KC\ell$) of total concentration 0.05M.

⧖ - Nafion 117 (EW 1100)

● - Nafion 125 (EW 1200)

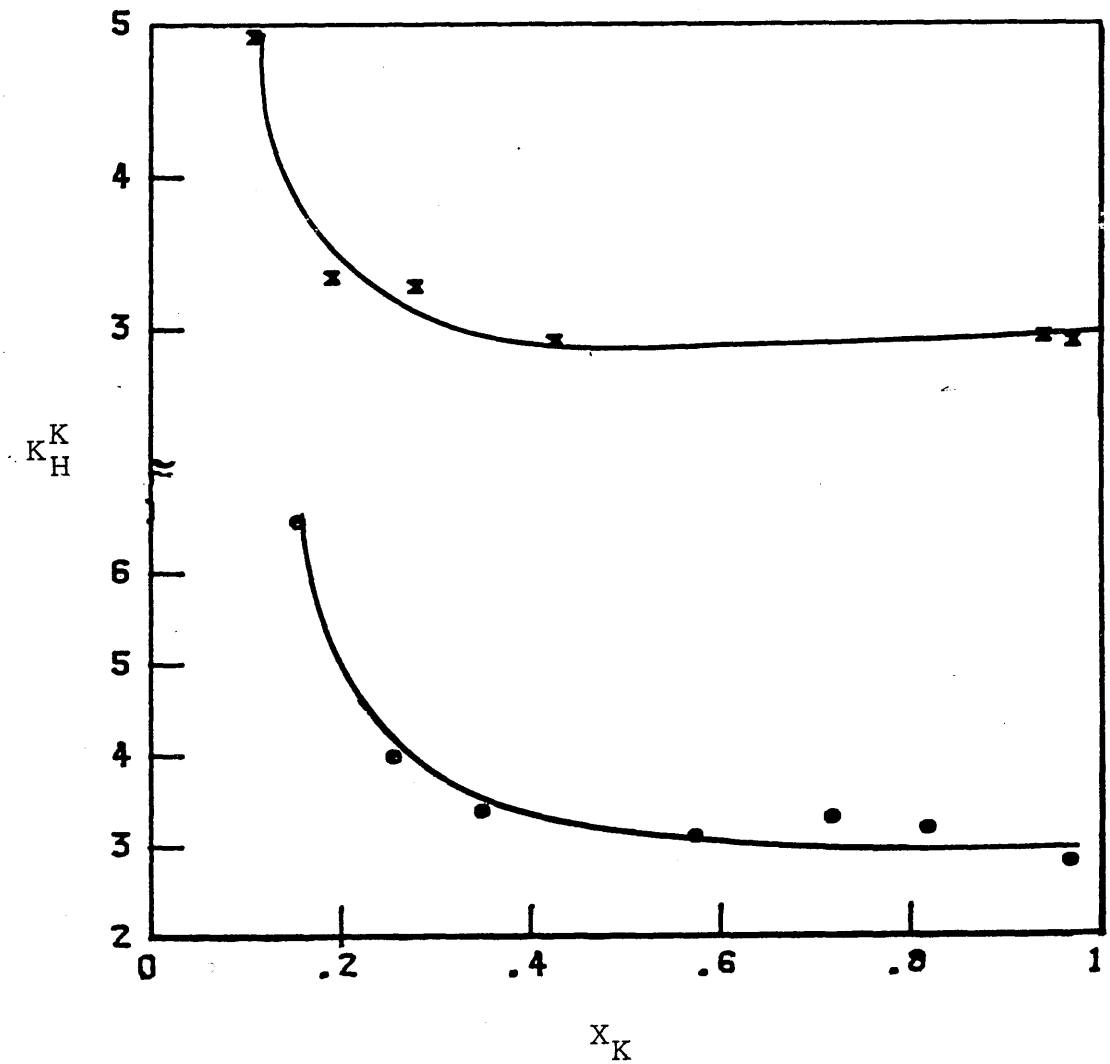
5
4
3
6
5
4
3
2
0
.2
.4
.6
.8
1
K_H^K
X_K

REFERENCES

1. O.D. Bonner, J. Phys. Chem., 59, 719 (1955).
2. H.L. Yeager and A. Steck, Anal. Chem., 51, 862 (1979).
3. D. Richenberg. In: "Ion Exchange". Ed. J. Marinsky. Marcel Dekker, New York, Vol. I, Chap. 7, 1966.
4. E. Roche, M. Pineri and R. Duplessix, J. Polym. Sci., 20, 107 (1982).
5. K.A. Mauritz, C.J. Hora and A.J. Hopfinger. In: "Ion in Polymers". Ed. A. Eisenberg. Adv. Chem. Ser. No. 107., Amer. Chem. Soc., Washington, D.C., p.198, 1980.
6. A. Eisenberg, Macromolecules, 3, 147 (1970).
7. T.D. Gierke,152nd Meeting of Electrochemical Society, Atlanta, Georgia, October, 1977.
8. W.Y. Hsu and T.D. Gierke,J. Memb. Sci., 13, 307 (1983).
9. T.D. Gierkeand W.Y. Hsu. In: "Perfluorinated Ionomer Membranes". Ed. A. Eisenberg and H.L. Yeager. Amer. Chem. Soc. Symp. Series No. 180, Am. Chem. Soc., Washington, D.C., p.283, 1982.
10. W.H. Koh and H.P. Silverman, J. Memb. Sci., 13, 279 (1983).
11. E. Högfeldt, R. Chiarizia, P.R. Danesi and V.S. Soldotov, Chemica Scripta, 18, 13 (1981).
12. G.V. Markovits and G.R. Choppin. In: "Progress in Ion Exchange and Solvent Extraction". Ed. J.A. Marinsky and Y. Marcus. Marcel Dekker, New York, Vol. 3, p.51, 1973.
13. P.R. Danesi and R. Chiarizia and G. Scibana, J. Inorg. Nuclear Chem., 35, 3926 (1973).
14. R.S. Lowry and K.A. Mauritz, J. Am. Chem. Soc., 102, 4665 (1980).

CHAPTER 5

Electrical Conductivity

5.1 INTRODUCTION

Perfluorinated ionomer membranes are widely used as separators in electrolytic and fuel cells. A primary consideration in such applications is the membrane conductivity, because ohmic losses due to membrane resistance can significantly increase energy consumption of electrolytic cells and energy loss of the fuel cell. Extensive studies of the conductivities of conventional (sulphonic acid) Nafion membranes in various industrially important electrolytes have been carried out in several laboratories in recent years. The conductivity of perfluorinated carboxylated membranes has been studied only in alkaline electrolytes because of its primary application in chlor-alkali industry.

These carboxylated polymers in the acid form are not desirable for other electrochemical applications because they have very high resistances (1) compared with Nafion membranes in SPE cells (solid polymer electrolyte) water electrolyser (2). This is primarily due to small membrane swelling and slight dissociation of the carboxylic acid group in water. The conductivity of Nafion membranes has been found to be strongly affected by the history of treatment of the membrane (3,4) and it is apparent that electrolyte uptake is an important factor in determining membrane conductivity and the voltaic efficiency of many membrane cells. The electrical conductivity of electrodialysis membranes is a fundamental property which is not constant but depends on the nature of the lesser counterion and to a lesser degree on the concentration of the solution with which the membrane is in equilibrium. To investigate this, Nafion 125 membrane (which has sulphonic acid groups) was studied in a variety of homoionic (H^+, K^+, Na^+, Li^+ and Ca^{2+}) forms

and in mixed H^+/K^+ forms over a complete range of loading. Charged membranes can include in their structure many ions or ionizable groups; one essential ionic component is chemically bound or otherwise retained by the polymeric matrix (the so-called fixed ion). The other essential ionic component is a mobile, replaceable ion (so-called counterion) which is electrostatically associated with the component. These membranes are in effect permeable only to the counterions, while resisting the direct flow of liquids and ions of opposite charge (co-ion).

Co-ion (in this case, chloride) uptake was effectively eliminated by examining the test membranes in sufficiently dilute electrolyte.

The internal ionic molalities of counterion per fixed sulphonic acid group in these Nafion 125 membranes were in the range of 4.6-7.3 mol kg^{-1} of solvent in the exchanger. They may therefore be considered to be very concentrated binary electrolytes. It should be noted that in this concentration range the average number of water molecules per ion pair of counterion and sulphonate fixed charge will be less than 12 molecules of water or less. It would be expected that the interactions between ions would be large since the membrane molalities for all but Li^+ and H^+ exceed saturation values to those of all common salts. It was expected, therefore, that water content would play an important part in determining the variation of conductivity of ion exchange membranes.

5.2 EXPERIMENTAL

The electrical conductivity of membranes may be measured in several ways; these fall in two broad categories.

The first is the direct method in which a constant voltage is applied to a strip of membrane and the current measured together with potential difference $\Delta\psi$ between two identical probe electrodes placed in a region of uniform current density, I (i/A). The electrical conductivity $\bar{\kappa}$ is calculated from the potential difference, $\Delta\psi$, the exposure area of the membrane, A, the current i, and the distance between electrodes, ℓ[5]

$$\bar{\kappa} = \frac{i\ell}{\Delta\psi A} \qquad (5\text{-}1)$$

There are several technical disadvantages to this method. These are the difficulty of overcoming the effect of interfacial resistances and the fact that the measurement is made along the length of the membrane strip, whereas most other transport measurements are made in the direction normal to the membrane surface. If the membrane is anisotropic then the results obtained by the direct method may be in error if they are used in conjunction with other properties which have been measured along different paths.

In this work an indirect method has been used for the conductance of a cell containing electrolyte, measured with and without a membrane as separator. The actual cell used in this work and in many previous studies in this laboratory[6] was constructed as described in the US manual for testing permselectivity membranes[7].

The cell, Fig. (5-1) is designed for use with membrane in dilute electrolyte. As long as the electrolyte is rather dilute ($C \ll \bar{X}$ the membrane capacity), the conductivity of the membrane which has higher ionic concentration (and is an excellent electrolytic conductor) is greater than the dilute electrolyte, there is difficulty in obtaining a precise value for the membrane conductivity. In order to increase the accuracy of the results, the cell design that the electrodes area and the electrolyte volumes have been made as large as is practicable and the exposed area of the membrane reduced to as small an area as is practicable (without measuring significant edge effect). The membrane area exposed was very small (0.0907 cm^2) compared to the whole disc area (13.85 cm^2).

When the cell had been assembled it was filled with pre-degassed solution, carefully ensuring that no air bubbles remained inside. The cell was placed in a polyethene bag, then the assembly was positioned in a thermostat water bath maintained at 25 ± 0.01°C; the bag collapsed around the cell, allowing good thermal contact, while preventing the conductivity cell from being contaminated by thermostat liquid.

The all-Perspex conductivity cell is a poor heat conductor and so although immersed in the thermostat bath as described, it would not allow efficient thermostat control of the cell solution. To overcome this difficulty and to ensure good temperature control of membrane and solution within the measurement all, the cell was connected to a thermostatted reservoir of electrolyte, Fig. (5-2), which could be trickled through the cell. The flow of the solution was stopped during measurements, which were taken at regular intervals over 90 min. Equilibrium thermal and chemical was indicated by constancy of measurement to ±0.1% otherwise the whole procedure was repeated.

To determine the electrical conductivity of a membrane in equilibrium with a particular electrolyte, the conductivity cell must be firstly used filled with electrolyte only and then the measurement of R_s.

The cell is then removed from the thermostat bath, dismantled and the test membrane, whose surface has been dried by plotting with fibre-free filter paper, placed in position. The cell is then returned to the thermostat bath and the thermal equilibrium process repeated as before. The conductivity and hence the resistance of the membrane is found by subtraction as follows:

$$R_m = R_{m+s} - R_s \qquad (5\text{-}2)$$

Conductivity $\bar{\kappa}$ of the membrane is then obtained

$$\bar{\kappa} = \frac{\ell}{A} \cdot \frac{1}{R_m} \qquad (5\text{-}3)$$

where ℓ is the membrane thickness and A the exposed area.

In the measurement of $\bar{\kappa}$ described above correction for edge effects[8] for an ℓ/A ratio of 0.2 or less is within the limits of experimental error. In this respect, membrane ℓ/A ratios smaller than 0.2 may be considered ideal in that the edge effect is negligible.

In this work Nafion 125 membrane with an ℓ/A ratio = 0.16, the edge effect may be neglected.

All measurements were made using a Wayne Kerr B331 conductivity bridge (Section 5-3) capable of accuracy of 0.01%.

5.2.1 Conductivity Bridge

Membrane conductance measurements were made using a Wayne Kerr Autobalance Precision Bridge, type B331 MKII. This instrument displayed capacitance and conductance simultaneously on two meters and six digital decades, three for capacitance and three for conductance, and allowed an accuracy of ± 0.01% to be attained. A "lead eliminator" circuit was incorporated to eliminate completely any error caused by the finite resistance of connecting leads. Measurements were made at an AC frequency of 1591.55 Hz, at which $\omega = 10^4$ rad/sec.

5.2.2 Tortuosity

A mobile species diffusing from ingoing face to outgoing face of the membrane is forced to take a path longer than the free solution path due to obstruction of the polymer segments. Attempts have been made to estimate this factor "tortuosity, Θ". There are different expressions which estimate tortuosity, Θ. Mackay and Meares,[9] on the basis of a lattice model, have calculated Θ to be Θ_m, where

$$\Theta_m = \left(\frac{2}{\bar{V}_w} - 1\right)^2 \qquad (5\text{-}4)$$

which has been widely tested. It has been found in this work, as in previous studies[6, 10] that a better correspondence between diffusion coefficients of exchanger and analogous electrolyte solutions is obtained when the tortuosity factor developed by Meares is reduced to

$$\Theta_m^* = \left(\frac{2}{\bar{V}_w} - 1\right) \tag{5-5}$$

where

$\Theta_m^* = \sqrt{\Theta_m}$, $\bar{V}_w$ = volume fraction of water in membrane

The other expression of Prager[11] provides the least arbitrary estimate of Θ, Θ_p in

$$\Theta_p = \frac{2}{\bar{V}_w} - \frac{0.5(\ln\bar{V}_w)^2}{(1 - \bar{V}_w + \bar{V}_w \ln\bar{V}_w)} \tag{5-6}$$

If $\bar{V}_w$ is close to unity only the first term $\left(\frac{2\bar{V}_{w-1}}{\bar{V}_{w+1}}\right)$ of the expansion of the series for $\ln\bar{V}_w$ need to be used. The equation now becomes

$$\Theta_p = \frac{2}{\bar{V}_w} - \frac{2}{1 + \bar{V}_w} \tag{5-7}$$

which is a form similar to eqn. (5-5) since, as $\bar{V}_w \to 1$, Θ_p leads to $\left(\frac{2}{\bar{V}_w} - 1\right)$ which is designated Θ_m^* in eqn. (5-5). Fig. (5-5) shows a plot of eqn. (5-5) and (5-6) over the range $0 \leqslant \bar{V}_w \leqslant 1$.

5.3 RESULTS AND DISCUSSION

5.3.1 Conductivity of Homoionic Forms

Electrical conductance $\bar{\kappa}$ of Nafion 125 perfluorosulphonic acid membrane (its main physical properties are given in Table (5-3)) at 25 ± 0.01°C in homoionic forms H^+, Na^+, K^+, Li^+ and Ca^{2+} are shown in Figs. (5-3a) and (5-3b) as a function of the concentration of the external solutions in which the membrane had been equilibrated. The equilibrium chloride solutions were ranged from 0.05-0.2M. Conductivity data are tabulated in Table (5-1). The overall impression is one of extreme complexity - there are no general trends. For example, in Fig. (5-3a) the H-form and K-form may be compared. The hydrogen form which has, as expected, the largest conductance after an initial drop in conductivity, shows a pronounced minimum in 0.1M HCℓ. Thereafter, an increase in the conductivity of the membrane is observed. The K-form on the other hand, has a conductance ten times smaller, but which decreases relatively little with change in equilibrating KCℓ concentration over the same range.

This overall impression of complexity is measured by observing the corresponding variations in the conductivity of other ionic forms: Na^+, Li^+ and Ca^{2+} forms are shown together with K^+ data of Fig. (5-3a) in Fig. (5-3b). Again we see that while the conductivity of Na^+ and Li^+ forms rise steeply with increased external solutions, conductivity of the calcium form increases also, but linearly.

On increasing the external electrolyte concentration, the Donnan uptake of electrolyte will increase which, accompanied with an

increase in the ionic concentration within the membrane, would be expected to increase the conductance. In some cases, however, the effect is reduced or even reversed by the (osmotic) shrinkage of the membrane phase in more concentrated electrolytes. Both effects are seen here in this membrane system.

One possible explanation which can be given for the observed trends in the conductivity is that the membrane swelling may have a particularly important effect in these perfluorosulphonic acid membranes, since they are known to have an island structure of sulphonic micelles in their less swollen forms.

The behaviour has already been observed[12] for Nafion 125 in homoionic forms in alkali (LiOH, KOH and NaOH). Those results are consistent with the above interpretation of results obtained with chloride salts in this work.

In other studies the conductivities of Nafion 125 were measured[13] in $NiC\ell_2$ and $NaC\ell$ solutions at different electrolyte concentrations. The conductivities of the membrane changed with electrolyte concentration but were higher in $NiC\ell_2$ solutions than in $NaC\ell$ solutions of comparable concentration. This is due to the smaller affinity of nickel ion for the charged sulphonic acid of the polyelectrolyte skeleton. Also the conductivity of Nafion 120 (1200 EW) was measured[14] at different $NaC\ell$ concentrations and it was found to increase rather steeply with increasing molalities of external solution as a result of increasing Donnan uptake of the salt.

The conductivities of Nafion 125 membrane in mixed H^+/K^+ forms were measured over a complete range of concentrations, Table (5-2). Conductivity, $\bar{\kappa}$, is shown as a function of ionic loading $\bar{X}_K$ ($=1-\bar{X}_H$) in Fig. (5-4).

5.3.2 Conductivity of mixed H^+/K^+ forms

The conductivity falls from 42.04×10^{-3} ohm^{-1} cm^{-1} for pure hydrogen form to 5.47×10^{-3} ohm^{-1} cm^{-1} for pure potassium form.

The ratio of these two conductivities is 8/1, which is somewhat larger than the similarity to the ratio of their mobilities in free solution. The conductivity of the mixed H^+/K^+ forms decreases as H^+ is replaced by K^+ and shows pronounced minimum with a slight rise in conductivity in the last few percent loading to pure K-form.

The linear curve, Fig. (5-4a) is that predicted by a simple mixture rule

$$\bar{\kappa}_{HK} = \bar{X}_H \bar{\kappa}^o_H + \bar{X}_K \bar{\kappa}^o_K \qquad (5\text{-}8)$$

and, by comparison, illustrates the very large negative deviations of the experimental data.

Such deviations have been observed before for Ca^2/Na^+ exchange on AMF C_{60} polystyrene sulphonic acid membranes.[6] They are observed also, but only to a much lesser degree, in concentrated salt mixtures in free solution in water.[15]

For Ca^{2+}/Na^+ exchange and for free salt solutions the effect is explained by the contribution of cation-to-cation coupling.[6] Miller

gave a number of precise measurements of these coupling coefficients, and showed that they could be predicted from the binary solution data (for coupling coefficients) with reasonable accuracy, using his own empirical relationships. Paterson reshaped these methods and applied them with success to the AMF C_{60} membrane[6] and successfully predicted the large negative deviations in the Ca^{2+}/Na^{+} exchange data on that membrane.

The application to the membranes involved the basic assumption that the mixture rule, eqn (5-8) applies to the direct mobility coefficients and that cation-to-cation coupling coefficients follow Miller's rules, transposed to a membrane-fixed (that is, an ion-fixed) frame of reference for flows.

A similar analysis was applied to these measurements. Insufficient data were available to make a complete analysis. Within the terms of the above method, the analysis was applied, but only to assess the deviations, due to coupling between H^{+} and K^{+} when their coupling coefficient in the membrane was at its maximum value at each composition. Any coupling coefficient L_{ik} may be positive or negative but is restricted in its magnitude by the laws of thermodynamics, such that

$$(L_{ik})^2 \leqslant L_{ii} L_{kk}$$

The square of the coupling coefficient must be lesser than or equal to the product of the direct mobility coefficients.

This requirement follows from the fact that the rate of production of entropy must be positive for a spontaneous (irreversible) process.

With this assumption of maximum coupling and application of the mixture rule to predict the direct coefficients, the conductivity of mixed ionic forms was predictable. Used with H^+/K^+ data, it gave a very reasonable prediction of the observed trends in the conductivity including a minimum in the curve, Fig. (5-4b). These predictions show deviations from the 'mixture rule' which are somewhat larger than observed as might be expected, since this is an estimate based upon a maximum coupling model. These calculations also made allowance for the very large changes in water content, and so included the changes in the tortuosity of the membrane phase as it was converted from H- to K-forms. This analysis therefore appeared both plausible and successful.

Transport numbers for H^+ and K^+ were obtained from bi-ionic potential measurements in Chapter 6. Direct experimental evidence was obtained there which showed that the H^+ and K^+ when each at 50% loading, had equal transport numbers:

$$\bar{t}_H = \bar{t}_K = 0.5$$

This remarkable and well substantiated result is discussed in detail in Chapter 6. It shows, however, that the basic assumption of the modified 'mixture rule' can not apply to Nafion membranes since the two ions H^+ and K^+, which have mobilities separated by almost one order of magnitude in solution, have equal mobilities in the membrane (at least

at 50/50 loading of H^+/K^+). Using irreversible thermodynamics, the transport numbers for H^+ and K^+ in the mixed forms are given by eqns. (2-21,22)

$$\bar{t}_H = \frac{L_{HH} + L_{HK}}{\alpha}$$

and

$$\bar{t}_K = \frac{L_{KK} + L_{HK}}{\alpha}$$

where $\alpha = \kappa/F^2$, eqn. (2-19) and $L_{HK} = L_{KH}$ by the Onsager reciprocal relationship. It is obvious therefore that the direct mobilities of H^+ and K^+ ions in the 50/50 mixed form are equal:

$$L_{HH} = L_{KK}$$

This precludes any possibility that we used the mixture to calculate L_{HH} and L_{KK} as in the model outlined above.

In that model the mobilities L_{HH} and L_{KK} are presumed to be proportional to their mole fractions, such that

$$L_{HH} = \bar{X}_H L^o_{HH} = \bar{X}_H \kappa_H/F^2$$

$$L_{KK} = \bar{X}_K L^o_{KK} = \bar{X}_K \kappa_K/F^2$$

where L^o_{HH} and L^o_{KK} are the mobilities of H^+ and K^+ in the pure homoionic membranes.

Although this calculation was further refined to include the scaling effects of changing tortuosity, it nevertheless remains obvious that L_{HH} and L_{KK} can never be equal. If a mixture rule applied, even approximately to the Nafion membrane.

The fact that it holds for AMF C_{60} membranes (for which a complete set of data was available) but not for Nafion membranes, suggests that they are very different in ionic transport mechanisms. Their water content is much lower in Nafion membranes which would make them less like ionic solutions. More important, however, is the 'island' structure or micelle structure which has been proposed by many workers[17,18,19] The membrane may therefore consist of a dispersion of highly concentrated electrolyte confined to island micelles in the polymer, with, largely or completely uncharged and unhydrated regions between. The conversion from H-form to K-form expels water from possibly increasing the effect. The current controlling step would therefore be transport of ions through largely uncharged, unhydrated regions, for which little information is available. Further work to resolve this mechanism is being considered.

The exercise was, however, a useful one, showing that a 'good-fit' does not necessarily signify a good explanation, especially if the test is based on a limited set of experimental measurements. This is particularly true of membrane studies.

Table (5-1)

Electrical conductivity $\kappa \times 10^3$ ($ohm^{-1}\ cm^{-1}$) of homoionic forms of Nafion 125 membrane at 25 ± 0.01°C in solutions of the corresponding chloride electrolyte at the concentrations given.

Ionic Forms / C(mol/L)	H^+	Li^+	Na^+	K^+	Ca^{2+}
0.025	-	-	-	-	1.251
0.05	59.88	2.048	4.371	5.588	1.491
0.10	42.04	3.818	7.160	5.466	2.027
0.20	46.77	4.799	7.304	5.356	-

Table (5-2)

Conductivities of mixed K^+/H^+ forms of Nafion 125 membrane at 0.1M ionic strength.

Ionic compositions				Electrical conductivity $\kappa \times 10^3$ $ohm^{-1}.cm^{-1}$
solution		membrane		
X_H	X_K	$\bar{X}_H$	$\bar{X}_K$	
0	1	0	1	5.47
0.08477	0.91522	0.0322	0.9678	1.72
0.2449	0.7551	0.1166	0.8834	2.34
0.4140	0.5860	0.1818	0.8182	3.70
0.5660	0.4340	0.2834	0.7166	5.25
0.6982	0.3018	0.4268	0.5732	17.69
1	0	1	0	42.04

X: ionic fraction in solution

$\bar{X}$: ionic fraction in membrane

Table (5-3)

Physical characteristics of Nafion 125 membrane at different loading of H^+/K^+ form. Equilibrating in 0.1M total concentration.

Capacity = 0.2364 mmol/disc

Dry weight = 0.3045gm

Physical Parameters \ X_H	0	0.10	0.30	0.50	0.70	0.90	1.00
Wet wt. of the disc (gm)	0.3369	0.3387	0.3411	0.3429	0.3454	0.3457	0.3548
Wt. of H_2O/ disc (gm)	0.0323	0.0342	0.0366	0.0384	0.0409	0.0412	0.0503
$\bar{d}$(gm/cm^3)	1.0014	1.0022	1.0019	1.0016	1.0013	1.0010	0.9987
$\bar{V}$(cm^3)	0.1623	0.1609	0.1605	0.1584	0.1586	0.1564	0.1589
$\bar{V}_w$	0.1991	0.2125	0.2279	0.2423	0.2577	0.2634	0.3165
m(molal /kg of pore H_2O)	7.3189	6.9122	6.4590	6.1563	5.7799	5.7378	4.6998
$\theta_m^* = (\frac{2}{\bar{V}_w} - 1)$	9.045	8.4118	7.7750	7.2522	6.7595	6.5930	5.3191
$\theta_m = (\frac{2}{\bar{V}_w} - 1)^2$	81.8157	70.7578	60.4510	52.5944	45.6903	43.4678	28.2930
$\theta_p^{**} =$	8.8847	8.3376	7.7892	7.3400	6.9176	6.7751	5.6874

* reference (9).

** reference (11)

Figure (5-1)

Conductivity cell

Legend

A	solution in
B	solution out
E	electrodes
M	membrane
S	solution chamber

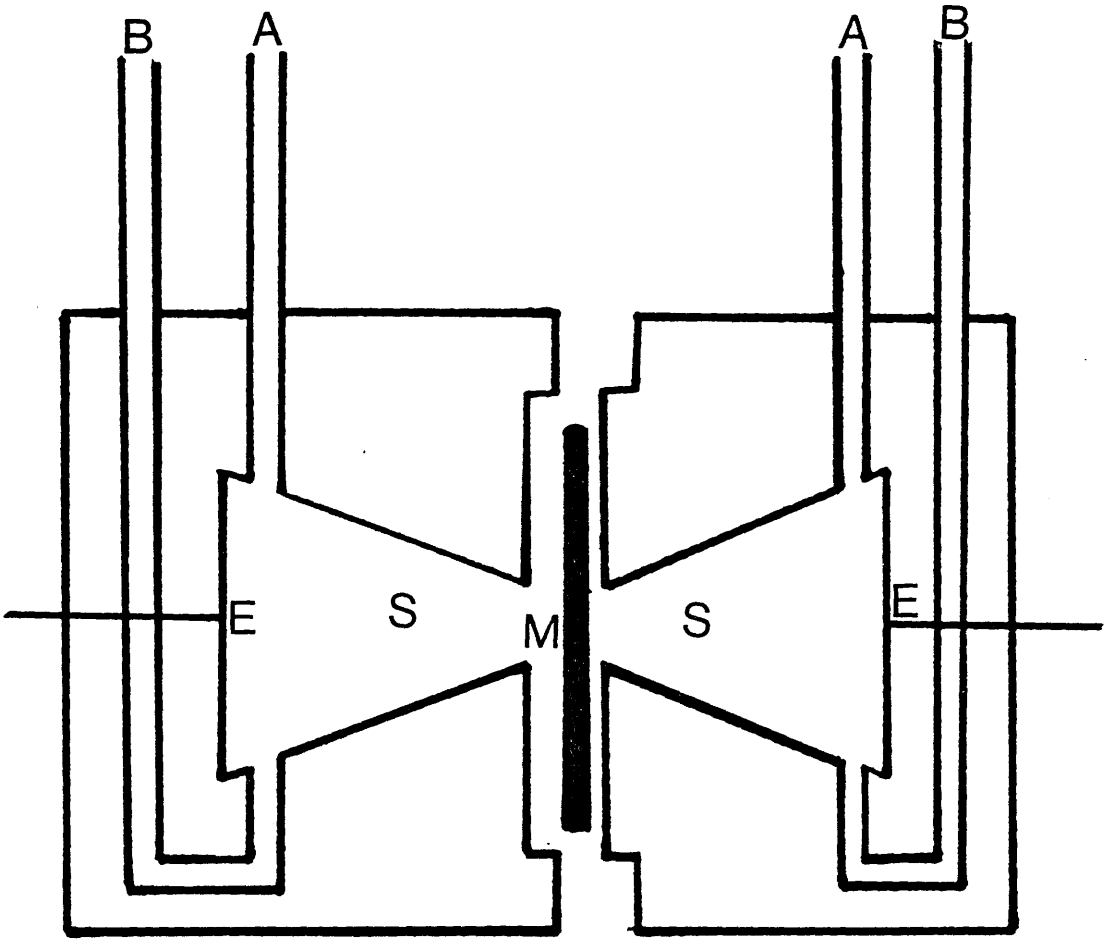
B
A
A
B
E
S
M
S
E

Figure (5-2)

Legend	
Th	thermometer
dw	double wall glass
WI	water in
WO	water out
sd	solution delivered
A and B	screw caps

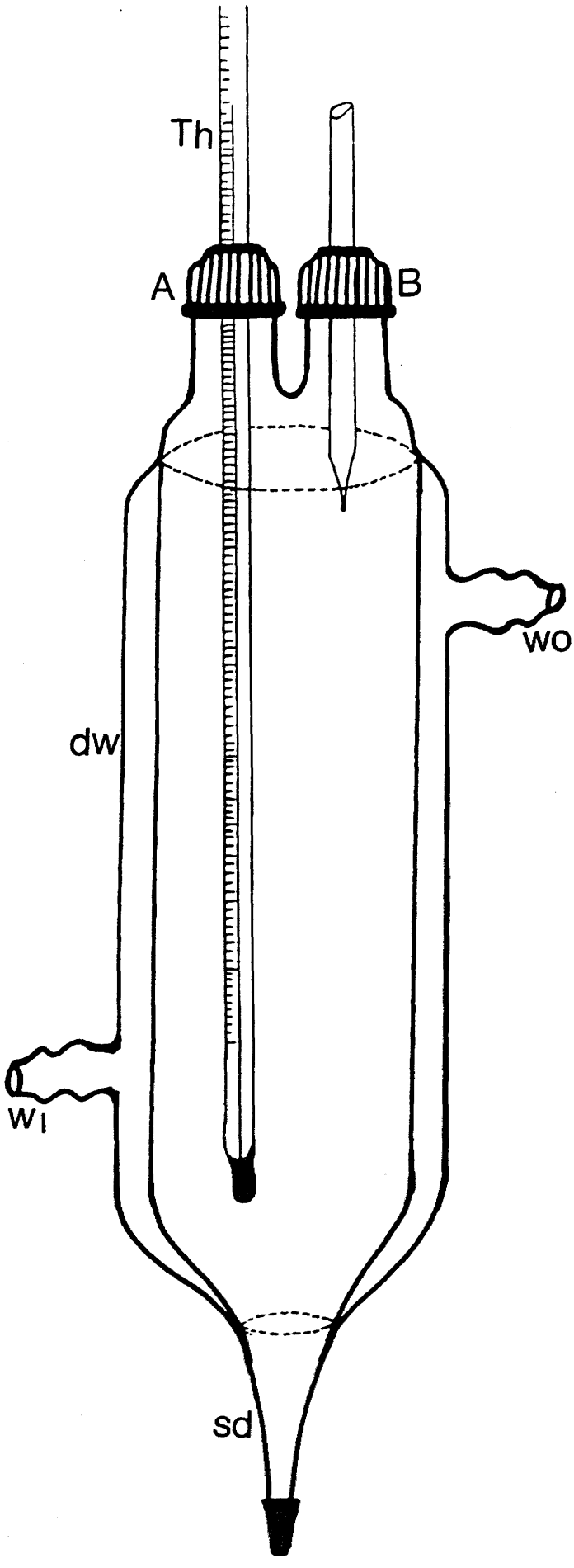
Th
A
B
wo
dw
wi
sd

Figure (5-3a)

Electrical conductance $\bar{\kappa}$ ohm^{-1} cm^{-1} of Nafion 125 membrane in hydrogen and potassium forms at 25 ± 0.01°C as a function of concentration of equilibrating solution of HCℓ or KCℓ respectively in mole/L.

⊙ - H^+ form and ● - K^+ form

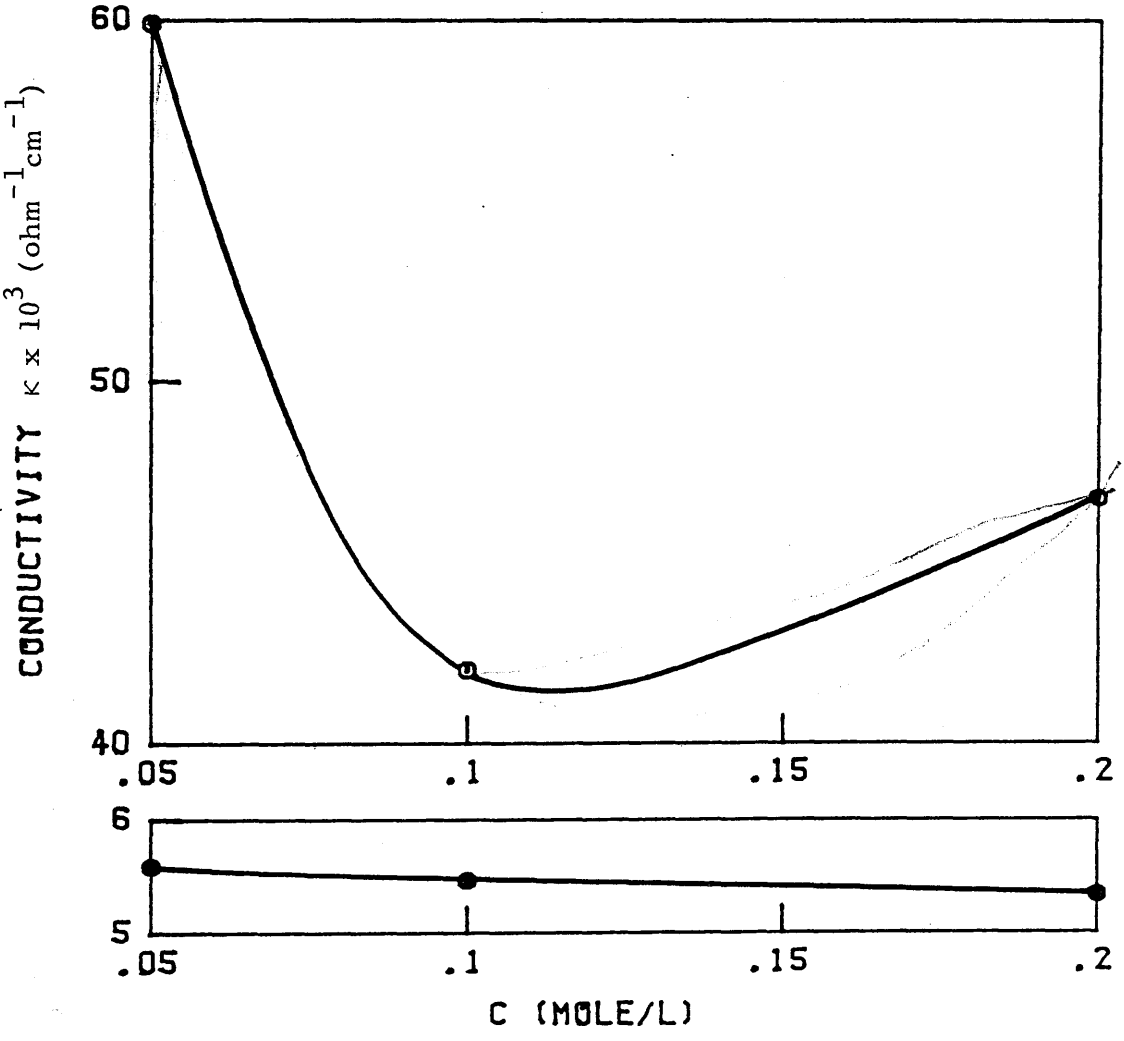
60
50
40
CONDUCTIVITY κ x 10^3 (ohm^-1 cm^-1)
.05
.1
.15
.2
6
5
.05
.1
.15
.2
C (MOLE/L)

Figure (5-3b)

Electrical conductance $\bar{\kappa}$ ohm^{-1} cm^{-1} of Nafion 125 at 25 ± 0.01°C as functions of the concentrations of equilibrating chloride solutions in mole/L:-

● - K^+ form, X - Na^+ form, ▲ - Li^+ form and ⊡ - Ca^{2+} form

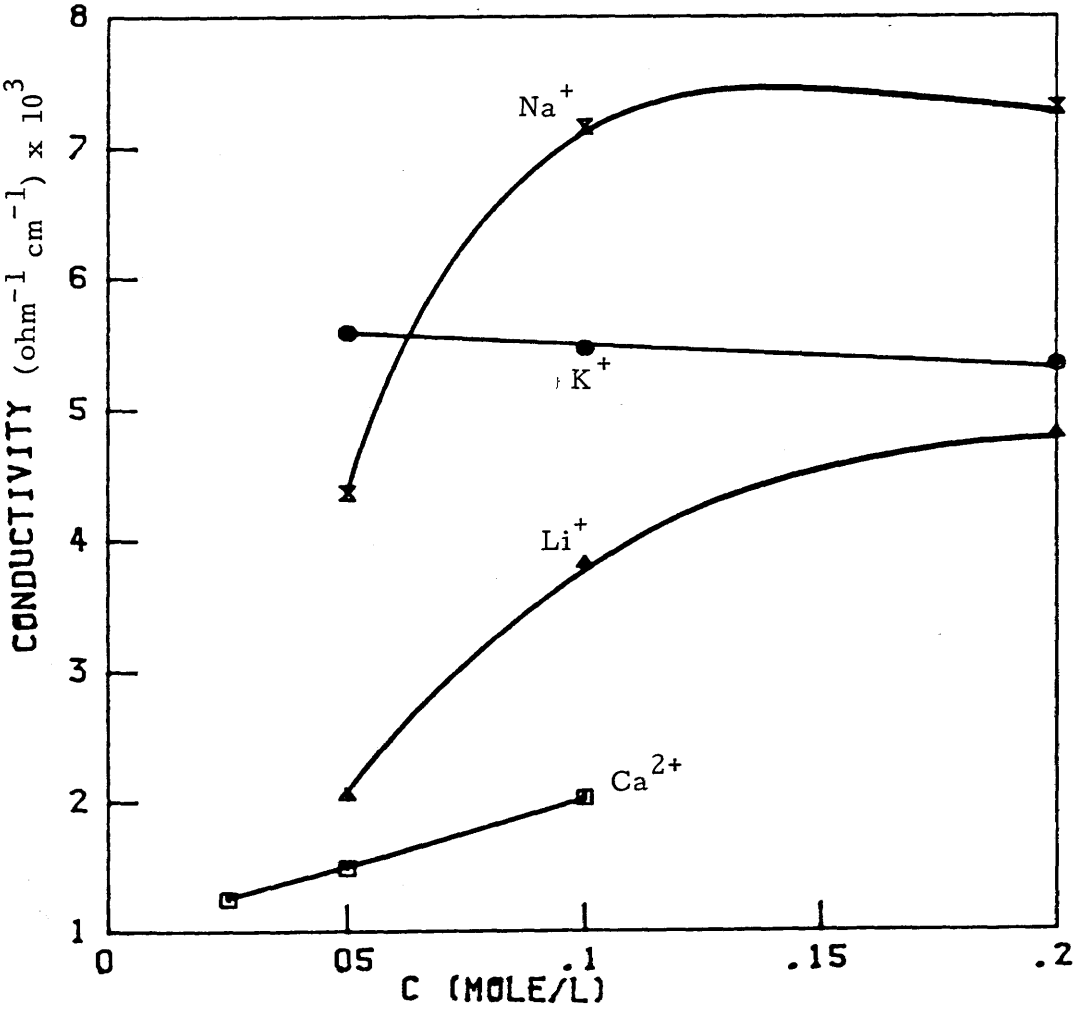
CONDUCTIVITY (ohm^{-1} cm^{-1}) x 10^3
8
7
6
5
4
3
2
1
0
05
.1
.15
.2
C (MOLE/L)
Na$^+$
K$^+$
Li$^+$
Ca^{2+}

Figure (5-4a)

Conductance $\bar{\kappa}$ ohm^{-1} cm^{-1} of Nafion 125 in mixed H^+/K^+ forms at 25 ± 0.01°C as a function of equivalent fraction of K^+ in the membrane, $\bar{X}_K$.

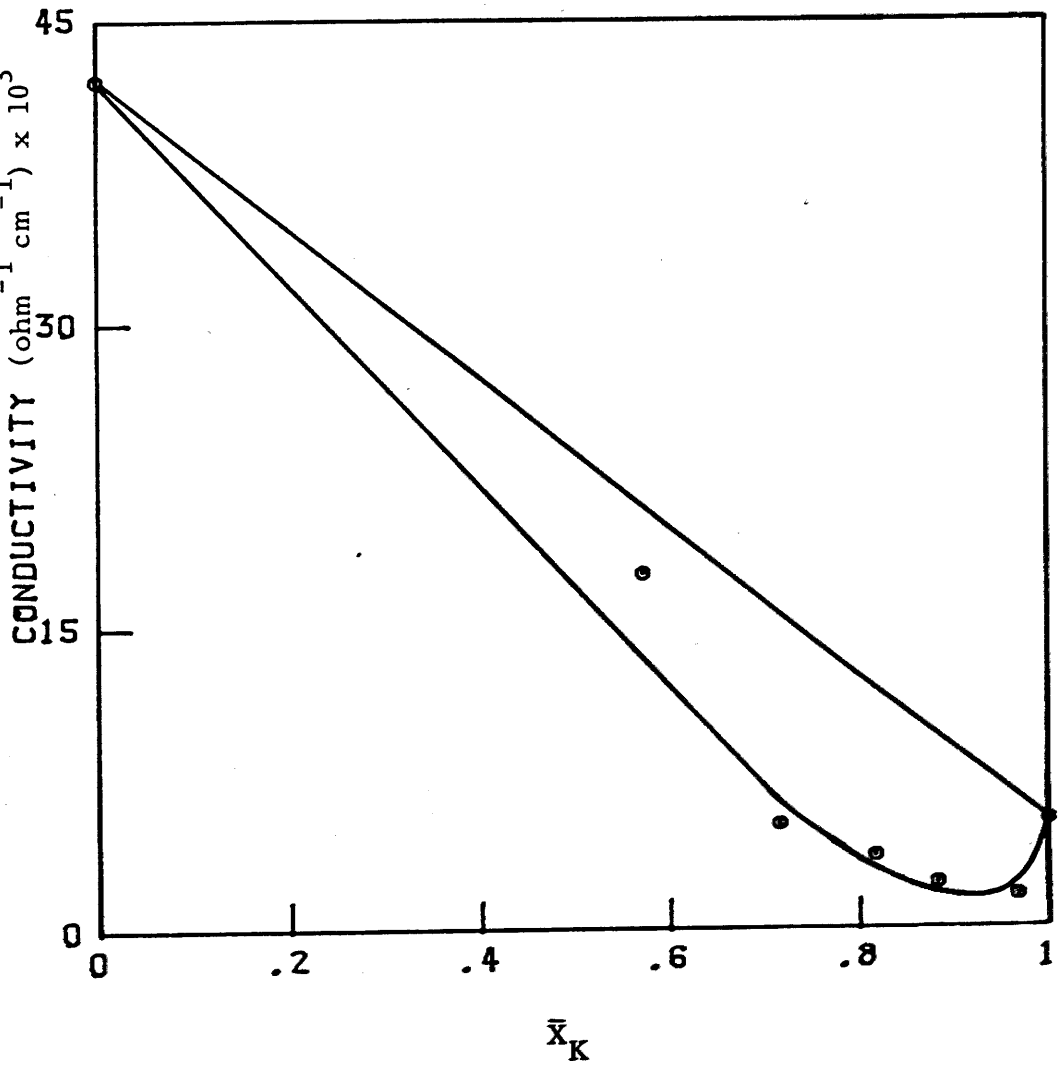
45
30
15
0
CONDUCTIVITY (ohm^{-1} cm^{-1}) x 10^3
0
.2
.4
.6
.8
1
$\bar{x}_K$

Figure (5-4b)

Electrical conductivity $ohm^{-1}\ cm^{-1}$

o experimental data

— in the absence of coupling

x estimate for maximum coupling made with omitting tortuosity

■ estimate for maximum coupling made by inclusion of tortuosity

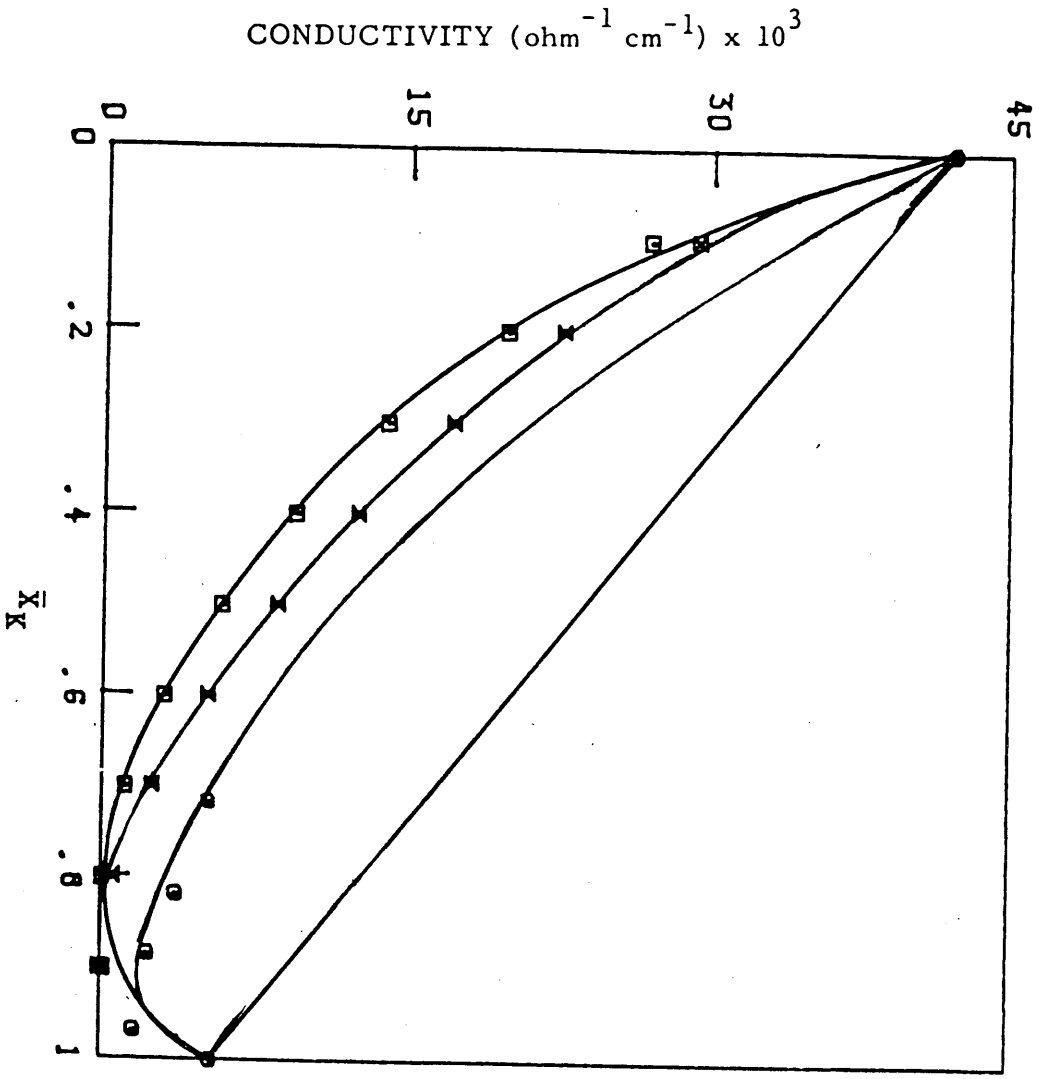
CONDUCTIVITY (ohm^{-1} cm^{-1}) x 10^3
0
15
30
45
0
.2
.4
.6
.8
1
$\frac{X}{K}$

Figure (5-5)

Tortuosity factor, Θ, plotted against the volume fraction of water '$\bar{V}_w$' in the Nafion 125 membrane.

⊙ - Meares Θ^*_m eqn. (5-5)

⧗ - Prager Θ_p eqn. (5-6)

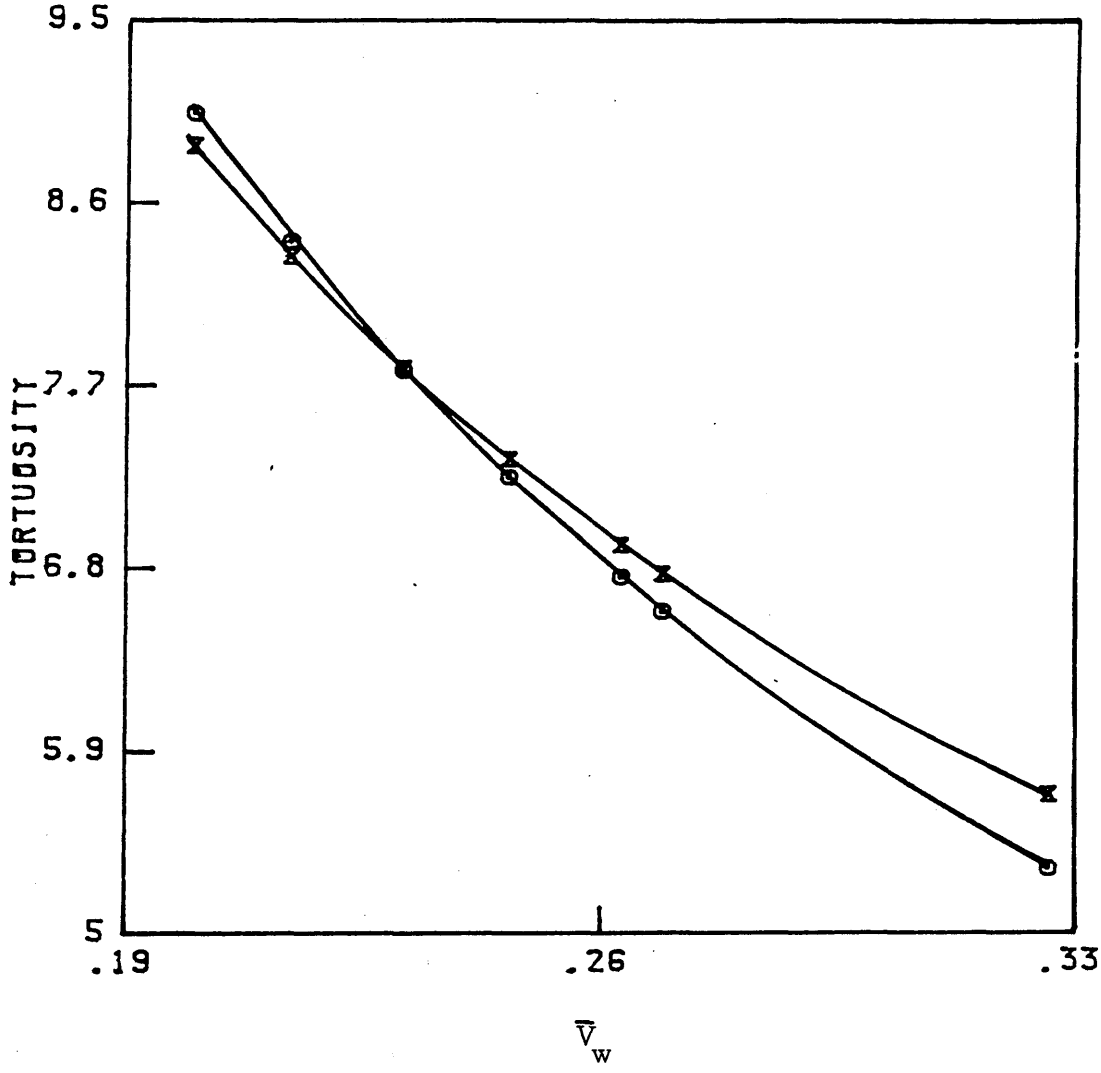
9.5
8.6
7.7
6.8
5.9
5
TORTUOSITY
.19
.26
.33
$\bar{V}_w$

REFERENCES

1. R.S. Yeo, S.F. Chan and J. Lee, J. Membrane Sci., 9, 273 (1981).
2. B.V. Tilak, P.W.T. Lu, J.E. Colman and S. Srinivasan. In: Comprehensive Treatise on Electrochemistry, Ed. O'M. Bockris, B.E. Conway, E.B. Yeager and R.E. White, Plenum Press, New York, p.1, Vol. 2, (1981).
3. R.S. Yeo and J. McBreen, J. Electrochem. Soc., 126, 1682 (1979).
4. R.S. Yeo and D.T. Chin, "ibid", 127, 549 (1980).
5. J.W. Lorimer, Discussion Faraday Soc., 21, 198 (1956).
6. R. Paterson, Pont. Acad. Sci. Scripta Varia, 40, 524 (1976).
7. 'Testing Manual for Permselective Membranes', U.S. Office of Saline Water Research, Report No. 77, January, 1964, P.B. 181575.
8. R.M. Barrer, J.A. Barrie and M.G. Rogers, Trans. Faraday Soc., 58, 2473 (1962).
9. J.S. Mackie and P. Meares, Proc. R. Soc. London, A234, 498 (1955).
10. H. Ferguson, G.R. Gardner and R. Paterson, J. Chem. Soc. Faraday I, 68, 2021 (1972).
11. S. Prager, J. Chem. Phys., 33, 122 (1960).
12. G. Sibona, C. Fabiani and B. Scuppa, J. Membrane Sci., 16, 37 (1983).
13. G. Fabiani, M. Defrancesco and L. Bimbi in: Ion Exchange Technology, Eds. D. Naden and M. Street, Ellis Horwood, Chichester, p.226 (1984). Proceedings of Soc. Chem. Ind. Conference, "IEX '84", Cambridge, England.
14. A. Narebska, S. Koter and W. Kujawski, J. Membrane Sci., 25, 153 (1985).
15. D.G. Miller, J. Phys. Chem., 71, 616 (1967).

16. S. Bonotto and E.F. Bonner, Macromolecules, 1, 510 (1968).

17. A. Eisenberg, "ibid", 3, 147 (1970).

18. R.S. Yeo and A. Eisenberg, Polym. Prepar., 16, 104 (1975).

CHAPTER 6

Single and Bi-ionic Membrane Potentials

6.1 INTRODUCTION

An electrical potential is developed when a membrane separates two ionic solutions which differ in composition and/or concentration. The resulting membrane potential may be used to determine the transport numbers of the ions in the membrane phase.

In this work the primary requirement was to study the bi-ionic membrane potentials developed when the membrane separated solutions of H^+/K^+ of differing composition.

Sollner[1,2] first showed that the bi-ionic potential (B.I.P.) was a function of the composition of exchanger and hence depended upon its selectivity as well as (more obviously) on the differing mobilities of the component ions. This now appears an obvious conclusion since the condition for steady state diffusion of ions across a membrane requires that there will be no electrical current, eqn. (6-1)

$$I = \sum_{i=1}^{n} z_i J_i F = 0 \qquad \text{for all ions, } i \tag{6-1}$$

where z_i, J_i are the signed valencies and flows, respectively. Since membrane flows may be expressed as a product of local concentration and ionic velocity, $J_i = \bar{c}_i V_i$, it is obvious that composition must play a major role, as Sollner observed.

Since our interests lay in comparing mobilities of the ions K^+ and H^+ in mixed forms of Nafion and other membranes, the B.I.P.s were measured for systems in which the membrane was $\bar{5}0/\bar{5}0$ in each ion ($\bar{X}_K = \bar{X}_H = 0.5$). The selectivity data of Chapter 4 showed that this composition would be obtained for a solution 0.01215M KCℓ, 0.03785M

HCℓ with total ionic strength 0.05M.

As before, this ionic strength was used as a working compromise to allow minimal co-ion (chloride) uptake and yet did not involve any other major side effects, such as in the measurement of conductivity, where membrane resistances in very dilute solutions posed problems or in diffusion where film diffusion effects might become significant and troublesome.

The interdiffusion of ions across charged membranes is usually much faster than salt or electrolyte diffusion and so such film effects would be expected to pose problems in this work unless dealt with by careful design of experiments (see Chapter 7).

Unstirred films at solid/liquid interfaces are unavoidable[3] and to minimise their effects it is usual to stir the solution phases vigorously. If this stirring is well defined hydrodynamically, even small residual effects of unstirred layers on transport and electrical potential measurements may be corrected by calculation.

Professor J.W. Lorimer has developed a new theoretical treatment based upon 'flowing junction' cells in which a jet of solution impinges on each side of the test membrane. Professor Lorimer's experimental verification of these theories was incomplete[4] when he visited the laboratory on Sabbatical leave. During this research, while he was in Glasgow, a new cell was designed and tested (most successfully) using single electrolytes and was later used for bi-ionic potential studies.

The value of these B.I.P. studies in understanding the behaviour and performance of Nafion membranes lay in the analysis of

the resulting transport numbers (and mobilities) of the hydrogen and potassium ions, $\bar{5}0/\bar{5}0$ in membrane ($\bar{X}_K = \bar{X}_H = 0.5$). Time did not allow analysis of the correlation of composition and transport number for the H^+/K^+ system over the complete range of loadings but the results of the $\bar{5}0/\bar{5}0$ system are strikingly unusual and suggest that such studies would be profitable.

The new membrane cell was used to study the H^+/K^+ system of B.I.P. centered on measurements in which one of the two solutions used was always that which created a $\bar{5}0/\bar{5}0$ composition in the membrane surface in contact with it. The other solutions, which need to be different from this reference, in order to obtain measured potentials, were those which generated membrane (surface) compositions, 100/0, 80/20, 60/40, 40/60, 20/80 and 0/100.

The membrane compositions are expressed as percent H^+ to percent K^+ in the membrane and later from the selectivity data of Chapter 4.

In all cases solutions with total ionic strength of 0.05M were used at 25 ± 0.01°C.

6.2 Theory

In some studies the 'membrane potential' is measured using two calomel (or similar) reference electrodes placed in the electrolytes diffusing across the membrane. The EMF of such a cell is sometimes defined by experimentalists as the 'membrane potential' since it is assumed that there is negligible differences in liquid junction potentials created at the reference electrodes in each half-cell.

There are fundamental objections to this, since by arbitrary assumption, membrane potentials are no more experimentally measurable than single electrode potentials are. It is, however, often a practical and seemingly reasonable (if arbitrary) definition of measurable membrane potentials.

In this work however, H^+/K^+ solutions of widely differing compositions were used in the B.I.P. studies and the assumption that the liquid junction potentials of calomel reference electrodes (with KCℓ salt bridges) are negligible would certainly cause large errors.

To avoid such problems, as in earlier studies [5,6] the EMF of the silver/silver chloride concentration cell was measured and used for a test of the diffusion film correction technique and to estimate transport numbers. This same set-up was used to determine the transport numbers of H^+ and K^+ in mixed ionic forms.

'Ag/AgCℓ|solution'|'membrane"|solution"|AgCℓ/Ag"

6.2.1 Single ion potentials

In the absence of unstirred layers in the solution phase the EMF of this cell, which is the difference in electrode potential, E, between electrode' and electrode" is $\psi'_{Ag}-\psi''_{Ag}$ (V) and is directly measurable.

$$E = (\psi'_{Ag}-\psi''_{Ag})=(\psi'_{Ag}-\psi'_{s})+(\psi'_{s}-\psi'_{m})+(\psi'_{m}-\psi''_{m})+(\psi''_{m}-\psi''_{s})+(\psi''_{s}-\psi''_{Ag}) \quad (6\text{-}2)$$

It may be identical, e.g. the algebraic of five electrical potentials.

$(\psi'_{Ag}-\psi'_s)$ and $(\psi''_{Ag}-\psi''_s)$ are the single electrode potentials of the silver/silver chloride electrodes where

$$(\psi^*_{Ag}-\psi^*_s) = E^\circ - K \ln a_{C\ell}{}^* \qquad (6\text{-}3)$$

where K = RT/F and the symbol * = ' or ".

$(\psi'_m-\psi'_s)$ and $(\psi''_m-\psi''_s)$ are the Donnan potentials between the membrane and its contact solutions at side ' and side " respectively. It is then easily shown that

$$(\psi^*_m-\psi^*_s) = - K \ln \left(\frac{\bar{a}_i}{a_i}\right)^{1/z_i} \qquad (6\text{-}4)$$

where $\bar{a}_i$ and a_i are the activities of ions involved in the equilibria, in this case, chloride and the single counterion. For B.I.P.s the two counterions, H^+ and K^+ (and $C\ell^-$) are represented. The remaining potential $(\psi'_m-\psi''_m)$ is the diffusion potential across the membrane and it is easily shown[6] that the potential is given by extended Henderson equation, quite analogous to that used to describe liquid junction potentials, eqn. (6-5), (see Chapter 2 for method of derivation).

$$(\psi'_m-\psi''_m) = \sum_{\text{all ions}} \int_{'}^{''} \frac{\bar{t}_i}{z_i} K \, d(\ln \bar{a}_i) + \int_{'}^{''} \bar{t}_3 \, K \, d(\ln \bar{a}_3) \qquad (6\text{-}5)$$

where K = RT/F.

The activities with barred superscripts refer to the membrane phase and the integration is taken across the membrane from one side

(side ') to the other (side "). $\bar{t}_i$ are ionic transport numbers, while $\bar{t}_3$ represents the transference number for water species 3.

In common with normal electrochemical procedures it is usual to define integral transport numbers $\bar{T}_i$ across the membrane, such that eqn. (6-5) becomes

$$(\psi'_m - \psi''_m) = \sum_{\text{all ions}} \frac{\bar{T}_i}{z_i} K \ell n \left(\frac{\bar{a}_i''}{\bar{a}_i'}\right) + \bar{T}_3 K \ell n \left(\frac{\bar{a}_3''}{\bar{a}_3'}\right) \qquad (6\text{-}6)$$

where $\bar{T}_3$ is the corresponding water transference number.

For a simple electrolyte $MC\ell_x$ ($x=|z_M|$), the total EMF, E, as defined in equation (6-2) becomes eqn. (6-7) using eqns. (6-3), (6-4) and (6-6) after some rearrangement).

$$E = (\psi'_{Ag} - \psi''_{Ag}) = \left(\frac{|z_M|}{z_M}\right) \bar{T}_M K \ell n \frac{[MC\ell_x''] \gamma''_{\pm}}{[MC\ell_x'] \gamma'_{\pm}} + \bar{T}_3 K \ell n \left(\frac{\bar{a}_3''}{\bar{a}_3'}\right) \qquad (6\text{-}7)$$

where $[MC\ell_x]$ and $\gamma_{\pm}$ are the molar concentration and mean molar activity coefficients of the electrolyte $MC\ell_x$.

6.2.2 Bi-ionic potentials

For B.I.P. the EMF, E, is once more defined as in eqn. (6-2) with each component potential defined as previously. This includes the diffusion potential, which has identical form to eqns. (6-5) and (6-6), but now the two ions are both counterions. A third ionic term in eqns. (6-5) and (6-6) would be added if chloride was present in significant amounts in the membrane phase.

The final equation, corresponding to eqn. (6-7) for a single ion or at least single potentials is, however, of a somewhat different form. For a B.I.P. in which only two counterions are involved eqn. (6-8) becomes

$$E = -K \ln a'_{C\ell} - K \ln \left(\frac{\bar{a}'_{C\ell}}{a'_{C\ell}}\right) + \frac{\bar{T}_H}{z_H} K \ln \left(\frac{\bar{a}''_H}{\bar{a}'_H}\right) + \frac{\bar{T}_K}{z_K} K \ln \left(\frac{\bar{a}''_K}{\bar{a}'_K}\right)$$

$$+ \bar{T}_3 K \ln \left(\frac{\bar{a}''_3}{\bar{a}'_3}\right) + K \ln \left(\frac{\bar{a}''_{C\ell}}{a''_{C\ell}}\right) + K \ln a''_{C\ell} \qquad (6\text{-}8)$$

(The Donnan potentials, eqn. (6-8) are expressed in terms of chloride here). Simplifying eqn. (6-8) becomes

$$E = (\psi'_{Ag} - \psi''_{Ag}) = \frac{\bar{T}_H}{z_H} K \ln \left(\frac{\bar{a}''_H \, \bar{a}''_{C\ell}{}^{z_H}}{\bar{a}'_H \, \bar{a}'_{C\ell}{}^{z_H}}\right) + \frac{\bar{T}_K}{z_K} K \ln \left(\frac{\bar{a}''_K \bar{a}''_{C\ell}{}^{z_K}}{\bar{a}'_K \bar{a}'_{C\ell}{}^{z_K}}\right)$$

$$+ \bar{T}_3 K \ln \left(\frac{\bar{a}''_3}{\bar{a}'_3}\right) \qquad (6\text{-}9)$$

The Donnan equilibrium condition, eqn. (6-10), allows ion activity products in the membrane to be expressed in terms of solution activities,

$$(\bar{a}_i \cdot \bar{a}_{C\ell})^{z_i} = (a_i \cdot a_{C\ell})^{z_i} \qquad (6\text{-}10)$$

It is also easily shown that the activities of water in the membrane and solution are equal, if defined relative to the same standard state (pure water, at 1 atm pressure, 298.15K), so that $\bar{a}_3^* = \bar{a}_3^*$ (* = ' or ") at each membrane surface (side ' and side "). The B.I.P. E, is therefore easily expressed in terms of solution activities, eqn. (6-11), expressed here for the H^+/K^+ B.I.P.

$$E = \frac{\bar{T}_H}{z_H} K \ln \left(\frac{a''_H \, a''_{C\ell}}{a'_H \, a'_{C\ell}}\right) + \frac{\bar{T}_K}{z_K} K \ln \left(\frac{a''_K \, a''_{C\ell}}{a'_K \, a'_{C\ell}}\right) + \bar{T}_3 K \ln \left(\frac{a''_3}{a'_3}\right) \quad (6\text{-}11)$$

since $a_H \, a_{C\ell} = [H^+][C\ell^-] \, \gamma^2_{HC\ell}$

and $a_K \, a_{C\ell} = [K^+][C\ell^-] \, \gamma^2_{KC\ell}$

where $\pm\gamma_{HC\ell}$ is the mean molar activity coefficient of $HC\ell$ in the solution, and similarly for $KC\ell$.

For the particular case considered here of a constant total ionic strength 0.05M and so a constant chloride concentration of same value, eqn. (6-11) becomes

$$E = \frac{\bar{T}_H}{z_H} K \ln \frac{[H^+]''}{[H^+]'} \cdot \frac{\gamma''_{\pm HC\ell}}{\gamma'_{\pm HC\ell}} + \frac{\bar{T}_K}{z_K} K \ln \frac{[K^+]''}{[K^+]'} \cdot \frac{\gamma''_{\pm KC\ell}}{\gamma'_{\pm KC\ell}}$$

$$+ \bar{T}_3 K \ln \left(\frac{a''_3}{a'_3}\right) \quad (6\text{-}12)$$

6.3 EXPERIMENTAL

6.3.1 Membrane cell

The cell was made of Perspex (pexiglass) and consisted of two symmetrical mains halves (A) basically similar to that described by Lorimer et al.[7] but completely different in design and operation, with many features which are absent in the original cell. Each half consisted of three parts, Fig. (6-1).

The main part (A) was fitted with 'Quickfit' tapered B10 glass cones mounted, using Araldite adhesive. The upper (B) held the flow meter (G), and the other below (C) was connected to the electrode chamber (H), Fig. (6-1). The screw seals (D and E) were designed to give the freedom to move the flowing tube (I). This carried a scale to record positions as they were moved forwards or backwards from the membrane surface during tests. Both seals were threaded and would move relative to each other and the main cell unit. Each was furnished with an O-ring to prevent leakage between the cell solution and the water bath.

6.3.2 Membrane holder

The membrane holder (F), Fig. (6-2) consisted of two discs turned and threaded to fit the main parts (A) of the cell. On one side a circular disc was milled out to hold the membrane, Fig. (6-2). The second disc correspondingly protruding to fit the milled depression in its partner. They were also equipped with O-rings designed to hold

the membrane and also to prevent leakage between the two halves of the cell and the water bath also. A number of membrane holders were made with different holes; these were made at diameters of 0.1, 0.2 and 0.3 cm. After testing measurements were taken with a hole 0.3 cm in diameter with bevelled edge to permit excess of flowing solution to flow freely from the membrane surface.

6.3.3 Solution reservoir

Solutions were kept in two reservoirs (J), each of ten litres capacity and fitted with thermometer (K). The reservoirs were placed 94 cm above the cell, and both were fitted with constant head devices (L) which gave a uniform flow through the cell, (Fig. 6-1). By circulating water at 30°C through double condenser jackets (P), the test solutions were maintained at a temperature of 25 ± 0.01°C. The solutions were stirred continuously, as shown in Fig. (6-1).

6.3.4 Electrode chamber

The electrode chamber (H), Fig. (6-1) consisted of two similar glass test tubes, one on each side of the connection to the joined main cell. These were interconnected by glass tubes and fitted with valves (V) to permit change of electrodes if necessary.

The electrode chamber was connected to the cell by a B10 cone (C) to fit its partner at the bottom of the cell, Fig. (6-1).

6.4 Silver/Silver Chloride Electrode

Silver/silver chloride electrodes (N) were prepared with bias potentials ranging between 0.02-0.065 mV. Four such electrodes giving the lowest bias potential were used, Fig. (6-1) in each experiment.

6.4.1 Silver/silver chloride electrode preparation

The electrodes were reversible silver/silver chloride electrodes prepared by the thermal-electrolytic method.[8] The electrodes consisted of a spiral (0.3 cm diameter) of 2-3 turns of platinum wire. This was sealed into a B10 standard taper joint with an extension. The platinum spirals were cleaned by boiling briefly in concentrated nitric acid followed by repeated rinsings with distilled water. The platinum spiral was then covered with a paste of silver oxide using a small spatula. The inside of the spiral was completely filled and the spiral totally covered with paste to form a ball of suitable dimension (0.4 or 0.5 cm in diameter). It was then heated, at first slowly, to 100°C to drive off water and preclude the possibility of sputtering by rapid formation of steam and to permit superficial drying.

The temperature was then raised at a uniform rate to 450°C . The electrodes were permitted to cool within the furnace to avoid thermal shock. For the second coat, a paste of much thinner consistency was used. The reduction of the second coat of silver oxide was performed in the same way.

6.4.2 Chloridization

The silver/silver electrodes prepared as above were then chloridized as anodes in 1M hydrochloric acid. A platinum spiral similar to those used for the preparation of silver electrodes, served as a cathode. A current of 10 mA was passed through an assembly consisting of six electrodes in series. The freshly prepared electrodes were white or light grey in colour. A batch of electrodes prepared in this way were short circuited and stored in a dilute KCℓ solution. After two weeks bias potentials were measured between pairs of electrodes. Pairs with a bias potential of greater than 0.1 mV were discarded. Several pairs of electrodes reproducibly gave bias potentials between 0.05-0.065 mV. Before each EMF measurement, the bias potentials were measured and the positive electrodes were placed in the dilute solution so that the corrections were always in the same direction.

6.5 Membranes and Reagents

Four types of membrane were used in these experiments. Nafion (125 and 117) perfluorinated sulphonic acid membrane (E.I. Du Pont de Nemours Co.) and AMF C_{60} graft copolymer membrane (American Machine and Foundry Co., Springdale, Connecticut, U.S.A.). This ion exchange membrane was prepared from low-density polyethylene and contained 35% styrene and up to 2% divinylbenzene. To complete the set of four membranes (uncharged) Visking dialysis membranes were included for comparison. Analytical grade KCℓ or NaCℓ was used, as previously.

6.5.1 Resistance measurement of membrane emf cell

The resistance of the cell was measured by inserting a piece of polythene sheet in place of the membrane. The two halves of the cell could be lined up reproducibly by means of six bolts and nuts. Very slight pressure on the polythene sheet was sufficient to prevent leakage.

The cell, with polythene membrane in place, was filled with potassium chloride solution. Electrodes were inserted and the whole assembly was supported horizontally by means of two clamps in the water bath at 25 ± 0.01°C. Its resistance was found to be 6.4 MΩ, measured by a Solartron 7075 digital voltmeter.

6.5.2 Test of the membrane cell

The membrane (M) was clamped between the two halves of the cell, Fig. (6-1) in such a way that six coupling nuts and bolts separated two solutions of the same concentration. The inflowing solutions impinged directly on the membrane surface and the outflowing solution passed through flow meters filled in the outlets of the cell (B). The flows, ranging from 0-1000 mL min^{-1} were measured by two calibrated Gilmont flowmeters F-1500, size 5, with 0.5 float diameter (G) and flow capacity ranging from 30-1900 mL min^{-1}.

The silver/silver chloride electrodes (N) were put in place and the whole assembly replaced in the water bath, maintained at 25±0.01°C. The electrodes were connected to the Solartron 7075 digital voltmeter to measure the potentials, Fig. (6-3).

6.6 RESULTS AND DISCUSSION

Two series of measurements were made on the new experimental flow cell. In the first, the EMF of simple concentration cells was measured,

$$Ag'/AgC\ell\,|MC\ell'\,|\text{'membrane''}\,|MC\ell''\,|AgC\ell/Ag''$$

Sodium and potassium chloride solutions were used with two perfluorosulphonic acid membranes (Nafion 125 and Nafion 117), a polystyrene sulphonic acid membrane (AMF C_{60}) and with an uncharged dialysis membrane (Visking). Bias potentials between pairs of electrodes in each half cell were never greater than 0.065 mV. In preliminary tests of the flow cell, it was assembled with a membrane in place and identical 0.1M KCℓ on either side. Membrane potentials under such circumstances should be zero since the cell is entirely symmetrical. At zero flow the measured potential was never greater than 0.03 mV. The system was tested with constant flows, equal on each side at the standardized flow rates used in the measurement of the experimental work; 100, 200, 300, 500, 700 and 1000 mL min^{-1}. These flows were read directly from Gilmont flow meters which had been independently calibrated and were shown to be reproducible to ± 1%.

These null potentials were measured at all flow rates and were zero within the limits ± 0.1 mV and were stable with time over a period of at least one hour, Fig. (6-3).

6.6.1 Single ion potential

For single salt measurements, all solutions were of Analar quality. They were prepared and analysed for chloride using potentiometric silver nitrate titration and Gran plot analysis, which was accurate to 0.2%. All measurements were made at 25 ± 0.01°C using temperature control units in the two solution reservoirs and the main water thermostat in which the membrane cell, Fig. (6-1) was placed.

EMF measurements were made at each of the standard flow rates in the range 0-1000 mL min^{-1}. The flow rates were adjusted and kept steady using fine control values on the solution outflow from each half cell.

Lorimer in his test[4] of this hydrodynamics theory was unable to observe all of the theoretical features of a plot of the EMF of a concentration cell and the flow rate (Q). In particular, although his experimental plots of EMF were in fact linear against $1/\sqrt{Q}$, the slopes were of the wrong sign, positive and negative, rather than negative all the time.

In a discussion with him, it was clear that the membrane cells used in his tests were of restricted value. Their major defect was firstly that the flow tube could not be adjusted so that the gap between its outlet and the membrane surface could be varied. The second limitation was that the effect of varying membrane area (exposed) was not measurable. In his cell, both were "arbitraryly" fixed.

In the present cell, Fig. (6-1) the flow tube (0.7 cm internal diameter, i.d.) could be adjusted to allow measurement at differing gaps

Also by fitting a range of three interchangeable membrane holders, the cell could be used with exposed membrane diameters 0.1, 0.2 and 0.3 cm. Preliminary tests showed that there were significant differences between the 0.1 and the 0.2 and 0.3 cm membrane diameter results. The two larger holders showed no significant differences in measurements made under otherwise identical conditions, but differed significantly from the 0.1 cm diameter holder. The holder with 0.3 cm diameter exposed membrane was used in all other work. The smallest area was obviously too small to allow the flow patterns expected by theory. A comparison of Table (6-1d) and (6-1f) shows the major effect of using the smallest membrane area of 0.1 cm diameter.

The impinging jet of the cell solution will be affected by the distance between this end of the outflow tube and the membrane surface. This too was tested and it was shown that if placed at a distance of 0.5 to 1 cm from the membrane surface, the system gave indistinguishable results. The effect of moving the outflow tube back from 0.5 cm to 1 cm (from 0.3 cm diameter membrane holder) is shown in a comparison of Table (6-2b) with (6-2d).

A typical plot of cell EMF versus flow, Q, (for Nafion 125 between 0.01 and 0.02M KCℓ) is shown in Fig. (6-4). As predicted by theory, a plot of EMF against the reciprocal of the square root flow rate ($^{1}/\sqrt{Q}$) was now found to be linear (in all cases studied here) with a well-defined intercept at infinite flow ($^{1}/\sqrt{Q} = 0$), Fig. (6-5). The data of Tables (6-1) to (6-4) were analysed in this way.

A linear least square curve fit was used to obtain the EMF extrapolated to infinite flow. Since in most cases these data were

obtained in several separate experiments, it was possible to show that for each concentration cell, slopes were reproducible to ± 0.3% and negative slopes (unlike the first tests by Lorimer) were of expected magnitude. The analysis of these data are summarised in Tables (6-5) to (6-8).

The EMF of a concentration cell is given by, eqn. (6-7)

$$E = (\psi'_{Ag} - \psi''_{Ag}) = \left(\frac{z_{|M|+1}}{z_M}\right) \bar{T}_M \, K \, \ell n \left[\frac{MC\ell_x''}{MC\ell_x'}\right] \frac{\gamma_{\pm}''}{\gamma_{\pm}'} + \bar{T}_3 \, K \, \ell n \left(\frac{a_3''}{a_3'}\right) \quad (6\text{-}7)$$

where $K = RT/F$

For all systems studied here, z_M, the valency of the cation of the electrolyte is unity. The mean molar activity coefficient may be calculated by Debye-Hückel equations.[9] The final osmotic term in eqn. (6-7) can only be evaluated if the transference number for water is available. This was not measured in these studies, but may be estimated by previous theory, which firmly predicts its maximum value and allows further refinement based on reasonable assumptions.[10]

Using this method the maximum value of $\bar{T}_3$ is the ratio of moles water n_3 to the moles of counterion n_M, n_3/n_M if a univalent counterion M or equivalently 55.51/m where m is the internal molality of the exchanger phase.

We may evaluate the water activities a'_3 and a''_3 in eqn. (6-7) This may be done using the osmotic coefficient, ϕ [11]. Such that $\ell n a_w = -2m\,\phi/55.51$ where m is the molality of solution and for 0.01009M KCℓ, $\phi = 0.9187$ and for 0.0201M KCℓ, $\phi = 0.8913$. Therefore the final

terms of eqn. (6-7) $\bar{T}_3$ K $\ell n \frac{a_3''}{a_3'}$ has a maximum value of 0.04 mV. The osmotic terms amount to less than 0.1 mV and may in any case be ignored.

The transport numbers for the counterions are given in Tables (6-5) to (6-8), calculated using eqn. (6-7).

It is seen that the counterion transport numbers are all between 0.9 and 1.0, except for Visking dialysis membrane, which has no (significant) charge on the polymer. The uptake of ions in this membrane will be (almost) equal for cations and anions and this is reflected in the transport numbers.

6.6.2 Bi-ionic potential

Bi-ionic potentials were measured in the flow cell, Fig. (6-1) for the cell system.

$Ag/AgC\ell'$	$HC\ell' + KC\ell'$ 0.05M	Nafion 125 membrane	$HC\ell'' + KC\ell''$ 0.05 M	$AgC\ell/Ag''$
	variable composition		constant reference	

The solution on the right hand side (RHS) of the cell, as shown above, was a constant, reference for all measurements. Its composition was 0.01215M KCℓ, 0.03785M HCℓ, and produced an equal loading of H^+ and K^+ on the equilibrium membrane surface (see Chapter 4). This will be referred to as the $\bar{5}0/\bar{5}0$ membrane or, in terms of ionic fractions, $\bar{X}_K = 0.5 = \bar{X}_H$. This reference was chosen so that when the transport numbers of potassium and hydrogen ions in equilibrium membranes were

determined, their values would reflect only the relative mobilities of the two ions since the contribution of ionic concentration would be equal in both for

$$\bar{t}_H = \frac{\bar{c}_H \bar{U}_H}{\bar{c}_H \bar{U}_H + \bar{c}_K U_K}$$

but

$$\bar{t}_H = \frac{\bar{U}_H}{\bar{U}_H + \bar{U}_K} \qquad \text{(for the } \bar{50}/\bar{50} \text{ membrane)}$$

B.I.P.s were measured for six solutions, each against this $\bar{50}/\bar{50}$ reference. These solutions were also chosen to give rounded concentrations in the membrane 100/0 (the pure potassium form in 0.05M KCℓ), 80/20, 60/40, 40/60, 20/80 and 0/100 (in pure hydrogen form in 0.05M HCℓ). The B.I.P.s were measured at flow rates of 100, 200, 300, 500, 700 and 1000 mL min^{-1}, as before. The results are shown in Fig. (6-6) and Table (6-9). The EMF was taken relative to the reference electrode, shown on the RHS in the figure. The cell potentials are shown to be relatively constant with increasing flow rate, Fig. (6-6).

Since the extrapolation method, by Lorimer, used in the single ion membrane potential studies is not applicable here, the B.I.P. was taken as the EMF of the cell at the highest flow rate (1000 mL min^{-1}) at which unstirred layer effects are known to be small. The configuration of the cell was unchanged from that used in standard measurements above, for single salts, as in Fig. (6-1)

A plot of B.I.P. against the variable solution composition of the LHS solution (expressed as ionic fraction of potassium in solution, X_K) is shown in Fig. (6-7). In section 6.2.2 and eqn. (6-12) the B.I.P., E, was shown to be

$$E = (\psi' - \psi'') = \frac{\bar{T}_H}{z_H} K \ln \frac{[H^+]'' \gamma''_{HC\ell}}{[H^+]' \gamma'_{HC\ell}} + \frac{\bar{T}_K}{z_H} K \ln \frac{[K^+]''}{[K^+]'} \cdot \frac{\gamma''_{KC\ell}}{\gamma'_{KC\ell}}$$

$$+ \bar{T}_3 K \ln \left(\frac{a''_3}{a'_3}\right)$$

where $K = RT/F$

In the above equation for B.I.P. the superscripts ' and " represent the variable (LHS) and reference solutions (RHS), respectively.

In dilute solutions the Debye-Hückel equation or its extended form (such as Davis equation) would be expected to give a good approximation for the activity coefficients ($\gamma_{HC\ell}/\gamma_{KC\ell}$). In such estimates activity coefficients defined only on the ionic strength of the solution. Since in all cases this was 0.05M, these estimates would all predict that $\gamma_{HC\ell}$ and $\gamma_{KC\ell}$ are equal under experimental conditions. Estimates using Pitzer's semi-empirical method[11] for mixed electrolytes show that at such low ionic strengths, $\gamma_{HC\ell} = \gamma_{KC\ell}$ within the limits of precision of the method. It is sufficient therefore to know the concentrations of the solution ions, to evaluate the first two logarithmic terms in eqn. (6-12).

The third and final osmotic contribution to the B.I.P. depends upon the integral reference number, $\bar{T}_3$, and the water activities a'_3 and a''_3 in the opposing solutions. As noted above, although no

measurements have been made of the electro-osmotic transference number ($\bar{T}_3$), its value cannot exceed 55.51/m, where m is the internal molality of the membrane phase. For the Nafion 125 membrane this predicts a maximum value of $\bar{T}_3$, 9.66 for the pure potassium form and 15.47 for the pure hydrogen form. Studies on similar Nafion membranes used in these earlier studies[10] show that this estimate of the transference number is further reduced by a coupling or slip-term, β, such that $t_3 = \beta\ (55.51/m)$ where typically β is close to unity for Nafion membranes in the potassium form and ~0.2 for the hydrogen form. For mixed ionic forms, as used here, in which the internal membrane molalities are in the range 4-7, we might expect $\bar{t}_3$ (and hence $\bar{T}_3$) to be in the range 5-8.

The final term of eqn. (6-12) may be estimated therefore if the water activities, a'_3 amd a''_3 are available. On a first order estimation, theory would be expected to be equal since the total ionic concentration and so the 'osmolarity' of the two solutions in each cell are equal.

Although water activities or equivalently osmotic coefficients, ϕ, are not available for mixed H^+/K^+ solutions at 0.05M, those for 0.05M KCℓ and 0.05M HCℓ were estimated using Pitzer's semi-empirical method.[11]

For 0.05M KCℓ, $\phi = 0.940$ and for 0.05M HCℓ, $\phi = 0.949$. From $\ell n a_w = -2m\phi/55.51$ we may evaluate $\ell n(a_{3(HC\ell)}/a_{3(KC\ell)})$ at 0.05M, from these osmotic coefficients. This has a value of $-2 \times 0.05 \times 0.009/55.51$. It is reasonable to assume that this estimate will be larger than any encountered for H^+/K^+ mixtures at 0.05M, used in the experimental cells. A maximum estimate of the osmotic concentration to the B.I.P., eqn. (6-12) will therefore be 0.003 mV, which is an order of magnitude smaller than the error of measure. It was therefore neglected.

Eqn. (6-12) may therefore be used without the final osmotic terms needed for activity coefficients correlations. Since $\bar{T}_K + \bar{T}_H = 1$, the integral transport numbers for potassium were calculated from eqn. (6-13)

$$\bar{T}_H = \frac{E - K \ln \frac{[K^+]''}{[K^+]'}}{K \ln \frac{[H^+]''[K^+]'}{[H^+]'[K^+]''}} \qquad (6\text{-}13)$$

where $K = RT/F$.

The results are given in Table (6-10). The integral transport number is the integrated value over the membrane for each cell, under steady state conditions. It does not apply to any one membrane composition.

To obtain an estimate of the transport numbers of H^+ and K^+ in the $\bar{5}0/\bar{5}0$ membrane, these integral transport numbers were plotted against the mole fraction of potassium ($\bar{X}_K$) on the LHS of the membrane. The other side was always maintained in the reference solution which defined a surface concentration of $\bar{5}0/\bar{5}0$ ($\bar{X}_K = \bar{X}_H = 0.5$). The plot, Fig. (6-8) shows that the integral transport numbers fall from unity in the pure forms to zero. They cross almost exactly at $\bar{X}_K = \bar{X}_H = 0.5$.

This is quite unexpected. It means that in these membranes we estimate that in the $\bar{5}0/\bar{5}0$ membranes with equal concentrations of H^+ and K^+ in the polymer matrix, each of these ions migrate with the same velocity. They have equal mobilities in an electric field. The ratio of the mobilities of H^+/K^+ in free aqueous solutions is ~6/1.

Examining other data sources in the literature provides no effect of similar magnitude. Meares[12] showed in Cs^+/Na^+ measurement of transport numbers (by direct methods), that the caesium ion is less mobile than the sodium ion, and concluded that the selective binding of caesium ion over sodium ion is the main cause. Even so this effect is small. The small previously high mobile proton is reduced to a mobility equal to that of potassium, which is largely effectively unhydrated and relatively strongly bound in the membrane.

It is tempting to speculate that this common mobility is due to particular features of the membrane structure of the Nafion perfluoro-sulphonic acid membranes.

There is a widely supported view that these membranes consist of island structures caused by at least partial, micelle formation of sulphonic groups in the polymer[13]. These 'inverted' micelles which contain most of the sulphonic acid groups, counterions and water, can be separated from other micelles by regions low in water and ions, largely hydrophobic polymer.

If there is transport of ions across the membrane, as here, then the ions must migrate across these hydrophobic regions and, since these regions would provide paths of high resistance, they would control the overall mobilities of the ions across the membrane. It is tempting to suggest that under such conditions and in paths without water (at least continuous water filled paths) the hydrated proton H_3O^+ would lose its enhanced mobility due to the proton jump mechanism and approach that of simple cation (unhydrated), like potassium.

If such hydrophobic paths were long, more than a few Angströms, then the exchange of counterions H_3O^+ and K^+ would require concurrent flow of chloride, coion.

This, although a minor component in the membrane, would therefore control the exchange of H^+/K^+ between micelles and make the mobilities of both K^+ and H_3O^+ equal to that of the exchange rate for chloride and so equal to one another.

Further investigations to test this tentative explanation of the phenomenon are now being planned.

Table (6-1a): EMF for Nafion N-125 Perfluorosulphonic Acid Membrane with (0.01009/0.0201) M Potassium Chloride Solutions

EMF mV	Flow rate (Q) mL min^{-1}							
	0	10	100	200	300	500	700	1000
Expt. 1	30.54 ±0.00	32.45 ±0.08	32.49 ±0.07	32.58 ±0.01	32.60 ±0.03	32.58 ±0.01	32.59 ±0.00	32.59 ±0.01
Expt. 2	30.85 ±0.00	32.58 ±0.03	32.62 ±0.02	32.69 ±0.02	32.68 ±0.03	32.68 ±0.01	32.70 ±0.02	32.72 ±0.00
Expt. 3	30.87 ±0.00	32.61 ±0.02	32.59 ±0.03	32.62 ±0.02	32.68 ±0.03	32.69 ±0.02	32.71 ±0.02	32.74 ±0.01
Expt. 4	30.83 ±0.00	32.57 ±0.05	32.66 ±0.03	32.70 ±0.02	32.69 ±0.03	32.70 ±0.05	32.70 ±0.05	32.74 ±0.00
Average	30.77 ±0.15	32.56 ±0.07	32.59 ±0.07	32.65 ±0.06	32.66 ±0.04	32.66 ±0.05	32.67 ±0.06	32.69 ±0.00

Membrane diameter exposed, 0.3 cm

Flow tube, i.d., 0.7 cm

Distance from flow tube to membrane surface, 0.5 cm

Table (6-1b): EMF for Nafion N-125 Perfluorosulphonic Acid Membrane with (0.01995/0.0503) M Potassium Chloride Solutions

EMF mV	Flow rate (Q) mL min^{-1}							
	0	10	100	200	300	500	700	1000
Expt. 1	39.05 ±0.00	39.26 ±0.01	39.36 ±0.02	39.47 ±0.01	39.48 ±0.00	39.50 ±0.00	39.53 ±0.00	39.56 ±0.00
Expt. 2	39.06 ±0.01	39.40 ±0.01	39.39 ±0.03	39.42 ±0.04	39.45 ±0.00	39.47 ±0.01	39.51 ±0.00	39.54 ±0.00
Expt. 3	39.09 ±0.00	39.34 ±0.01	39.37 ±0.01	39.42 ±0.00	39.44 ±0.01	39.45 ±0.00	39.46 ±0.00	39.48 ±0.02
Average	39.07 ±0.02	39.33 ±0.07	39.37 ±0.01	39.44 ±0.03	39.46 ±0.01	39.47 ±0.02	39.50 ±0.03	39.52 ±0.03

Membrane diameter exposed, 0.3 cm

Flow tube, i.d., 0.7 cm

Distance from flow tube to membrane surface, 0.5 cm

Table (6-1c): EMF for Nafion-125 Perfluorosulphonic Acid Membrane with (0.0496/0.0102) M Potassium Chloride Solutions

EMF mV	Flow rate (Q) mL min^{-1}						
	0	100	200	300	500	700	1000
Expt. 1	31.53	32.00	31.98	32.00	32.00	32.08	32.07
	±0.03	±0.09	±0.01	±0.02	±0.01	±0.00	±0.02
Expt. 2	31.59	32.03	31.98	31.98	32.00	32.03	32.08
	±0.01	±0.02	±0.01	±0.01	±0.01	±0.03	±0.01
Expt. 3	31.55	32.06	31.98	31.98	32.00	32.05	32.06
	±0.02	±0.00	±0.01	±0.06	±0.06	±0.02	±0.07
Average	31.56	32.03	31.98	32.00	32.00	32.05	32.07
	±0.03	±0.03	±0.00	±0.01	±0.00	±0.02	±0.04

Membrane diameter exposed, 0.3 cm

Flow tube, i.d., 0.7 cm

Distance from flow tube to membrane surface, 0.5 cm

Table (6-1d): EMF for Nafion-125 Perfluorosulphonic Acid Membrane with (0.05/0.1) M Potassium Chloride Solutions

EMF mV	Flow rate (Q) mL min^{-1}						
	0	100	200	300	500	700	1000
Expt. 1	30.72 ±0.04	31.65 ±0.02	31.71 ±0.09	31.83 ±0.05	31.65 ±0.22	31.88 ±0.07	31.81 ±0.04
Expt. 2	30.76 ±0.01	31.65 ±0.06	31.67 ±0.01	31.65 ±0.07	31.74 ±0.06	31.82 ±0.03	31.83 ±0.03
Average	30.74 ±0.03	31.65 ±0.00	31.69 ±0.03	31.74 ±0.13	31.70 ±0.06	31.85 ±0.04	31.82 ±0.01

Membrane diameter exposed, 0.3 cm

Flow tube, i.d., 0.7 cm

Distance from flow tube to membrane surface, 1.0 cm

Table (6-1e): EMF for Nafion N-125 Perfluorosulphonic Acid Membrane with (0.01002/0.0503) M Potassium Chloride Solutions

EMF mV	Flow rate (Q) mL min^{-1}						
	0	100	200	300	500	700	1000
Expt. 1	71.45 ±0.02	72.53 ±0.04	72.74 ±0.14	72.94 ±0.06	72.94 ±0.06	73.12 ±0.01	73.16 ±0.02
Expt. 2	71.32 ±0.03	72.54 ±0.06	72.70 ±0.07	72.83 ±0.07	72.89 ±0.03	73.00 ±0.05	73.64 ±0.05
Expt. 3	71.37 ±0.01	72.54 ±0.08	72.91 ±0.14	72.96 ±0.06	72.97 ±0.02	73.21 ±0.02	73.18 ±0.03
Average	71.39 ±0.08	72.54 ±0.00	72.79 ±0.11	72.91 ±0.07	72.93 ±0.04	73.11 ±0.10	73.12 ±0.00
Additivity test:	Σ(0.01009/0.0201 + 0.01995/0.0503) See Tables (6-1a) and (6-1b)						
	69.84	71.96	72.09	72.12	72.14	72.18	72.22

Membrane diameter exposed, 0.3 cm

Flow tube, i.d., 0.7 cm

Distance from flow tube to membrane surface, 0.5 cm

Table (6-1f): EMF for Nafion-125 Perfluorosulphonic Acid Membrane with (0.05/0.1) M Potassium Chloride Solutions using 0.1cm diameter of the Membrane Area

EMF mV	Flow rate (Q) mL min^{-1}					
	0	200	300	500	700	1000
Expti 1	16.17	16.30	16.47	18.62	25.42	30.08
Expt. 2	16.97	17.37	17.59	19.62	25.87	29.98
Expt. 3	16.89	19.55	19.73	20.17	24.60	27.94
Expt. 4	16.51	17.23	18.47	19.17	-	30.32
Expt. 5	16.38	17.36	-	20.05	-	29.87
Expt. 6	-	18.53	19.35	20.50	-	-
Average	16.58	17.72	18.32	19.69	25.30	29.64

Membrane diameter exposed, 0.1 cm

Flow tube, i.d., 0.7 cm

Distance from flow tube to membrane surface, 0.5 cm

Table (6-2a): EMF for AMF C_{60} Membrane with (0.00994/0.0495) M Potassium Chloride Solutions

EMF mV	Flow rate (Q) mL min^{-1}						
	0	100	200	300	500	700	1000
Expt. 1	67.56 ±0.02	70.55 ±0.01	70.67 ±0.08	70.77 ±0.05	70.57 ±0.05	71.01 ±0.04	71.04 ±0.01
Expt. 2	67.91 ±0.03	70.62 ±0.05	70.86 ±0.02	70.91 ±0.04	70.96 ±0.09	71.03 ±0.02	71.18 ±0.03
Expt. 3	67.57 ±0.01	70.63 ±0.04	70.79 ±0.03	70.90 ±0.07	70.99 ±0.05	70.99 ±0.01	71.00 ±0.01
Expt. 4	67.52 ±0.09	70.54 ±0.05	70.74 ±0.05	70.79 ±0.05	70.68 ±0.10	70.77 ±0.08	71.05 ±0.01
Average	67.69 ±0.15	70.58 ±0.05	70.77 ±0.08	70.84 ±0.07	70.80 ±0.20	70.95 ±0.12	71.07 ±0.02

Membrane diameter exposed, 0.3 cm

Flow tube, i.d., 0.7 cm

Distance from flow tube to membrane surface, 0.5 cm

Table (6-2b): EMF for AMF C_{60} Membrane with (0.0495/0.1012) M Potassium Chloride Solutions

EMF mV	Flow rate (Q) mL min^{-1}						
	0	100	200	300	500	700	1000
Expt. 1	29.08 ±0.00	30.77 ±0.04	30.92 ±0.01	30.97 ±0.04	30.97 ±0.06	31.01 ±0.02	31.04 ±0.01
Expt. 2	29.35 ±0.00	30.69 ±0.10	30.91 ±0.07	31.03 ±0.01	31.01 ±0.01	31.02 ±0.01	31.06 ±0.02
Expt. 3	29.42 ±0.00	30.82 ±0.02	31.06 ±0.01	31.09 ±0.05	31.11 ±0.02	31.14 ±0.01	31.20 ±0.01
Average	29.28 ±0.18	30.76 ±0.07	30.96 ±0.08	31.03 ±0.06	31.03 ±0.07	31.06 ±0.07	31.10 ±0.01

Membrane diameter exposed, 0.3 cm

Flow tube, i.d., 0.7 cm

Distance from flow tube to membrane surface, 0.5 cm

Table (6-2c): EMF for AMF C_{60} Membrane with (0.00986/0.1002) M Potassium Chloride Solutions

EMF mV	Flow rate (Q) mL min^{-1}						
	0	100	200	300	500	700	1000
Expt. 1	95.78 ±0.01	101.52 ±0.10	102.31 ±0.08	102.37 ±0.02	-	102.72 ±0.05	102.38 ±0.07
Expt. 2	95.75 ±0.01	101.46 ±0.03	102.11 ±0.12	102.37 ±0.06	102.31 ±0.05	102.55 ±0.12	102.79 ±0.03
Expt. 3	95.64 ±0.00	101.45 ±0.01	102.30 ±0.01	102.58 ±0.01	102.43 ±0.04	102.60 ±0.05	102.89 ±0.06
Expt. 4	95.78 ±0.02	101.55 ±0.03	102.30 ±0.03	102.58 ±0.04	102.60 ±0.11	102.82 ±0.09	103.02 ±0.01
Average	95.74 ±0.07	101.50 ±0.04	102.25 ±0.10	102.46 ±0.10	102.45 ±0.15	102.68 ±0.12	102.78 ±0.28
Additivity test: Σ(0.00994/0.0495 + 0.0495/0.1012) See Tables (6-2a) and (6-2b)	96.97	101.34	101.73	101.87	101.83	102.01	102.17

Membrane diameter exposed, 0.3 cm

Flow tube, i.d., 0.7 cm

Distance from flow tube to membrane surface, 0.5 cm

Table (6-2d): EMF for AMF C_{60} Membrane with (0.0495/0.1012) M Potassium Chloride Solutions.

EMF mV	Flow rate (Q) mL min^{-1}						
	0	100	200	300	500	700	1000
Expt. 1	29.48 ±0.00	30.99 ±0.07	31.23 ±0.10	31.28 ±0.07	31.69 ±0.09	31.25 ±0.04	31.32 ±0.01
Expt. 2	29.44 ±0.02	30.96 ±0.04	31.12 ±0.02	31.16 ±0.02	31.15 ±0.01	31.18 ±0.02	31.21 ±0.04
Average	29.46 ±0.03	30.98 ±0.02	31.18 ±0.08	31.22 ±0.08	31.42 ±0.38	31.22 ±0.05	31.27 ±0.08

Membrane diameter exposed, 0.3 cm

Flow tube, i.d., 0.7 cm

Distance from flow tube to membrane surface, 1.0 cm

Table (6-3a): EMF for Nafion-117 Perfluorosulphonic Acid Membrane with (0.02986/0.05995) M Sodium Chloride Solutions

EMF mV	Flow rate (Q) mL min^{-1}							
	0	10	100	200	300	500	700	1000
Expt. 1	31.47 ±0.06	32.69 ±0.06	33.07 ±0.01	33.12 ±0.00	33.17 ±0.00	33.23 ±0.00	33.46 ±0.00	-
Expt. 2	31.54 ±0.09	32.87 ±0.10	33.08 ±0.00	33.21 ±0.00	33.22 ±0.02	33.35 ±0.01	33.33 ±0.04	33.47 ±0.00
Expt. 3	31.48 ±0.03	32.66 ±0.01	33.20 ±0.00	33.33 ±0.00	33.35 ±0.00	33.35 ±0.00	33.40 ±0.00	33.42 ±0.01
Expt. 4	31.60 ±0.05	32.70 ±0.62	33.18 ±0.01	33.46 ±0.02	33.46 ±0.02	33.45 ±0.00	33.49 ±0.00	33.51 ±0.00
Average	31.52 ±0.06	32.73 ±0.10	33.13 ±0.07	33.28 ±0.±5	33.30 ±0.±2	33.34 ±0.09	33.42 ±0.08	33.46 ±0.00

Membrane diameter exposed, 0.3 cm

Flow tube, i.d., 0.7 cm

Distance from flow tube to membrane surface, 0.5 cm

Table (6-3b): EMF for Nafion 117 Perfluorosulphonic Acid Membrane with (0.05995/0.10007) M Sodium Chloride Solutions

EMF mV	Flow rate (Q) mL min^{-1}							
	0	10	100	200	300	500	700	1000
Expt. 1	-	23.77 ±0.02	23.89 ±0.00	23.93 ±0.00	23.90 ±0.01	23.85 ±0.02	24.28 ±0.09	24.27 ±0.07
Expt. 2	22.83 ±0.00	23.60 ±0.03	23.87 ±0.02	23.94 ±0.00	23.97 ±0.00	24.00 ±0.05	24.13 ±0.00	24.14 ±0.03
Expt. 3	22.86 ±0.04	23.64 ±0.04	23.88 ±0.01	23.92 ±0.00	23.94 ±0.00	23.91 ±0.01	24.07 ±0.04	23.98 ±0.00
Expt. 4	22.80 ±0.00	23.69 ±0.00	23.78 ±0.01	23.78 ±0.01	23.86 ±0.01	23.90 ±0.00	23.84 ±0.05	24.00 ±0.00
Average	22.83 ±0.03	23.67 ±0.07	23.86 ±0.05	23.89 ±0.08	23.92 ±0.05	23.92 ±0.06	24.08 ±0.18	24.10 ±0.13

Membrane diameter exposed, 0.3 cm

Flow tube, i.d., 0.7 cm

Distance from flow tube to membrane surface, 0.5 cm

Table (6-3c): EMF for Nafion-117 Perfluorosulphonic Acid Membrane with (0.02986/0.01002) M Sodium Chloride Solutions

EMF mV	Flow rate (Q) mL min^{-1}							
	0	10	100	200	300	500	700	1000
Expt. 1	54.65	56.09	56.31	56.44	56.47	56.48	56.50	56.53
	±0.01	±0.01	±0.00	±0.00	±0.00	±0.01	±0.00	±0.00
Expt. 2	54.74	56.10	56.28	56.34	56.37	56.36	56.40	56.48
	±0.03	±0.02	±0.00	±0.01	±0.01	±0.00	±0.01	±0.01
Expt. 3	54.77	56.12	56.33	56.45	56.47	56.46	56.48	56.50
	±0.01	±0.01	±0.00	±0.00	±0.00	±0.00	±0.00	±0.00
Average	54.72	56.10	56.27	56.41	56.44	56.44	56.46	56.50
	±0.06	±0.02	±0.07	±0.06	±0.05	±0.06	±0.05	±0.06
Additivity test:	Σ(0.02986/0.05995 + 0.05995/0.10007)				See Tables (6-3a) and (6-3b)			
	54.36	56.41	56.99	57.17	57.22	57.26	57.50	57.56

Membrane diameter exposed, 0.3 cm

Flow tube, i.d., 0.7 cm

Distance from flow tube to membrane surface, 0.5 cm

Table (6-4a): EMF for Visking Dialysis Membrane with (0.05995/0.10007) M Sodium Chloride Solutions

EMF mV	Flow rate (Q) mL min^{-1}							
	0	10	100	200	300	500	700	1000
Expt. 1	10.07 ±0.00	10.22 ±0.00	10.25 ±0.00	10.27 ±0.00	10.27 ±0.00	10.27 ±0.00	10.27 ±0.00	10.28 ±0.00
Expt. 2	10.09 ±0.02	10.20 ±0.00	10.24 ±0.00	10.27 ±0.00	10.27 ±0.00	10.27 ±0.00	10.28 ±0.00	10.29 ±0.00
Expt. 3	10.08 ±0.02	10.22 ±0.00	10.25 ±0.00	10.28 ±0.00	10.29 ±0.00	10.28 ±0.00	10.29 ±0.00	10.30 ±0.00
Expt. 4	10.09 ±0.00	10.22 ±0.00	10.25 ±0.00	10.28 ±0.00	10.29 ±0.00	10.28 ±0.00	10.29 ±0.00	10.29 ±0.01
Average	10.08	10.22 ±0.00	10.25 ±0.00	10.27 ±0.00	10.28 ±0.00	10.28 ±0.00	10.28 ±0.00	10.29 ±0.01

Membrane diameter exposed, 0.3 cm

Flow tube, i.d., 0.7 cm

Distance from flow tube to membrane surface, 0.5 cm

Table (6-4b): EMF for Visking Dialysis Membrane with (0.02986/0.05995) M Sodium Chloride Solutions

EMF mV	Flow rate (Q) mL min^{-1}							
	0	10	100	200	300	500	700	1000
Expt. 1	13.93 ±0.01	14.66 ±0.01	14.65 ±0.00	14.70 ±0.00	14.72 ±0.01	14.76 ±0.02	14.77 ±0.01	-
Expt. 2	-	14.57 ±0.00	14.65 ±0.01	14.72 ±0.01	14.74 ±0.00	14.75 ±0.01	14.75 ±0.02	14.75 ±0.00
Expt. 3	13.94 ±0.00	14.44 ±0.01	14.52 ±0.02	14.58 ±0.02	-	14.63 ±0.00	14.64 ±0.00	14.64 ±0.01
Expt. 4	13.87 ±0.01	14.38 ±0.01	14.47 ±0.00	14.66 ±0.00	14.66 ±0.01	14.68 ±0.00	14.68 ±0.01	14.70 ±0.02
Average	13.91 ±0.04	14.51 ±0.12	14.57 ±0.09	14.67 ±0.06	14.71 ±0.04	14.71 ±0.06	14.71 ±0.06	14.70 ±0.06

Membrane diameter exposed, 0.3 cm

Flow tube, i.d., 0.7 cm

Distance from flow tube to membrane surface, 0.5 cm

Table (6-4c): EMF for Visking Dialysis Membrane with (0.02986/0.10002) M Sodium Chloride Solutions

EMF mV	Flow rate (Q) mL min^{-1}							
	0	10	100	200	300	500	700	1000
Expt. 1	23.81 ±0.00	24.18 ±0.00	24.32 ±0.02	24.45 ±0.00	24.48 ±0.01	24.49 ±0.00	24.51 ±0.00	24.55 ±0.01
Expt. 2	23.81 ±0.00	24.19 ±0.00	24.35 ±0.00	24.48 ±0.00	24.52 ±0.00	24.5 ±0.00	24.56 ±0.01	24.59 ±0.01
Expt. 3	-	-	24.40 ±0.00	24.53 ±0.00	24.56 ±0.00	24.56 ±0.01	24.58 ±0.01	24.63 ±0.00
Expt. 4	23.82 ±0.02	24.25 ±0.00	24.41 ±0.00	-	24.57 ±0.00	24.57 ±0.00	24.59 ±0.01	24.64 ±0.00
Average	23.81 ±0.00	24.21 ±0.04	24.37 ±0.04	24.49 ±0.04	24.53 ±0.04	24.54 ±0.04	24.56 ±0.03	24.60 ±0.04
Additivity test:	23.99	24.72	24.82	24.94	24.99	24.98	24.99	24.95

$\Sigma(0.02986/0.05995 + 0.05995/0.10007)$ See Tables (6-4a) and (6-4b)

Membrane diameter exposed, 0.3 cm

Flow tube, i.d., 0.7 cm

Table (6-5): Potassium Ion Integral Transport Numbers in Nafion-125 Membranes in Potassium Chloride Solutions at 298.15K

Potassium chloride concentrations mol L^{-1}	Least square fit EMF mV	slope $x10^{-3}$ V min^{-1}	sodium transport number $\bar{t}_{+}$ $mol\ F^{-1}$	Max flow EMF* mV
0.01009/0.0201	32.65	-1.320	0.975	32.59±0.01
	32.76	-1.225	0.978	32.72±0.00
	32.79	-2.165	0.979	32.74±0.00
	32.74	-7.766	0.978	32.74±0.06
0.01995/0.0503	39.63	-2.572	0.912	39.56±0.00
	39.58	-2.071	0.911	39.54±0.00
	39.63	-2.572	0.912	39.48±0.02
0.0496/0.1012	32.09	-1.188	0.962	32.07±0.02
	32.05	-5.188	0.961	32.08±0.01
	32.03	-1.076	0.961	32.06±0.07
0.01002/0.0503	73.42	-9.040	0.946	73.16±0.02
	73.24	-7.189	0.944	73.04±0.05
	73.32	-5.392	0.944	73.18±0.03

* At 1000 mL min^{-1}

Table (6-6): Potassium Ion Integral Transport Numbers in AMF C_{60} Membranes in Potassium Chloride Solutions at 298.15K

Potassium chloride concentrations mol L^{-1}	Least square fit EMF mV	slope $x10^{-3}$ V min^{-1}	sodium transport number $\bar{t}_+$ mol F^{-1}	Max flow EMF* mV
0.00994/0.0495	71.12	-6.207	0.920	71.04±0.01
	71.34	-7.214	0.923	71.18±0.03
	71.07	-5.331	0.919	71.00±0.01
	71.07	-5.331	0.919	71.05±0.01
0.0495/0.1012	31.15	-3.621	0.934	31.04±0.01
	31.09	-5.357	0.935	31.06±0.02
	31.35	-4.949	0.940	31.20±0.01
0.00986/0.1002	103.11	-14.0	0.937	102.38±0.07
	103.26	-17.4	0.938	102.79±0.03
	103.62	-18.0	0.941	102.89±0.06
	103.62	-20.0	0.941	103.02±0.01

* At 1000 mL min^{-1}

Table (6-7): Sodium Ion Integral Transport Number in Nafion-117 Membranes in Sodium Chloride Solutions at 298.15K

Sodium chloride concentrations mol L^{-1}	Least square fit EMF mV	slope $\times 10^3$ V min^{-1}	sodium transport number $\bar{t}_+$ mol F^{-1}	Max flow EMF* mV
0.02986/0.05995	33.53	-5.128	1.046	-
	33.56	-5.015	1.047	33.47±0.00
	33.51	-2.907	1.045	33.42±0.00
	33.67	-4.347	1.046	33.51±0.00
0.05995/0.10007	24.30	-4.933	0.740	24.27±0.07
	24.23	-3.840	0.738	24.14±0.03
	24.06	-1.914	0.733	23.98±0.00
	24.08	-3.161	0.744	24.00±0.00
0.02986/0.1002	56.63	-3.015	1.005	56.53±0.00
	56.57	-2.228	1.004	56.50±0.00
	56.57	-3.633	1.004	56.48±0.00

* at 1000 mL min^{-1}

Table (6-8): Sodium Ion Integral Transport Numbers in Visking Dialysis Membranes in Sodium Chloride Solutions at 298.15K

Sodium chloride concentrations mol L^{-1}	Least square fit EMF mV	slope $\times 10^{-3}$ V min^{-1}	sodium transport number $\bar{t}_+$ mol F^{-1}	Max flow EMF* mV
0.02986/0.05995	14.84	-1.864	0.462	-
	14.81	-1.395	0.461	14.75±0.00
	14.71	-1.853	0.458	14.64±0.01
	14.82	-3.103	0.461	14.70±0.02
0.05995/0.10007	10.29	-0.3983	0.311	10.28±0.00
	10.30	-0.5961	0.312	10.29±0.00
	10.32	-0.6027	0.312	10.30±0.00
	10.31	-0.5169	0.312	10.29±0.00
0.02986/0.1002	24.65	-3.146	0.378	24.55±0.01
	24.70	-3.301	0.378	24.59±0.01
	24.72	-3.657	0.378	24.63±0.00
	24.73	-3.141	0.379	24.64±0.00

* At 1000 mL min^{-1}

Table (6-9). Bi-ionic Potential Across Nafion-125 Membrane in H^+/K^+ Form at Different Flow Rates

Equivalent ionic fraction in solutions		Flow Rate (Q) mL min^{-1}					
X_H	X_K	100	200	300	500	700	1000
0	1	-31.19 ± 0.09	-32.19 ± 0.03	-32.20 ± 0.02	-32.30 ± 0.02	-32.71 ± 0.05	-32.96 ± 0.03
0.48	0.52	- 8.04 ± 0.05	- 8.13 ± 0.07	- 8.15 ± 0.00	- 8.14 ± 0.02	- 8.15 ± 0.04	- 8.24 ± 0.02
0.70	0.30	- 1.77 ± 0.06	- 1.78 ± 0.07	- 1.79 ± 0.05	- 1.76 ± 0.09	- 1.78 ± 0.07	- 1.79 ± 0.05
0.757	0.242	0	0	0	0	0	0
0.835	0.165	3.04 ± 0.04	3.07 ± 0.02	3.07 ± 0.02	3.08 ± 0.02	3.09 ± 0.02	3.11 ± 0.02
0.951	0.049	4.48 ± 0.03	4.50 ± 0.02	4.52 ± 0.02	4.55 ± 0.03	4.55 ± 0.02	4.56 ± 0.01
1	0	4.86 ± 0.02	4.86 ± 0.01	4.88 ± 0.01	4.88 ± 0.01	4.88 ± 0.00	4.89 ± 0.03

Table (6-10). Integral Transport Numbers of Potassium and Hydrogen of Nafion-125 Membrane in H^+/K^+ Form at Different Potassium Equivalent ionic fractions in Membrane.

$c_{K(=0.05-c_H}$ mol L^{-1}	$\bar{X}_{K(=1-\bar{X}_H)}$	$X_{K(=1-X_H)}$	E^* mV	$\bar{T}_K$ V F^{-1}	$\bar{T}_H$ V F^{-1}
0.05000	1.0	1.0	-32.96 ± 0.03	1	0
0.02600	0.8	52	- 8.25 ± 0.02	0.639	0.361
0.01500	0.6	30	- 1.79 ± 0.05	0.513	0.487
0.01215	0.5	0.5	0	–	–
0.00825	0.4	0.165	3.11 ± 0.02	0.453	0.547
0.00245	0.2	0.049	4.56 ± 0.01	0.222	0.778
0	0	0	4.89 ± 0.03	0	1

* E at 1000 mL min^{-1}

$$\bar{T}_H = \frac{E - (\frac{RT}{zF}) \log \frac{[K]''}{[K]'}}{(\frac{RT}{zF}) \log \frac{[H]''.[K]'}{[H]'.[K]''}}$$

Figures (6-1) and (6-2)

Legend

A	Main part of cell (half cell shown here)
B	B10 to fit flowmeter
C	B10 to fit electrode chamber
G	Flowmeter
H	Electrode chamber
D and E	Two units designed to give freedom to move the flow tube
I	Flow tube
F	Membrane holder
J	Solution reservoir
K	Thermometer
L	Constant head device
N	Ag/AgCℓ electrode
P	Glass coil to heat up or cool the solution

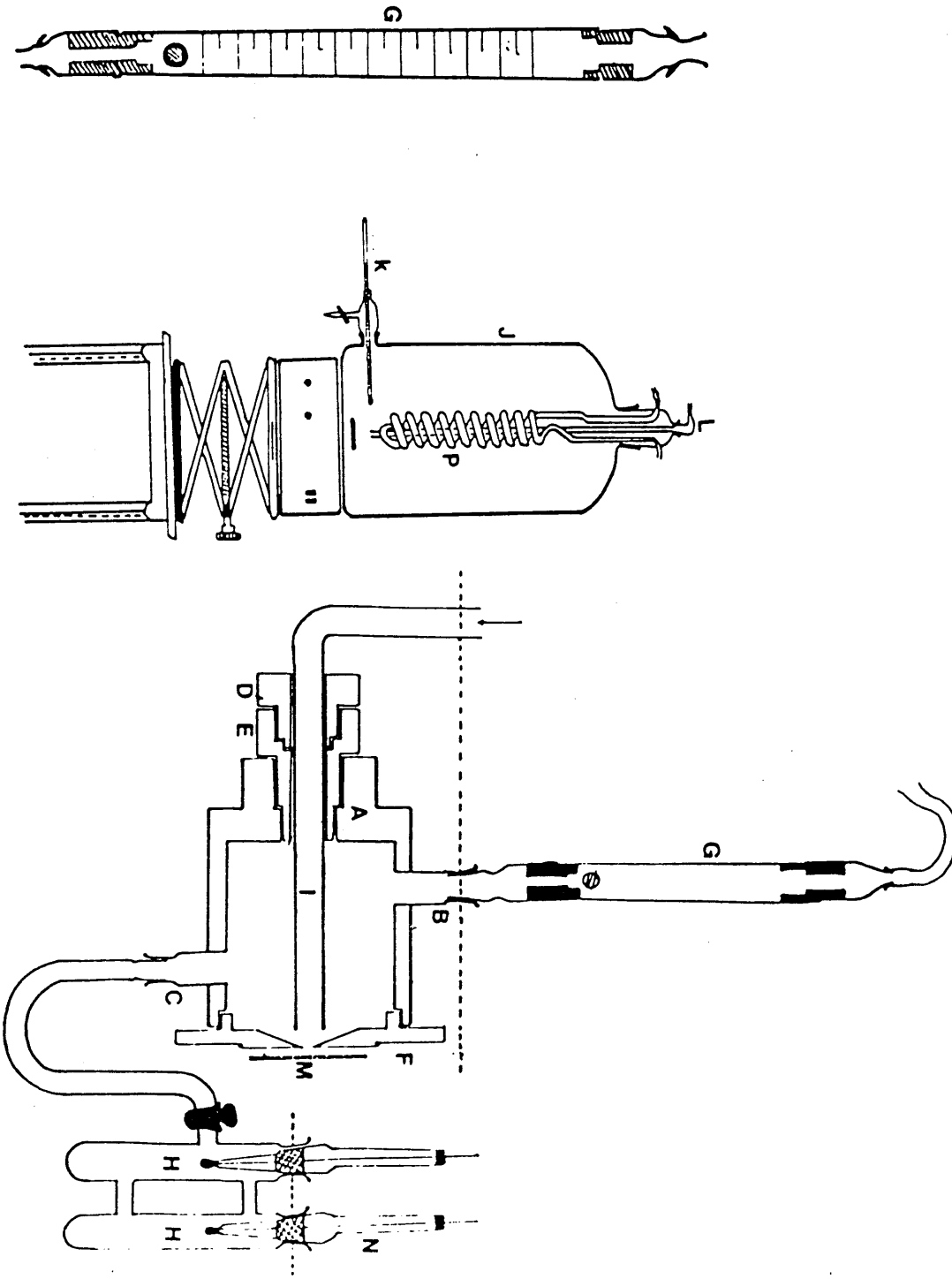

Figure (6-1)

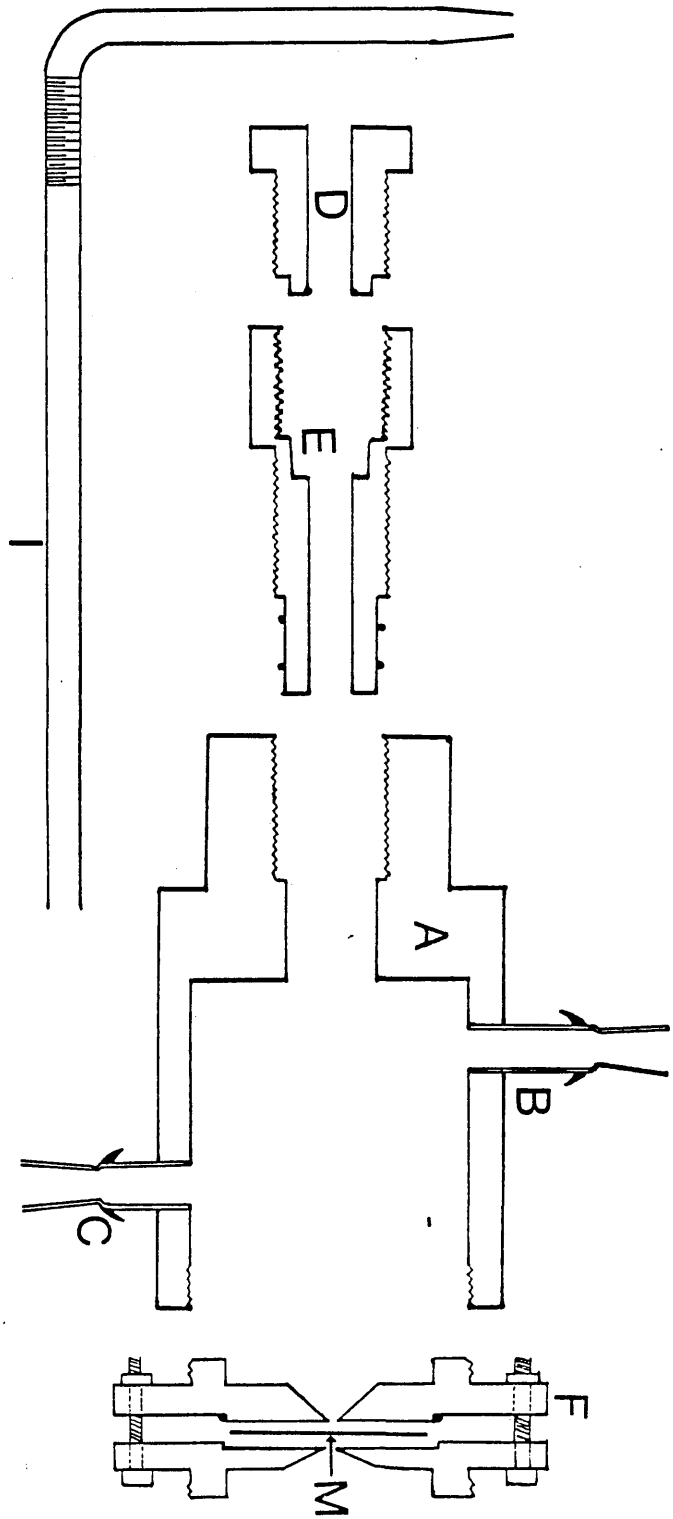

Figure (6-2)

Figure (6-3)

Zero voltage test for the cell

$$Ag/AgC\ell|0.1M\ KC\ell|membrane|0.1M\ KC\ell|AgC\ell/Ag$$

The membrane was Nafion 125 perfluorosulphonic acid membrane and a constant flow rate, Q, 500 mL min^{-1} was maintained.

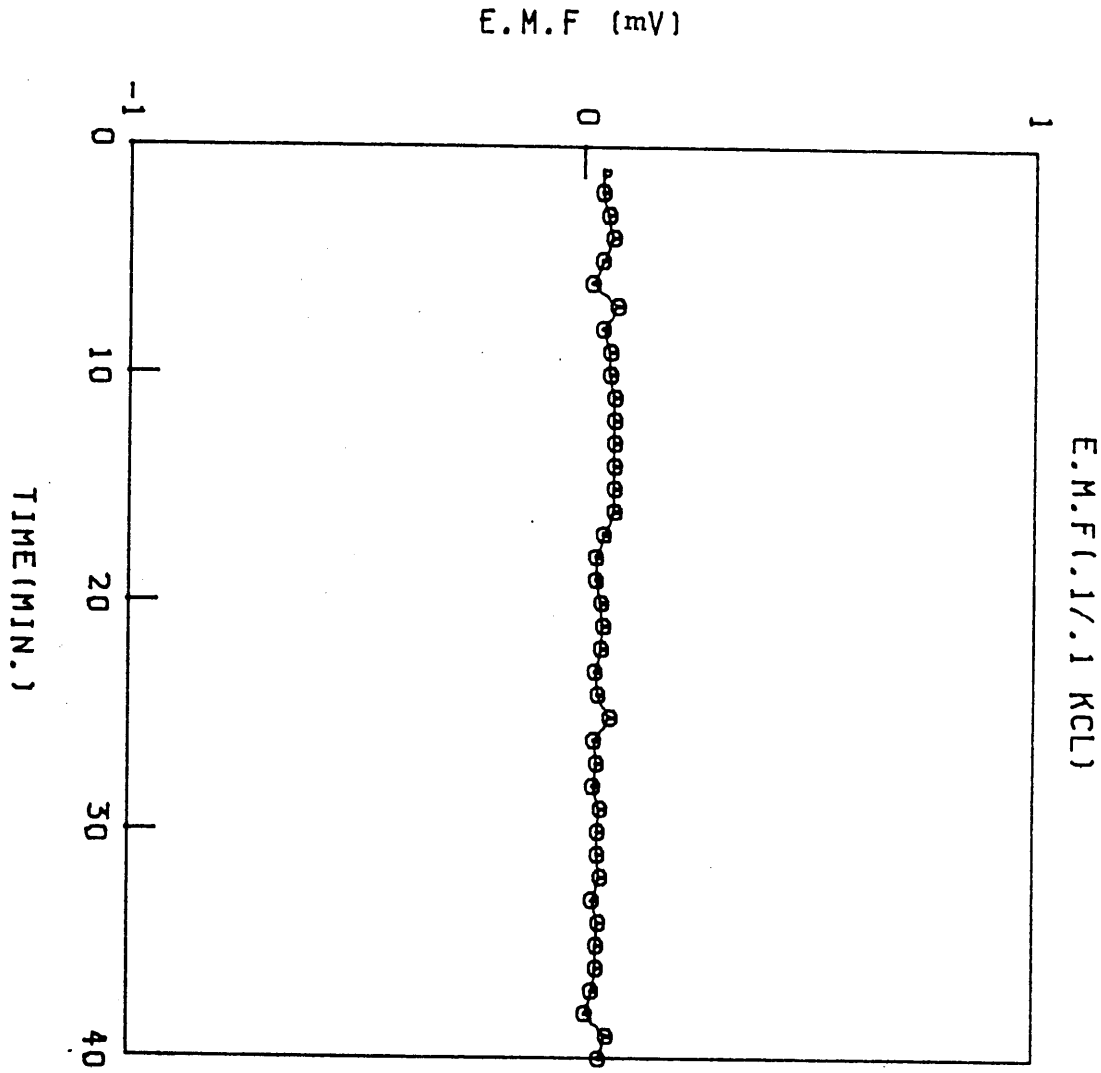
E.M.F (mV)
-1
0
1
0
10
20
30
40
TIME(MIN.)
E.M.F(.1/.1 KCL)

Figure (6-4)

EMF as a function of flow rate of the solution mL min^{-1}.

Figure (6-5)

EMF as a function of reciprocal of the flow rate, $\sqrt{Q}$.

Membrane: Nafion 125 in K-form

Solutions: 0.01/0.02M KCℓ

Membrane diameter exposed 0.3 cm.

Nafion 125 membrane (0.01/0.02) M KCℓ solution

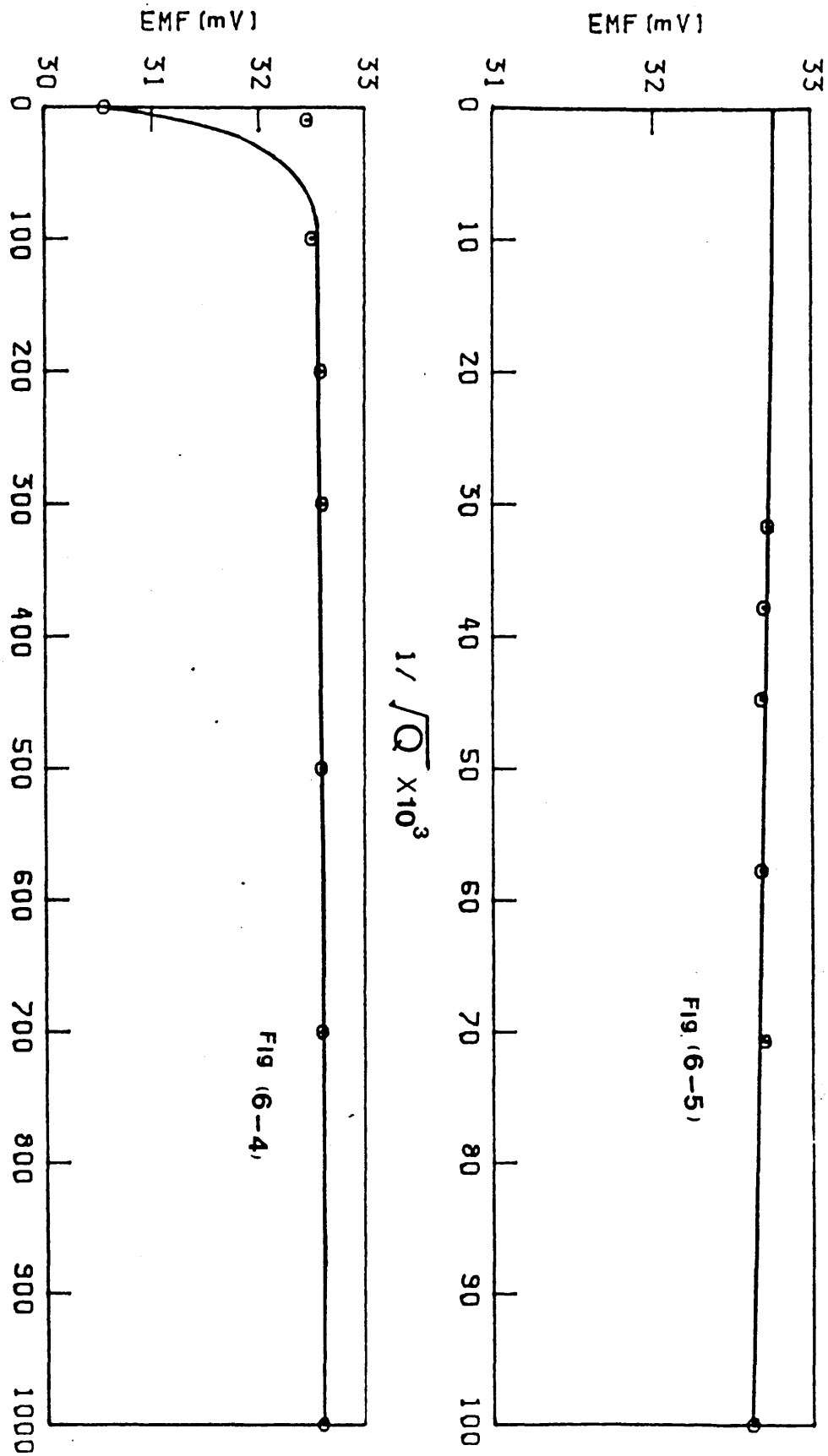

Fig (6-5)

Fig (6-4)

Figure (6-6)

A plot of the measured B.I.P. for a H^+/K^+ system with Nafion 125 membrane in which the total ionic strength in solution was maintained constant, 0.05M.

The solution on the RHS was held constant at $X_K = 0.245$ ($\bar{X}_K = 0.50$) while in a series of measurements in which the LHS solution was changed progressively, as shown.

- ● $X_K = 1.00$ ($\bar{X}_K = 1.00$)
- ⧗ $X_K = .520$ ($\bar{X}_K = 0.80$)
- ▲ $X_K = .300$ ($\bar{X}_K = 0.60$)
- ■ $X_K = 0.165$ ($\bar{X}_K = 0.40$)
- ◆ $X_K = 0.049$ ($\bar{X}_K = .20$)
- • $X_K = 0.00$ ($\bar{X}_K = .00$)

The corresponding ionic fractions of potassium ion in the equilibrium surface of the membrane are shown ($\bar{X}_K$) in brackets. Data of Chapter 8.

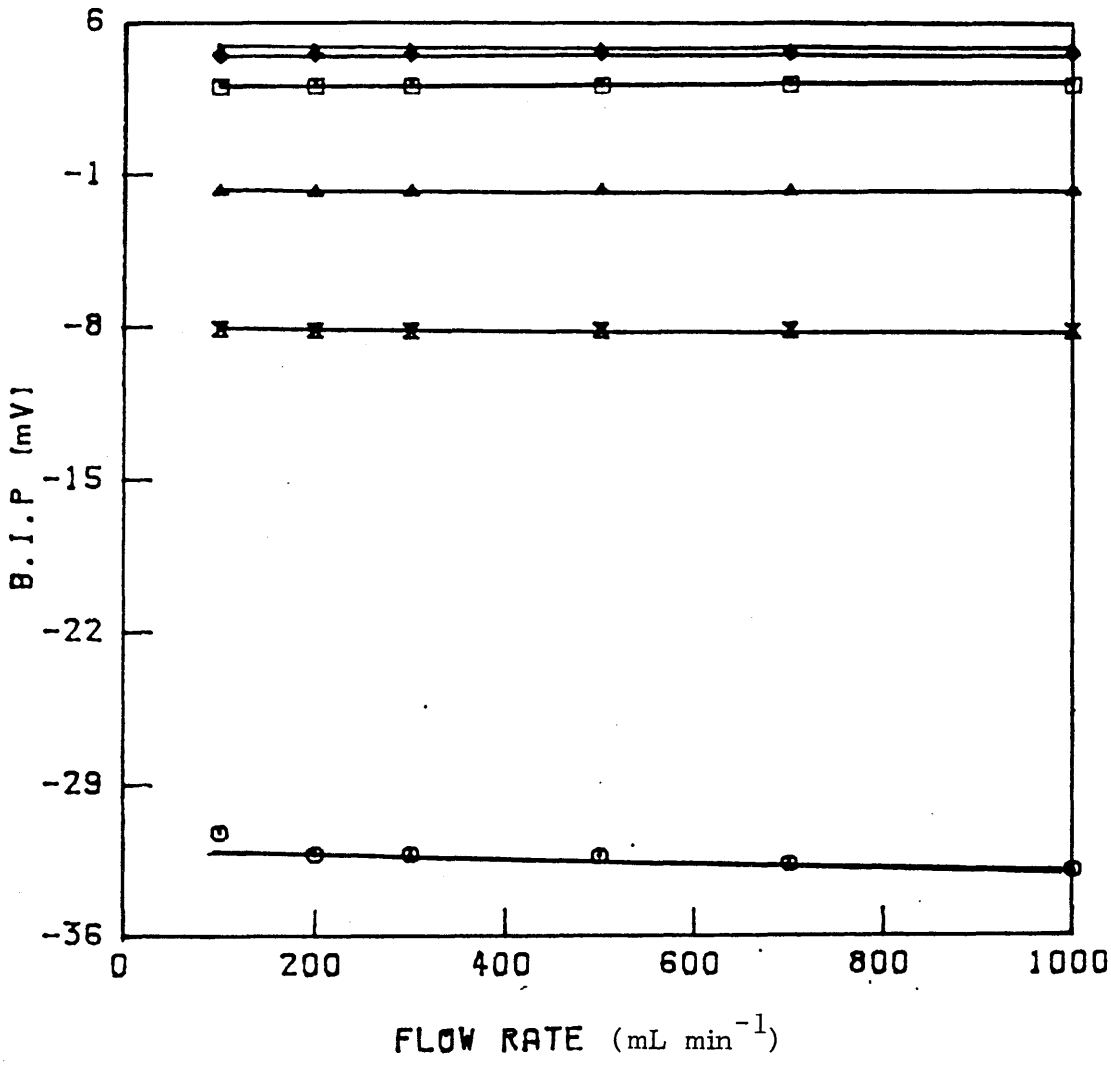
6
-1
-8
-15
-22
-29
-36
B.I.P (mV)
0
200
400
600
800
1000
FLOW RATE (mL min^{-1})

Figure (6-7)

B.I.P. for H^+/K^+ system, with Nafion 125 membrane, as shown in Table (6-9), for maximum flow rate 1000 mL min^{-1}. The abscissa is the ionic fraction of K^+ in the mixed H^+/K^+ solution on the LHS of the cell (as shown in the text), measured against the standard reference solution.

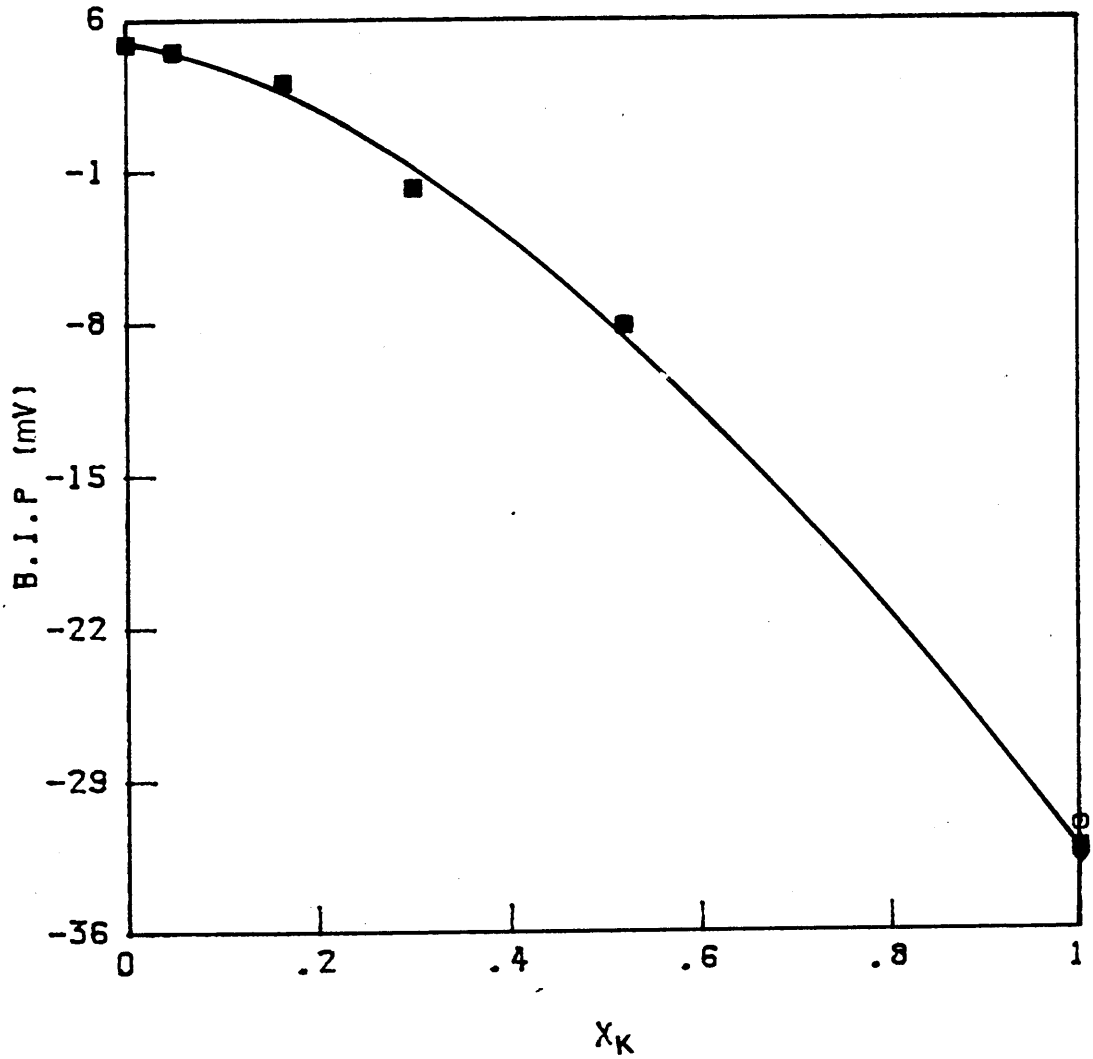
6
-1
-8
-15
-22
-29
-36
B.I.P (mV)
0
.2
.4
.6
.8
1
X_K

Figure (6-8)

Integral transport numbers, $\bar{T}_i$ in Nafion 125 perfluorosulphonic acid membrane in H^+/K^+ mixed form ($\bar{X}_H = \bar{X}_K = 0.5$) against equivalent fraction of K^+ in the membrane $\bar{X}_K$.

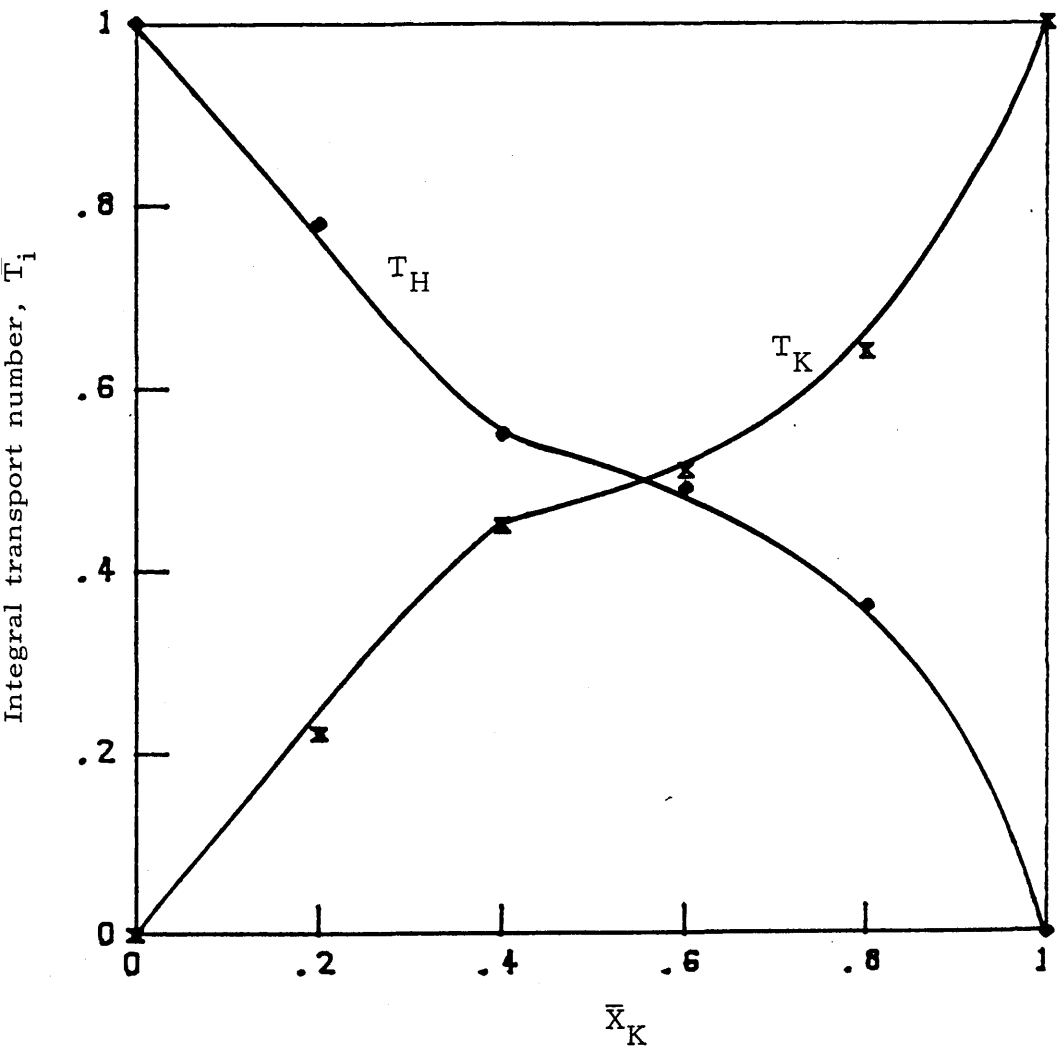
1
.8
.6
.4
.2
0
0
.2
.4
.6
.8
1
T_H
T_K
Integral transport number, $\bar{T}_i$
$\bar{X}_K$

References

1. K. Sollner, J. Phys. Chem., 53, 1211 and 1266 (1949).
2. K. Sollner, S. Dray, E. Grim and R. Neihof, in 'Ion Transport Across Membranes', Eds. H.T. Clarke and D. Nachmansohn, Acad. Press, N.Y., p.144 (1954).
3. D. Mackay and P. Peares, Koll.-Zeit., 171, 139 (1960).
4. J.C. Hipfner, M.Sc. Thesis, University of Western Ontario, (1970).
5. C.R. Gardner, Ph.D. Thesis, University of Glasgow, (1970).
6. C. McCallum, Ph.D. Thesis, University of Glasgow, (1971).
7. J.W. Lorimer, E.I. Boterenbroad and J.J. Hermans, Discuss. Faraday Soc., 21, 141 (1956).
8. J.G. Ives and G.J. Janz, 'Reference Electrodes , Theory and Practice', Acad. Press, N.Y., (1961).
9. H.S. Harned and B.B. Owen, 'Physical Chemistry of Electrolytic Solutions', Amer. Chem. Soc. Monogr. No. 137, Reinhold, N.Y., p.490 (1958).
10. R. Paterson, in Pontificae Academiae Scientiarum Scripta Varia, 40, 517 (1976).
11. K.S. Pitzer and J.J. Kim, J. Am. Chem. Soc., 96, 5701 (1974).
12. P. Meares and A.H. Sutton, J. of Colloid and Interface Sci., 28, 118 (1968).
13. R.S. Yeo and A. Eisenberg, Poly. Prepr., 16 104 (1975).

CHAPTER 7

Diffusion and Permeability by the Time-Lag Method

7.1 INTRODUCTION

In gas diffusion studies the time-lag method is commonly used to determine both the diffusion coefficient and the permeability of gases in polymer membranes. It was first used by Daynes (1). Typically a test membrane is mounted between two halves of an evacuated cell. To begin the experiment, gas is admitted to one side of the cell. Constant pressure is established almost immediately, defining $t=0$. The quantity of gas permeating $Q(t)$ into the other half of the cell may then be measured by monitoring the pressure increase in that half with time. The steady state flow $\dot{Q}(t)$ is obtained after a sufficient length of time. From this the permeability, P, is obtained, eqn. (7-3) and the corresponding diffusion coefficient, from time-lag τ, eqn. (7-2), see Fig. (7-3).

The method is convenient, rapid and relatively accurate. Till recently (2) it has not been possible to use it for membrane diffusion processes in condensed systems in which the permeant was dissolved in a liquid. This was because it is a technique which depends upon producing well-defined boundary conditions and, in particular, creating a sharp concentration step at time zero.

In this laboratory, these problems were overcome using a new technique employing solution sprays (3). A membrane cell was designed in which one side of a test membrane was in contact with a small volume of solvent or test solution. As a preliminary to the diffusion experiment, the other side of the membrane (which was open to the air) was sprayed with the same solvent or test solution and equilibrium conditions were

established. To begin the experiment the first spray was switched off and 'simultaneously' a second spray containing diffusant switched on. In this way a well-defined concentration step was applied to the outer membrane surface and the diffusion experiment began with precise initial conditions. Independent tests showed that the concentration step could be made in less than a tenth of a second (3). For electrolyte diffusion studies a pair of conductivity electrodes were used to monitor ionic concentrations in the solution-filled half of the cell as diffusion proceeds.

Because the electrical conductivity of electrolyte solutions are strongly temperature dependent, careful temperature control of sprays and test solutions is required.

Since the major topic of this thesis is the transport properties of bi-ionic forms of charged membranes, it was decided to apply this method to such problems (and the related oscillatory wave method (3), next chapter) to obtain interionic exchange diffusion coefficients during the ion exchange process. To evaluate the technique, salt diffusion experiments were repeated using Visking dialysis membranes, Nafion 125 perfluorosulphonic acid membranes and AMF C60 sulphonic acid ion exchange membranes, for which a considerable amount of transport data was known from previous studies in this laboratory (4-12). The last two membranes were used in mixed potassium-hydrogen forms in which potassium/hydrogen concentration is 3/1.

The basic design of the experiments with Nafion 125 was to determine the interdiffusion coefficient for hydrogen/potassium ion, in a membrane in which these ions were at equal concentration, 50% in each.

Previous studies to determine the selectivity coefficient for this exchange over the complete range of loadings (Table (4-1)) defined the composition of the equilibrium solution required. To obtain loading of 50% for each ion the equilibrating solution was richer in hydrogen ion than potassium since this Nafion 125 perfluorosulphonic acid membrane selects potassium ion over hydrogen. The sprayed solutions were either HCℓ or KCℓ or mixed H^+/K^+ solutions (0.05M) which provided well-defined compositions on the outer membrane surface. When these were made to be different from the inner solution, which maintained a 50:50 loading in hydrogen and potassium, on the inner membrane surface, an ion exchange diffusion process was initiated:

$$H^+ + RSO_3^-K^+ \rightleftharpoons K^+ + RSO_3^-H^+$$

Previous analysis had shown that the exclusion of chloride (coion) was virtually complete for the test solutions used here, in which the total ionic strength was always 0.05M. Since chloride is not involved in the exchange process under these conditions, it was possible to follow by measuring the electrical conductivity of the cell solution as a function of time. Calibration tests showed that the method was sufficiently sensitive for this work due to the large difference in the mobilities of hydrogen and potassium ions. (This, to a large degree, was the reason for their choice). In a typical experiment, conductivity changes were ≈5%. Since the conductivity of the electrolyte is itself temperature dependent (≈1% per degree), very careful temperature control was required, particularly with the sprays.

7.2 Theory of the Time-Lag Method

The time-lag method is standard for gaseous diffusion and so its application to a liquid system posed only technical problems. By spray techniques the solution in contact with the outer surface may be stepped up or down sharply from the equilibrium value to a new level, which if maintained creates a concentration step. If we assume that there are no significant unstirred layers of solution on the side being sprayed and that efficient stirring will remove them effectively in the collecting volume, the problem of implementation reduces to a decision on the optimum exposed area for the membrane and the size of the collecting volume itself.

Most applications of the time-lag method use a mathematical solution valid for an infinite collecting volume. In practical applications changes in pressure or concentration in the collecting volume are used to determine the quantity of permeant diffused and these are most easily and accurately measured if the collecting volume is small. This strictly irrational situation is normally resolved by choosing a collecting volume which, although finite and small enough to allow accurate pressure/concentration measurement, also remains large enough in relation to the system parameters to ensure that the errors due to the application of the infinite volume analysis to a limited volume system remain acceptably small.

If a planar membrane, area A, thickness ℓ, is exposed to a concentration step Δc, the quantity of that solute which will have permeated at time t, Q(t) is approximated by eqn. (7-1) (for an infinite collecting volume) at large times

$$Q(t) = \frac{AD\Delta\bar{c}}{\ell}\left(t - \frac{\ell^2}{6D}\right) \qquad (7\text{-}1)$$

where D is the diffusion coefficient and $\Delta\bar{c}$, the difference in permeant concentration in the membrane phase from outer to inner surface. In the simplest experiments, diffusion is against solvent on the inner side and $\Delta\bar{c}$ becomes simply $\bar{c}$ the value at the outer surface. The ratio $\bar{c}/c = \alpha$, the distribution coefficient, defined as the ratio of membrane to solution concentrations at equilibrium (in this paper barred symbols represent quantities in the membrane phase). From eqn. (7-1) it is obvious that a plot of Q(t) against time, t, will be linear at large times (when the system is in a steady state) and have slope $AD\Delta\bar{c}/\ell$ and intercept on the time axis, τ, according to eqn. (7-2)

$$\tau = \ell^2/6D \qquad (7\text{-}2)$$

The linear portion of the plot, see Fig. (7-3) is obtained from the slope at times $\geqslant 2.5\ \tau$ (13-15). Eqns.(7-1) and (7-2) were obtained for infinite bath conditions. For most measurements Q(t) is determined by measurement of concentration (or pressure for gaseous studies) in a collecting volume of finite volume, V, since $c = Q(t)/V$ (and pressure = $Q(t)RT/V$).

From the slope $\dot{Q}(t)$, the steady state flow, $J = \dot{Q}(t)/A$, defines the permeability, P (Eqn. (7-3))

$$J = D\Delta\bar{c}/\ell = P\Delta c \qquad (7\text{-}3)$$

where

$$P = (D\Delta\bar{c}/\Delta c)/\ell \qquad (7\text{-}4)$$

(If permeant diffuses against solvent, eqn. (7-4) becomes $P = D\alpha/\ell$).

It is necessary to determine the system parameters which will allow confident application of these equations for systems with finite collecting volumes, V. The parameters of free choice are time t, membrane area under test A, and collecting volume V. Those over which the experimenter has little or no control are such factors as membrane thickness ℓ, and the parameters to be measured, diffusion coefficient D, distribution coefficient α, or permeability, P.

The limited volume problem may be solved analytically either by use of Laplace transforms or non-orthogonal sine series, as shown in the Appendix A.7.6. This analysis becomes indistinguishable from the infinite volume case, if eqns. (7-6,7) are satisfied. In eqn. (7-7), t_f is the upper time limit for agreement, which should exceed 3τ, as discussed below.

$$\alpha A\ell/V \ll 1 \qquad (7\text{-}6)$$

and

$$t_f \ll \ell V/(\alpha AD) \qquad (7\text{-}7)$$

Jenkins et al., (15) have given different conditions which stress only requirements for linearity in Q(t) vs. t. In designing experiments aimed at a precision of $\approx$1% in diffusion coefficient and permeability, the adjustable parameters, A and V, need to be chosen to reduce $\alpha A\ell/V$ to $\leqslant 0.01$ and to increase t_f to $\geqslant 6\tau$. The first limitation, eqn. (7-6), is

the more stringent. For the experimental dialysis membrane $\alpha A\ell/V$ is typically 0.005, while $t_f \approx 3.10^4$ s. For salt diffusion from dilute solutions through ion exchange membranes eqn. (7-6) proves even less limiting since the distribution coefficient α, is very small due to Donnan exclusion.

7.3 EXPERIMENTAL

7:3:1 Diffusion cell

The diffusion cell was made from a rectangular block of Perspex of dimensions 3.3 x 4 x 8 cm^3. This was drilled horizontally and vertically to provide two intersecting cylinders, Fig. (7-1). The vertical one was plugged at the bottom to hold a "Spin fin" stirrer (Bel Art) which was driven magnetically from outside the cell. The upper portion of the vertical tube was threaded and sealed with a Teflon screw top which held a pair of platinised platinum wires which served as conductance electrodes. The bottom of this screw top was a hemispherical hollow to improve mixing in the cell. It also contained a capillary to aid the removal of entrapped bubbles. The horizontal hole passed through the block. On one side, Fig. (7-1b) it defined the exposed membrane area, 0.771 cm^2, on the other it too was threaded and sealed with a Teflon screw, which held two thermistors, one used as temperature probe and the second as a heater.

The cell, which held a solution volume 2 mL, was bolted to a large Perspex (spray) box. The membrane aperture was defined by the coincident holes in the cell and a flanged template, Fig. (7-1).

7.3.2 Spray assemblies and their use

The sprays used were two plastic nozzles manufactured by Shandon Southern Products Ltd., which were not subject to corrosion by the acid. These were operated by a 30 psi compressed air supply which was laid on as a service to the laboratory. A coarse spray of solution was produced immediately when this air supply was connected to the spray heads. The air jet was directed across the mouth of the tube containing the solution at right angles to it. To ensure minimum delay in generating the spray, a small but steady trickle of solution was allowed to flow from the solution filled tube, when not in use. The jet spray was then formed immediately when the compressed air was switched on.

Switching from one spray to another was performed by a small computer which opened and closed solenoid valves. The computer system also provided the time base and was programmed to read the electrical conductivity of the cell solution at preset intervals. The sprays were mounted on rods which could be wound back and forward to move the sprays nearer or further from the face of the membrane. This was required for temperature control.

7.3.3 Solenoids

The solenoids were manufactured by R.S. Supplies. They were opened or shut by signals sent from a microcomputer by means of soft switches. The algorithm for switching is given in Fig. (7-10) and the program derived therefrom is given in Appendix A.7.1. The

The computer had an inbuilt clock which was used as a timer to switch the solenoids on and off at predetermined times as required.

7.3.4 Temperature Control

As noted in the Introduction, accurate temperature control of the sprays and the diffusion cell was particularly important. The requirement was not so much due to the basic sensitivity of the membrane diffusion coefficients to varying temperature, but to the method of detection. Here electrical conductivity was used, and during a typical exchange diffusion experiment it might change no more than 5%, due to diffusion, but would vary also by $\approx$1%/°C for a change in temperature. Since temperature fluctuations of several degrees could easily occur on switching sprays, special attention was needed.

Considerable adiabatic cooling occurred when solutions were sprayed. To counter this, 2 litre flasks of stock solutions were maintained at a suitably high temperature, $\approx$40°C, in a water thermostat placed $\approx$1m from the spray jets. The solution-filled tubes leading from the stock flasks and the air line to each spray were also thermostatted with hot water. In this way, by carefully controlling the temperature of the thermostat, the distance of the jets from the membrane surface (18 cm) and the circulation of water, it was possible to maintain the jets at 25 ± 1°C and eliminate any significant temperature fluctuation when the sprays were switched to create the concentration step. The spray temperatures were measured on a digital thermometer placed close to the exposed membrane surface.

Temperatures inside the cell were measured by a thermistor and logged on the computer. A test in which the two sprays were identical proved the efficiency of these methods, (Fig. 7-2a,b).

7.3.5 Operation of the Diffusion Cell

The diffusion cell was assembled with the (blotted) membrane in position and quickly filled with degassed solution. In all cases the membrane had been pre-equilibrated with this solution. The conductivity electrodes mounted in a Teflon screw plug were fitted. The excess solution was displaced through a fine capillary in the plug itself. In this way the cell was filled completely and contained no air bubbles. The electrodes were platinised platinum wires which were passed through the plug and cemented in place. The membrane surface was sprayed by the same solution as that in the cell at 25°C. Since the diffusion cell was made from a single block of Perspex, some difficulty was found in adjusting the cell solution to 25°C initially. For this purpose a second thermistor was fitted. This was used as a small electrical heater. Using an external source, small currents were passed and the solution temperature raised as required. An initial condition of equilibrium was established. To ensure this, the solution temperature and conductivity within the cell were monitored and shown to be constant for at least 20 minutes before switching to the second spray and starting the experiment.

7.3.6 Data Acquisition and Handling

The experiment was performed under computer control. During the experiment a PET microcomputer monitored both the conductivity of the cell solution and its temperature at regular intervals, usually 15s, but chosen freely as needed. The cell conductivity was measured on a Wayne-Kerr conductivity bridge (type B905A) to a precision of ±0.05%. The conductance bridge was linked to the computer via a IEEE 488 interface. The controlling program is listed in Appendix A.7.2. The conductivity measurements were converted to solution compositions using data from separate calibration experiments (Table (7-6)). In most experiments several hundred compositions and times were collected. These were transferred from the PET computer, where they were stored on magnetic tape, to Apple II+ computer where they were transferred to disk storage. In this form they were suitable for plotting on a digital plotter (Watanabe Digiplot), printing, and processing. In this case least-square linear curve fitting. The standard programs used for these processes are given in Appendices A.7.3, A.7.4 and A.7.5.

7.4 Test of the System

A membrane was clamped into the diffusion cell (Fig. (7-1)). The conductivity and temperature of the solution within the diffusion cell was monitored. The membrane was first sprayed with a solution at a concentration equal to that in the filled cell, until the system was shown to be at thermal and chemical equilibrium. It was then consecutively sprayed at equal times with solution A and solution B. The

cell solution and the sprayed solutions A and B were identical. Typical results are shown in Figs. (7-2a) and (7-2b).

7.5 RESULTS AND DISCUSSION

Data were Collected by Computer

Computers are capable of rapid calculations and can store large amounts of data. Probably one of the most important features is their ability to communicate with the outside world by accepting codified electrical signals from measuring devices or sensors.

In the diffusion cell, the conductance, G needed to be measured at time intervals, which the computer can do by monitoring the conductance through an interfaced conductivity bridge. Time was generated by a real-time clock in the computer and the results can be stored and recalled for further calculation or for plotting purposes, as required. These data were required to transfer from the PET computer where they were collected and stored on magnetic tape to Apple II+ computer where they were transferred to disk storage. In this form they were suitable for plotting on a digital plotter (Watanabe Digiplot). A sample of raw results is shown in Table (7-1).

7.5.1 Salt Diffusion

The time-lag method was tested by determining salt diffusion through uncharged Visking dialysis membrane, using a concentration step wave (i.e. spray with distilled water and then spray with salt solution). To measure the salt flow of sodium chloride solution, the

membrane was placed in distilled water which frequently changed for several days prior to being used in the experiment. The membrane was placed in the cell and sprayed with distilled water and the conductance in the collecting volume was continuously monitored, only when it had stayed constant for a period of the same order as the time for which the membrane was sprayed with salt solution. The run was started by spraying the membrane with salt solution (0.05M NaCℓ). After a sufficient period of time a pseudo-steady state condition was obtained and conductance increased linearly with time. This linear portion cut the time axis at $\tau = \ell^2/6D$ (eqn. (7-2)), and from this cut-off (knowing the membrane thickness, ℓ cm), the diffusion coefficient, D, can be found. Results from these runs are given in Table (7-3). The resultant diffusion coefficients were reproducible to ± 10%. A computer simulation of actual experimental results was run using data for a Visking dialysis membrane obtained from an experimental run (Table (7-2)). This simulation was compared with the experimental run itself and the result shown in Fig. (7-3).

Earlier work done on the same Visking dialysis membrane (2) at 0.13M potassium chloride gave diffusion coefficient, $D_{KC\ell}$, 2.75×10^{-6} $cm^2.s^{-1}$, compared with work which used 0.05M NaCℓ and gives $D_{NaC\ell}$ 2.95×10^{-6} $cm^2.s^{-1}$.

7.5.2 Interionic Diffusion

Interionic diffusion of H^+/K^+ in commercial electro-dialysis ion-exchange membranes. Two membranes were used, the first being AMF C_{60} graft copolymer membrane, manufactured by American Machine and Foundery Company, Springdale, Connecticut, U.S.A. This membrane is prepared from low-density polyethylene, containing 35% styrene (sulphonated) and up to 2% divinylbenzene. The second membrane was the perfluorosulphonic acid membrane (E.I. du Pont de Nemours and Co.), where the co-ion uptake in 0.05M mixed HCℓ + KCℓ solution is < 1%. The ionic exchange process therefore is solely for cations, eqn. (7-8)

$$H^+ + ROSO_3^- K^+ \underset{2}{\overset{1}{\rightleftharpoons}} ROSO_3^- H^+ + K^+ \qquad (7\text{-}8)$$

When the membrane, contacting on the inner side with a mixture (0.025M HCℓ + 0.025M KCℓ) is sprayed from the outer side with either 0.05M HCℓ or 0.05M KCℓ, the conductivity in the collecting volume will either rise or fall, depending on whether the exchange is in direction 1 (gave D_{HK}) or 2 (gave D_{KH}) as defined by eqn. (7-8) and Figs. (7-4), (7-5).

From the time-lag runs, graphs of conductance G against time were obtained, Figs. (7-6) and (7-7), which by using eqn. (7-2) immediately gave the diffusion coefficient, D. The slope $\frac{dG}{dt}$ could be converted from conductance per second to rates of change of concentration, $\frac{dc}{dt}$. To achieve this we required to calibrate the cell

over the complete range of concentrations used.

A series of standard mixtures of HCℓ + KCℓ solutions at a total concentration of 0.05M were prepared using precise conductivity measurements (Table (7-6)). A linear relationship of conductance, G to the composition of X_H in the solution was obtained (Fig. (7-9)) from the slope and the intercept. We can use these data in the actual cell to determine the quantity of ions exchanged, as follows:

$$G = m\, c_H + c \tag{7-9}$$

where G is the conductance in mmho, m the slope, c_H the HCℓ concentration in the mixed solution and c a constant.

Equation (7-9) may be rearranged,

$$G - G^o = m(c_H - c_H^o) \tag{7-10}$$

where G^o and c_H^o are the conductance and concentration of HCℓ in the standard solution. Dividing eqn. (7-10) by G^o, we obtain,

$$\frac{G - G^o}{G^o} = \frac{m}{G^o}(c_H - c_H^o) \tag{7-11}$$

Differentiating eqn. (7-11) with respect to t, we obtain,

$$\frac{dG/G^o}{dt} = m^* \frac{dc_H}{dt} \tag{7-12}$$

where $m^* = \frac{m}{G^o}$ which should be independent of the cell used.

Eqn. (7-12) now becomes,

$$\frac{dG}{dt} = m^* G^o \frac{dc_H}{dt} \tag{7-13}$$

Since all experiments were conducted at 0.05M total ionic strength,

$$c_H + c_K = 0.05 \tag{7-14}$$

$$\frac{dc_H}{dt} + \frac{dc_K}{dt} = 0 \tag{7-15}$$

Therefore the flux of ions in the steady state for each ion is equal in magnitude but opposite in sign (direction)

$$\dot{Q}_H = \frac{dc_H}{dt} \cdot V \quad \text{and} \quad \dot{Q}_K = \frac{dc_K}{dt} \cdot V$$

where V is the cell volume, since the steady state flux through the membrane is

$$f = \dot{Q}_H \tag{7-16}$$

The flux density, J can be obtained (knowing the cell volume, V and the membrane exposed area, A), eqn. (7-17).

$$J = \frac{dc_H}{dt} \cdot \frac{V}{A} \tag{7-17}$$

We may solve for $\frac{dc_H}{dt}$ from eqn. (7-13) and substituting eqn. (7-17) we obtained

$$J = \frac{1}{m^* G^o} \cdot \frac{dG}{dt} \cdot \frac{V}{A} \qquad (7\text{-}18)$$

where G^o is the conductance of the reference solution $\overline{50}/\overline{50}$ and $\frac{dG}{dt}$ the experimental slope of Figs. (7-6) and (7-7). From the flux in the steady state, J, we can obtain the permeability and diffusion coefficient as follows:

$$P = J/\Delta c \qquad (7\text{-}19)$$

$$\bar{D} = \frac{\ell . J}{\Delta \bar{c}} \qquad (7\text{-}20)$$

where ℓ is the membrane thickness in cm.

Typical experimental results are shown in Figs. (7-6) and (7-7), respectively. These graphs show a constant linear steady initial conductance. The switching on of the second spray solution to start the diffusion run is indicated by a line stroke on the time axis (t=0). To determine τ, eqn. (7-2), the intercept of the two linear portions of the graphs was required.

A short computer program was written which included a linear least square fitting routine, (Appendix A.7.5). By inspection of the plotted data, suitable portions were chosen to represent the best linear regions and from the mark of switching of the second spray (t=0) and the intercept gives τ. The resultant was used directly to

obtain the diffusion coefficient, eqn. (7-2), and the slope $\frac{dG}{dt}$ was proportional to the change in the relative concentration of H^+ and K^+ in the cell, which is required to convert from mmho per second to mole per second.

A wealth of experimental results has been collected for these membrane systems and is given in Tables (7-4) and (7-5). The average of these are reproducible to ± 3-8%.

Earlier interionic diffusion runs done on Nafion 125, when the membrane, sprayed with 0.05M KCℓ, eqn. (7-8), and its inner surface in contact with a mixed solution of 0.025M HCℓ + 0.025M KCℓ (which gave unequal loading of H^+ and K^+ ions in the membrane, i.e., $\bar{X}_H = 0.25$ and $\bar{X}_K = 0.75$). The resulting interionic diffusion coefficient, D_{KH}, was 5.42×10^{-7} cm^2 s^{-1} ($\pm 0.20 \times 10^{-7}$) while, when sprayed with 0.05M HCℓ and its inner surface in contact with the same solution (as above) the diffusion coefficient, D_{HK}, was 6.51×10^{-7} cm^2 s^{-1} ($\pm 0.11 \times 10^{-7}$), (Table (7-5)). The two diffusion coefficients were not expected to be equal in these two experiments since the membrane was studied with quite different loadings of H^+ and K^+ ions.

For the main experiment we chose to equilibrate the Nafion membrane with 0.012M KCℓ + 0.038M HCℓ, at a total concentration of 0.05M, which gave equal loading of H^+ and K^+ ions in the membrane phase ($\bar{X}_H = \bar{X}_K = 0.5$). This composition was obtained from corresponding equilibrium data for HCℓ + KCℓ exchange on Nafion membrane previously obtained (Chapter 4, Table (4-1), Fig. (4-1)).

At equilibrium the cell and spray solution were of this standard composition. To perform a diffusion experiment, the first

spray was switched off and the second spray immediately turned on. The switching over at the membrane surface was ≈ 0.1s. Several such spray solutions were employed since the diffusion flux is, as observed above, dependent on the membrane composition. These spray solutions were such as would give a H^+/K^+ loading on the outer membrane surface in the run, Fig. (7-11). $\bar{X}_H/\bar{X}_K$ = 80/20; 60/40; 50/50; 40/60; 20/80; 0/100.

Since all solutions were mixtures of HCℓ + KCℓ at total concentrations of 0.05M, the membrane contained only K^+ and H^+ ions (co-ion uptake of chloride was negligible).

For convenience and clarity, further reference to a particular solution will be given solely as X_H or $\bar{X}_H$, the ionic fractions of hydrogen ion in the solution and membrane respectively.

Typical results of this experiment were shown in Table (7-7); average data of 4-6 runs for each solution used gave τ, together with standard deviation reported.

The striking feature of this experiment is that although there is a considerable swelling on converting from the K^+ to H^+ forms, the interionic diffusion coefficients D_{HK} and D_{KH} are equal and relatively constant, 2.70×10^{-7} cm^2 s^{-1} ($\pm 0.04 \times 10^{-7}$), Fig. (7-8). It is notable also from earlier experiments on Nafion 125 membrane at unequal loading of H^+ and K^+ ions ($\bar{X}_H = 0.25$ and $X_H = X_K$ (solution)), that the interionic diffusion coefficients D_{HK} and D_{KH} are not equal then, Table (7-5), and that their values are almost double the interdiffusion coefficients obtained here from the time-lag when the inner membrane surface was equally loaded with H^+ and K^+ ions. The permeability, P,

eqn. (7-19) is also relatively constant, while calculated interdiffusion coefficients, eqn. (7-20), were in very poor agreement with that obtained directly from the time-lag, eqn. (7-2), apart from that at $\bar{X}_H = 0$ which agreed very well, Table (7-7).

These data obtained from the time-lag method will be compared with the oscillatory method in Chapter 8.

There is little or no comparable data in the litereature on these membranes. Will (16) has studied bromine (Br_2) diffusion in Nafion membranes for varying polymer equivalent weight membrane pretreatment and solute concentration. The electrolytes used in these experiments were 2M $ZnBr_2$ and 4M NaBr solutions, the Br_3^- being the predominant bromine species in such media, although molecular bromine (Br_2) would appear to be responsible for transport across the membrane. The measured diffusion coefficients of Br_3^- for Nafion 125 membrane are 1.78×10^{-7} cm^2 s^{-1} and 6.2×10^{-8} cm^2 s^{-1}, at room temperature.

The values of D increased with decreasing equivalent weight of the polymer and with decreasing solution concentration. This would support the view that membrane water content is an important factor in determining membrane diffusion coefficients.

The diffusion coefficients and solubilities of hydrogen, oxygen and nitrogen were examined using time-lag method (17) in dried Nafion 125 membrane. It was found that the acid form which contained more water than potassium form, had lower gas solubilities and greater gas diffusitivities than K-form.

The diffusion coefficient value for K-form Nafion was smaller than that for acid form. These comparisons show that the data obtained

by the time-lag method may be used for membrane characterization in liquid environments in much the same way as it has been applied traditionally for gas diffusion and permeability studies.

Table (7-1)

Sample of raw data collected by computer during a time-lag experiment

Time (s)	Conductance (ohm^{-1} cm^{-1})	Time (s)	Conductance (ohm^{-1} cm^{-1})
30	7.06E-03	758	7.044E-03
45	7.058E-03	773	7.044E-03
60	7.057E-03	788	7.045E-03
75	7.057E-03	803	7.043E-03
90	7.058E-03	819	7.043E-03
105	7.057E-03	834	7.045E-03
121	7.059E-03	849	7.044E-03
136	7.056E-03	864	7.043E-03
151	7.056E-03	879	7.042E-03
166	7.055E-03	895	7.043E-03
181	7.057E-03	910	7.043E-03
196	7.056E-03	925	7.043E-03
211	7.057E-03	940	7.042E-03
226	7.054E-03	955	7.039E-03
242	7.055E-03	970	7.036E-03
257	7.054E-03	986	7.034E-03
272	7.052E-03	1001	7.028E-03
287	7.053E-03	1016	7.022E-03
302	7.052E-03	1031	7.018E-03
318	7.052E-03	1047	7.014E-03
333	7.054E-03	1062	7.007E-03
348	7.05E-03	1077	6.999E-03
363	7.051E-03	1092	6.994E-03
378	7.051E-03	1107	6.987E-03
394	7.051E-03	1123	6.977E-03
409	7.049E-03	1138	6.971E-03
424	7.05E-03	1153	6.962E-03
439	7.049E-03	1168	6.953E-03
454	7.047E-03	1184	6.946E-03
470	7.05E-03	1199	6.939E-03
485	7.049E-03	1214	6.931E-03
500	7.048E-03	1229	6.923E-03
515	7.05E-03	1245	6.915E-03
530	7.047E-03	1260	6.905E-03
545	7.047E-03	1275	6.899E-03
561	7.047E-03	1290	6.893E-03
576	7.048E-03	1305	6.885E-03
591	7.047E-03	1321	6.877E-03
606	7.046E-03	1336	6.866E-03
621	7.046E-03	1351	6.861E-03
637	7.048E-03	1366	6.854E-03
652	7.047E-03	1381	6.847E-03
667	7.045E-03	1397	6.839E-03
682	7.044E-03	1412	6.83E-03
697	7.047E-03	1427	6.826E-03
713	7.046E-03	1442	6.819E-03
728	7.046E-03	1457	6.811E-03
743	7.042E-03	1472	6.803E-03

Table (7-2)

Typical experimental parameters for the diffusion cell and Visking dialysis membrane, with sodium chloride as diffusant.

Diffusion coefficient for sodium chloride	D	2.95×10^{-6} cm^2 s^{-1}
Membrane thickness	ℓ	0.0195 cm
Cell output volume	V	2.064 cm^3
Area of membrane exposed	A	0.771 cm^2
Distribution coefficient for sodium chloride	α	0.75

Table (7-3)

Diffusion coefficient and steady state fluxes obtained from the time-lag method using Visking dialysis membrane. The diffusant was 0.05M NaCℓ against water in the cell. Two experiments were carried out.

Time-Lag τ (s)	Salt Diffusion Coefficient $D_{NaC\ell}$ $cm^2\ s^{-1} \times 10^6$	Steady State Flux of Salt $J_{NaC\ell}$ $mol\ cm^{-2}\ s^{-1} \times 10^6$	Distribution Coefficient $\alpha = \bar{c}/c$ -
21.5	2.93	5.63	0.75
21.5	2.93	5.30	0.70

Table (7-4)

Experimental results obtained from the time-lag method by using C_{60} sulphonic acid membrane; thickness = 0.031 cm and area = 0.771 cm^2; the diffusants were 0.05M KCℓ and 0.05M HCℓ against 0.025M HCℓ + 0.025M KCℓ in the cell; total concentration is equal to 0.05M

Diffusant 0.05M KCℓ		
No. of Exp.	Time-Lag τ (s)	Diffusion Coefficient D_{KH} $cm^2\ s^{-1} \times 10^6$
1	62	2.58
2	64	2.50
3	62	2.58
		average 2.55 ± 0.05 3%
Diffusant 0.05M HCℓ		
No. of Exp.	Time-Lag τ (s)	Diffusion Coefficient D_{HK} $cm^2\ s^{-1} \times 10^6$
1	51	3.14
2	48	3.34
3	49	3.27
4	50	3.20
		average 3.24 ± 0.09 6%

Table (7-5)

Experimental results obtained from the time-lag method on Nafion 125 membrane; thickness = 0.0141 cm and area = 0.771 cm^2; the diffusants were 0.05M KCℓ and 0.05M HCℓ against HCℓ + KCℓ (HCℓ = KCℓ = 0.025M) in the cell ($\overline{X}_H$ = 0.25); total concentration is equal to 0.05M

Diffusant 0.05M KCℓ		
No. of Exp.	Time-Lag τ (s)	Diffusion Coefficient D_{KH} $cm^2\ s^{-1} \times 10^7$
1	60	5.52
2	62	5.34
3	64	5.18
4	59	5.62
	average	5.42 ± 0.20 8%
Diffusant 0.05M HCℓ		
No. of Exp.	Time-Lag τ (s)	Diffusion Coefficient D_{HK} $cm^2\ s^{-1} \times 10^7$
1	50	6.63
2	51	6.50
3	52	6.41
	average	6.51 ± 0.11 3%

Table (7-6)

Electrical conductivity measurements at different HCℓ + KCℓ composition (total concentration 0.05M)

Concentration of HCℓ (M)	Conductance (mmho)
0.05	0.5548
0.045	0.5163
0.040	0.47891
0.035	0.44125
0.030	0.40360
0.025	0.36742
0.020	0.33094
0.015	0.29346
0.005	0.21727

Table (7-7). Exchange diffusion of H^+/K^+ across Nafion 125 perfluorosulphonic acid membranes in mixed 0.012M KCℓ + 0.038M HCℓ solution of total ionic strength 0.05M ($\bar{X}_H = \bar{X}_K = 0.5$)

spray composition		membrane outer surface		time-lag	conductance of reference solution	expt. slope	composition	flux	permeability	expt.* diffusion coefficient	calc** diffusion coefficient
X_H	ΔC_H mol cm^{-3}	$\bar{X}_H$	$\Delta C_H \times 10^4$ mol cm^{-3}	τ (s)	$G^\circ \times 10^3$ mmho	$\frac{dG}{dt} \times 10^7$ mmho s^{-1}	$\frac{dC_H}{dt} \times 10^9$ mol cm^{-3} s^{-1}	$J \times 10^8$ mol cm^{-2} s^{-1}	$P \times 10^4$ cm s^{-1}	$D \times 10^7$ cm^2 s^{-1}	$D \times 10^7$ cm^2 s^{-1}
0.0	-0.03785	0.0	-7.42	123.85 ± 22	6.631	-5.04 ±0.79	4.70	-1.414	3.736	2.74 ±0.44	2.71
0.47	-0.01385	0.20	-4.46	126.30 ± 11		1.78 ±0.18	1.66	-0.498	3.596	2.66 ±0.21	1.61
0.76	0.00285	0.40	-1.48	123.60 ± 2.0		-0.34 ±0.1	0.32	-0.096	3.368	2.72 ±0.04	0.92
0.76	0	0.50	0	0		0	0	0	—	—	—
0.833	0.0039	0.60	1.49	123.62 ± 0.6		0.38 ±0.20	0.35	0.11	2.733	2.72 ±0.1	1.05
0.95	0.0097	0.80	4.52	127.20 ± 21		1.19 ±0.04	1.11	0.334	3.443	2.64 ±0.4	1.05
1.0	0.01215	1.0	7.65	126.30		1.81	1.69	0.509	4.189	2.66	0.94

average of 20 experiments

* eqn. (7-2)

** eqn. (7-20)

Figure (7-1)

Diagram of spray diffusion cell

Legend

M	Membrane
Sb	Sides of the spray box
E	Conductivity Electrodes
St	Magnetic stirrer
Th	Thermistor (temperature probe)
EF	Thermistor (heating probe)
Mg	Magnet
Te	Flanged template defining membrane area exposed to spray input

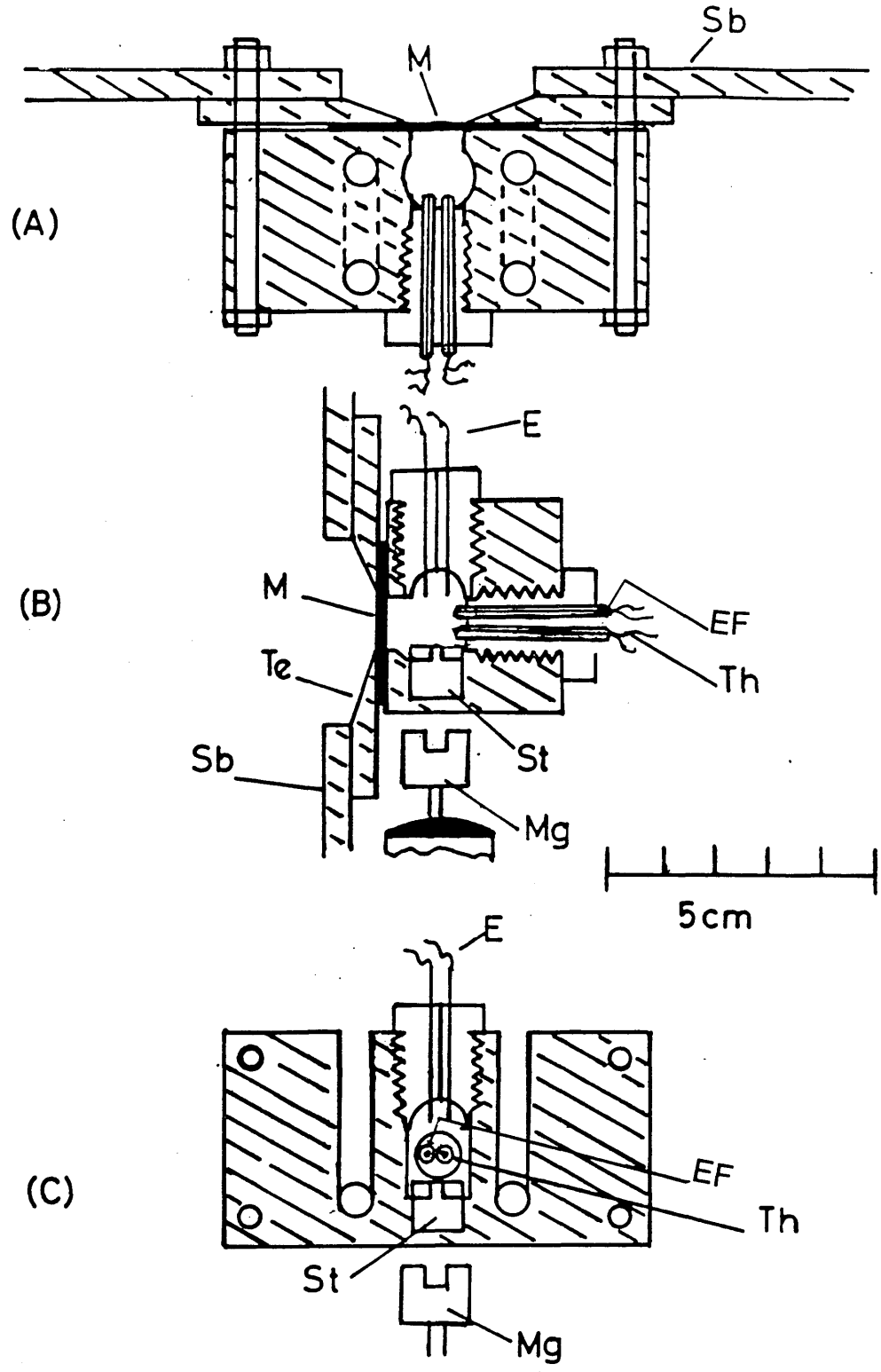
(A)
Sb
M
(B)
E
M
EF
Te
Th
Sb
St
Mg
5cm
(C)
E
EF
Th
St
Mg

Figure (7-2) a and b

Test to show that no temperature or conductivity fluctuations occurred on switching between spray A and spray B. The cell solution and the sprayed solutions A and B were identical ($HC\ell + KC\ell$). (a) and (b) show the corresponding plots of temperature and electrical conductance, respectively.

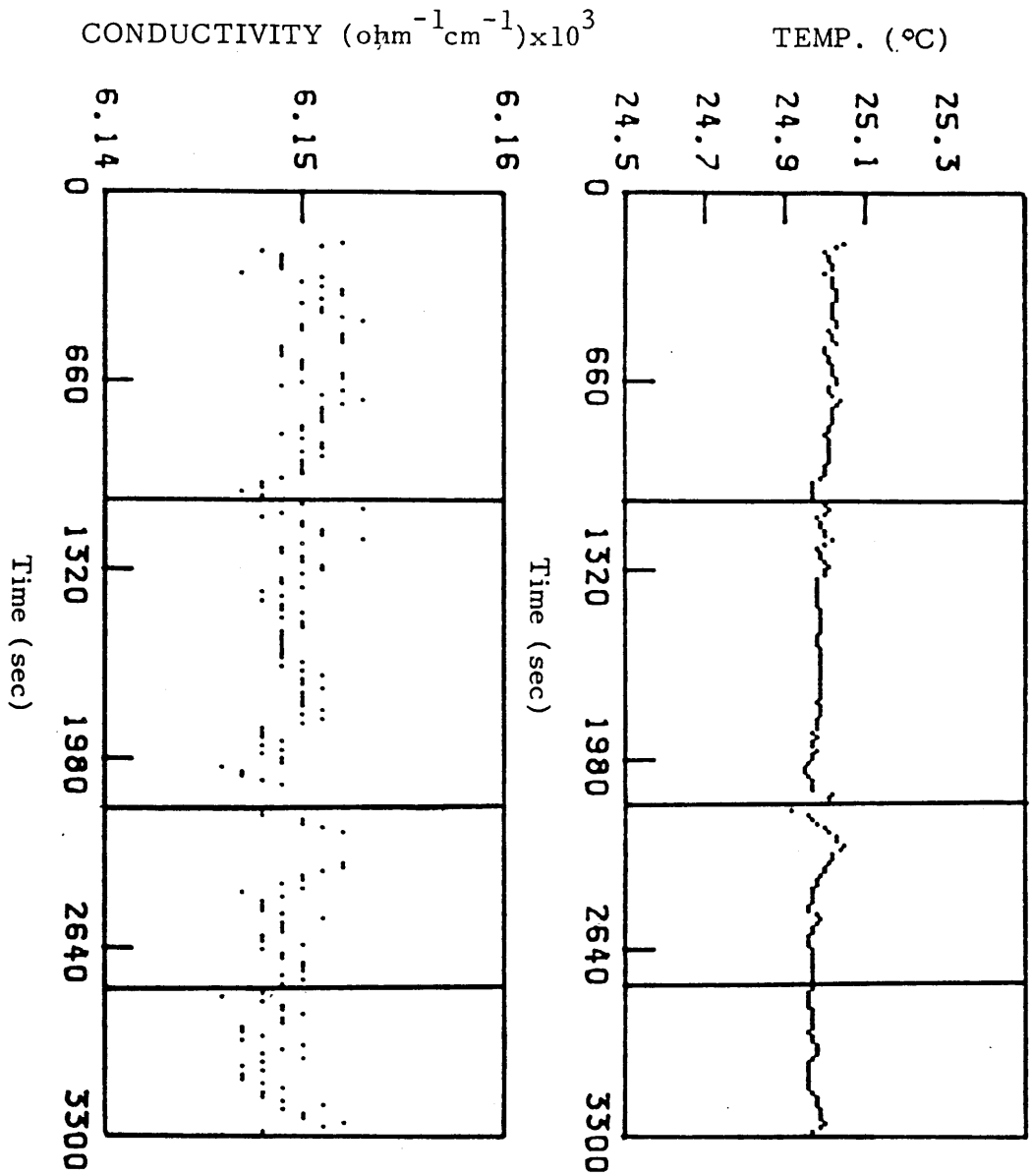
CONDUCTIVITY (ohm^{-1}cm^{-1})x10^{3}
6.14
6.15
6.16
0
660
1320
1980
2640
3300
Time (sec)
TEMP. (°C)
24.5
24.7
24.9
25.1
25.3
0
660
1320
1980
2640
3300
Time (sec)

Figure (7-3)

A plot of conductivity within the collecting volume as a function of time, following the establishment of a concentration step (▲). These data were obtained with a Visking dialysis membrane, thickness 0.0195 cm, cell collecting volume 2.0638 cm^3, and exposed membrane area 0.771 cm^2. The concentration step was 0.05M NaCℓ against water. From the time-lag, τ, eqn. (7-2) and slope, $D_{NaC\ell} = 2.95 \times 10^{-6}$ cm^2 s^{-1} and $\alpha = 0.75$ were obtained. The complete experiment was simulated by network method (2) using these data as input (—)

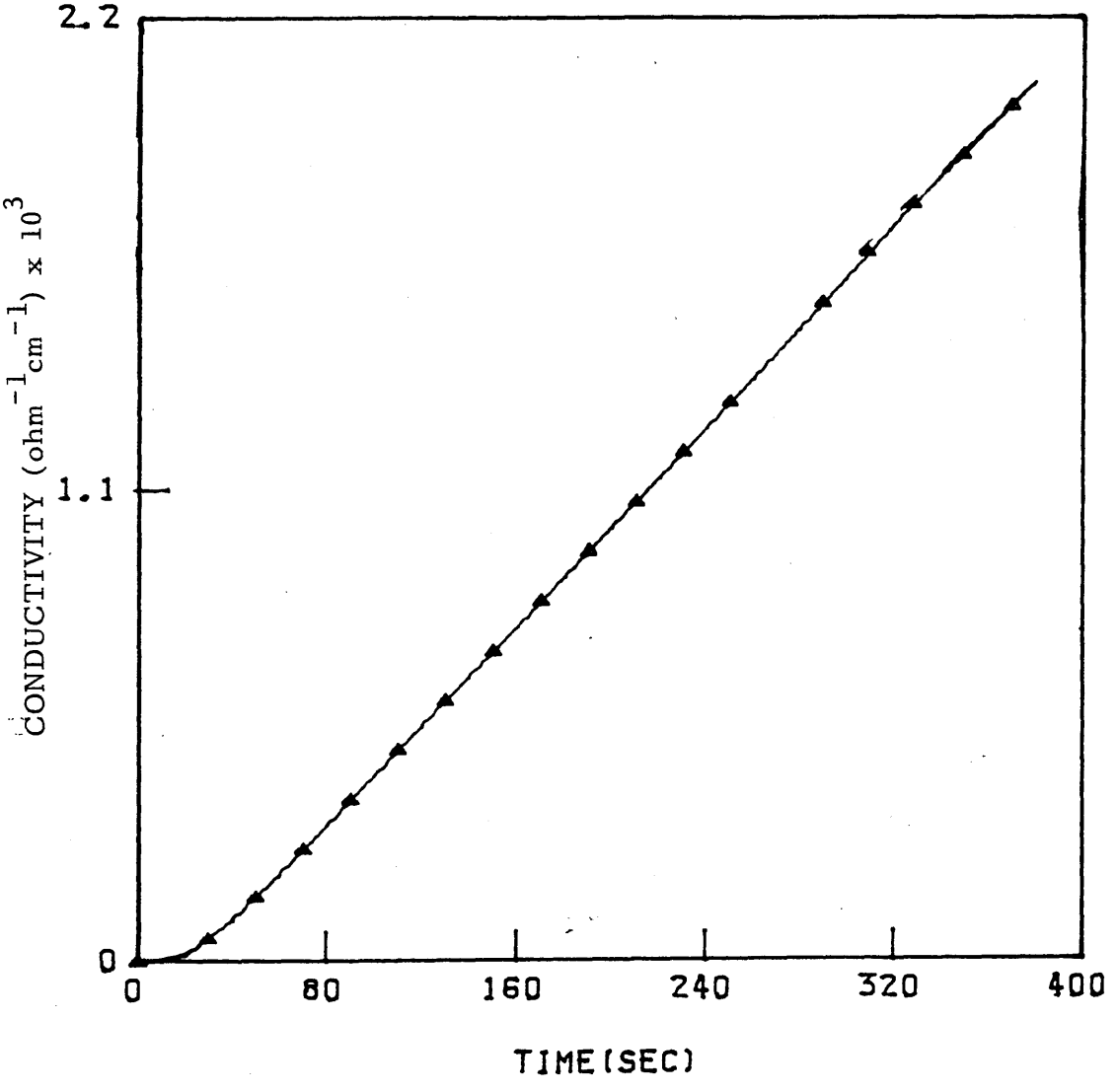
2.2
1.1
0
CONDUCTIVITY (ohm^{-1}cm^{-1}) x 10^{3}
0
80
160
240
320
400
TIME(SEC)

Figures (7-4) and (7-5)

Typical experimental results obtained by the time-lag method, using sprayed external solutions, 0.05M HCℓ and 0.05 KCℓ, respectively. The membrane was Nafion 125. The membrane composition on the inner surface, facing the collecting volume was $\bar{X}_H$ / $\bar{X}_K$ = .25 / .75 ($H^+ = K^+ = 0.025M$)

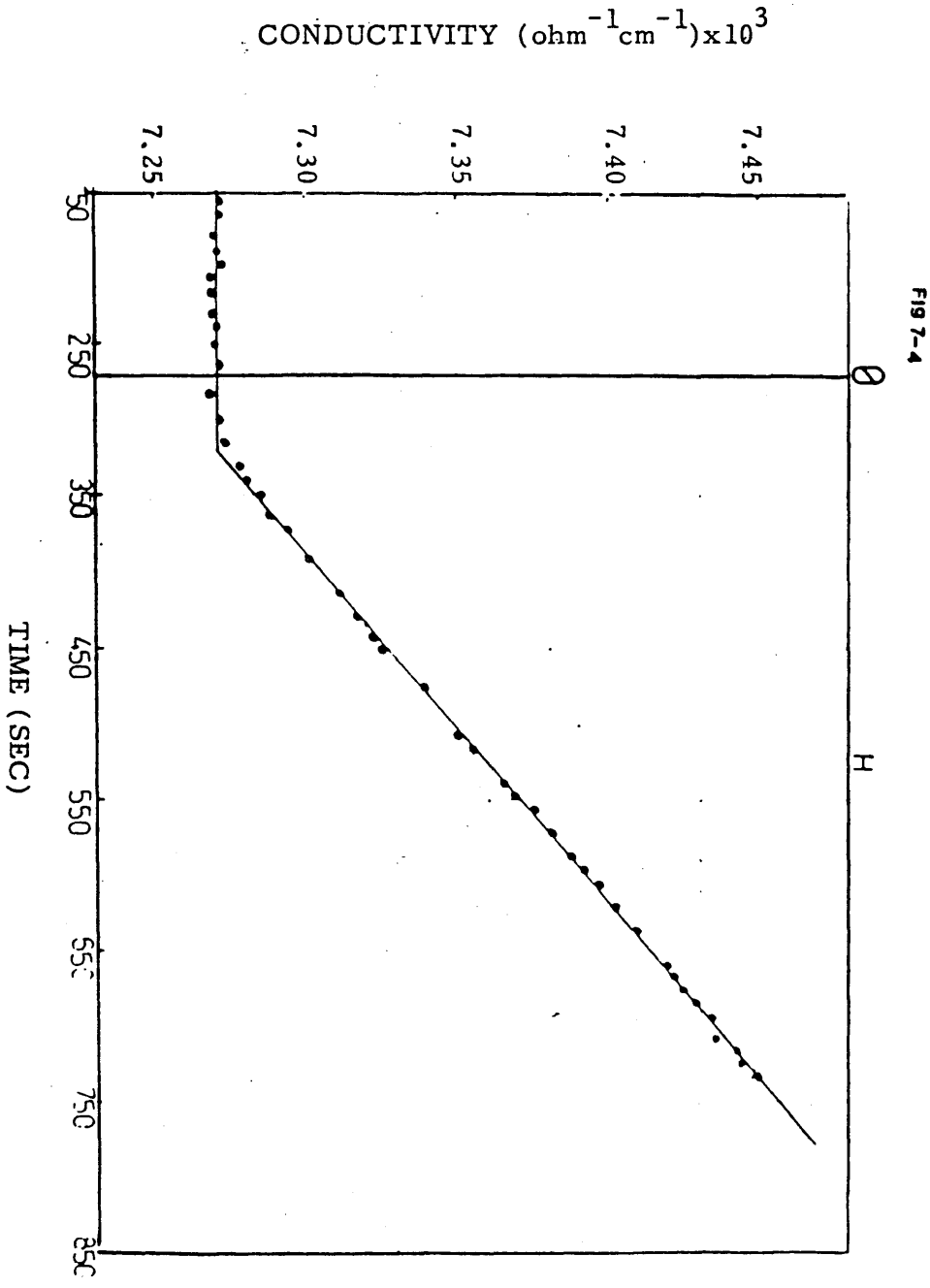
CONDUCTIVITY (ohm^{-1}cm^{-1})x10^{3}
7.25
7.30
7.35
7.40
7.45
50
250
350
450
550
750
850
TIME (SEC)
0
H

Fig 7-4

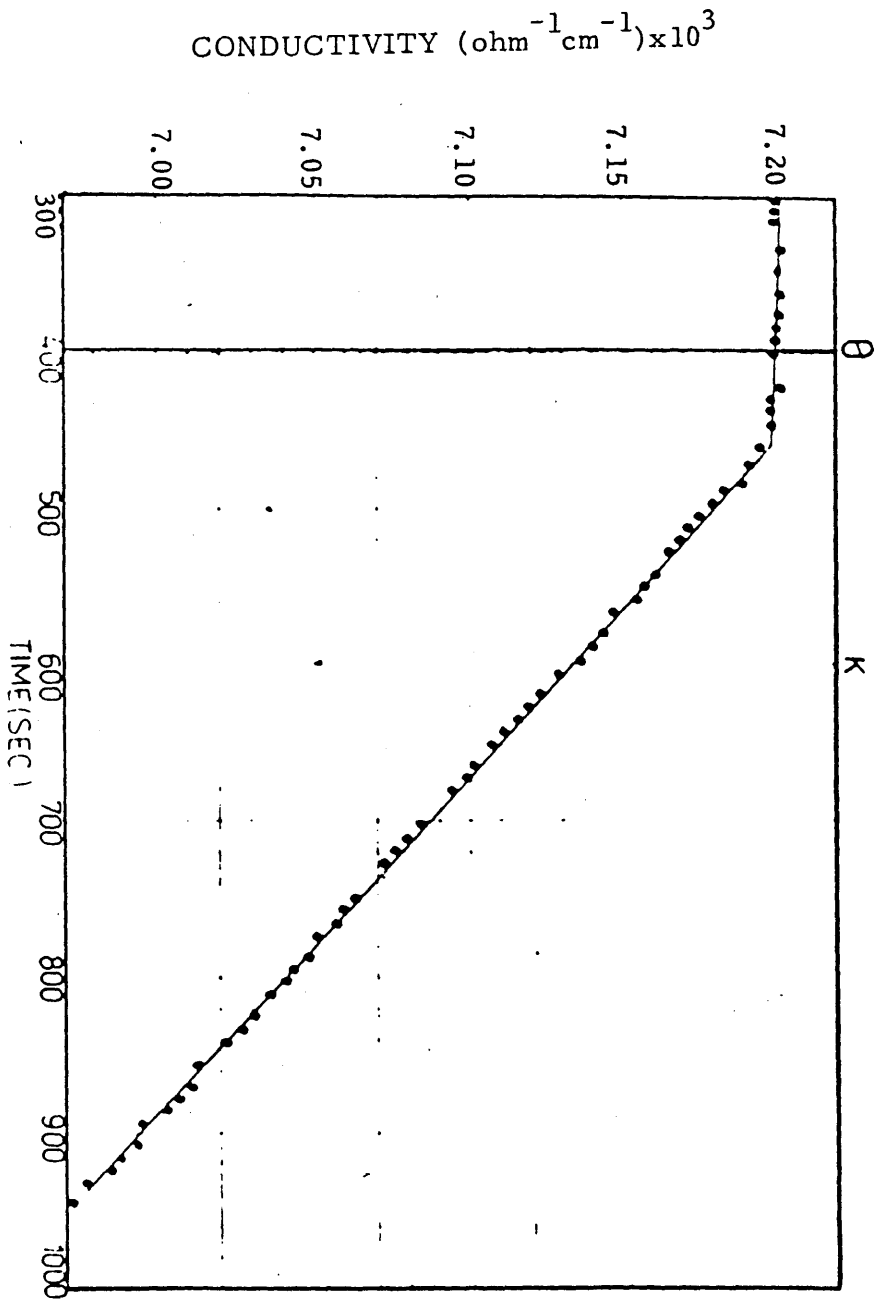
CONDUCTIVITY (ohm^{-1}cm^{-1})x10^3
7.00
7.05
7.10
7.15
7.20
300
400
500
600
700
800
900
1000
TIME(SEC)
θ
K

Fig7-5

Figures (7-6) and (7-7)

Typical experimental results obtained by the time-lag method, using 0.955 and 0.47 mole fraction of HCℓ in the sprayed external solution which had at total concentration 0.05M, made up with KCℓ. The membrane was Nafion 125 perfluorosulphonic acid membrane. The membrane composition on the inner surface, facing the collecting volume was $\bar{X}_H = \bar{X}_K = 0.5$ ($H^+/K^+ = 50/50$). The thickness = 0.0141 cm and membrane exposed area = .771 cm^2.

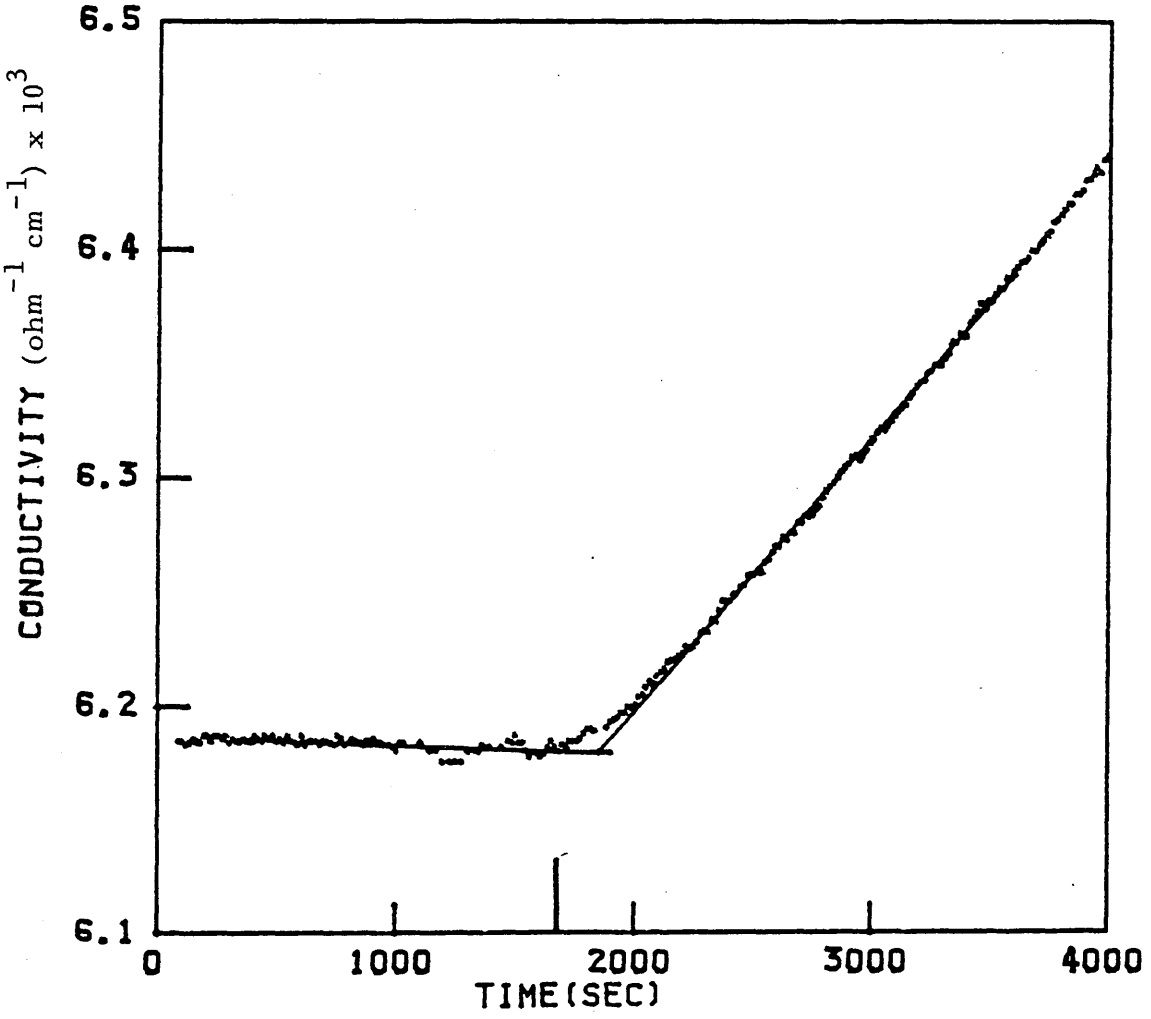
6.5
6.4
6.3
6.2
6.1
CONDUCTIVITY (ohm^{-1} cm^{-1}) x 10^3
0
1000
2000
3000
4000
TIME(SEC)

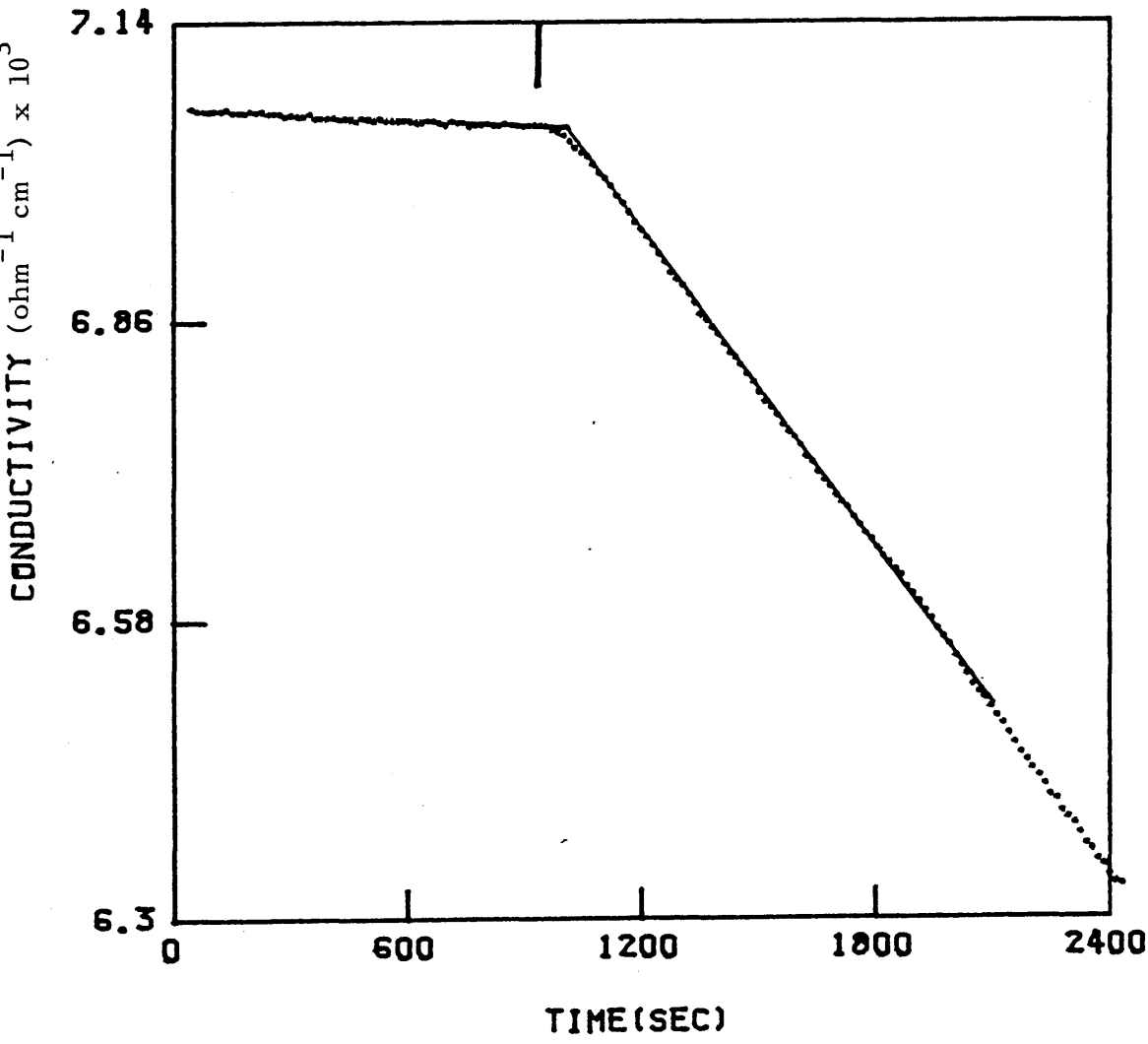
7.14
6.86
6.58
6.3
CONDUCTIVITY (ohm^{-1} cm^{-1}) x 10^{3}
0
600
1200
1800
2400
TIME(SEC)

Figure (7-8)

A plot of coupled diffusion coefficient, (D_{HK}), and flux, J, against mole fraction of HCℓ in the sprayed solution. Total concentration, 0.05M using Nafion 125 perfluorosulphonic acid membrane. With equal loading ($\bar{X}_H = \bar{X}_K = 0.5$). The thickness = 0.0142 cm, membrane exposed area = 0.771 cm^2 and volume = 2.32 cm^3.

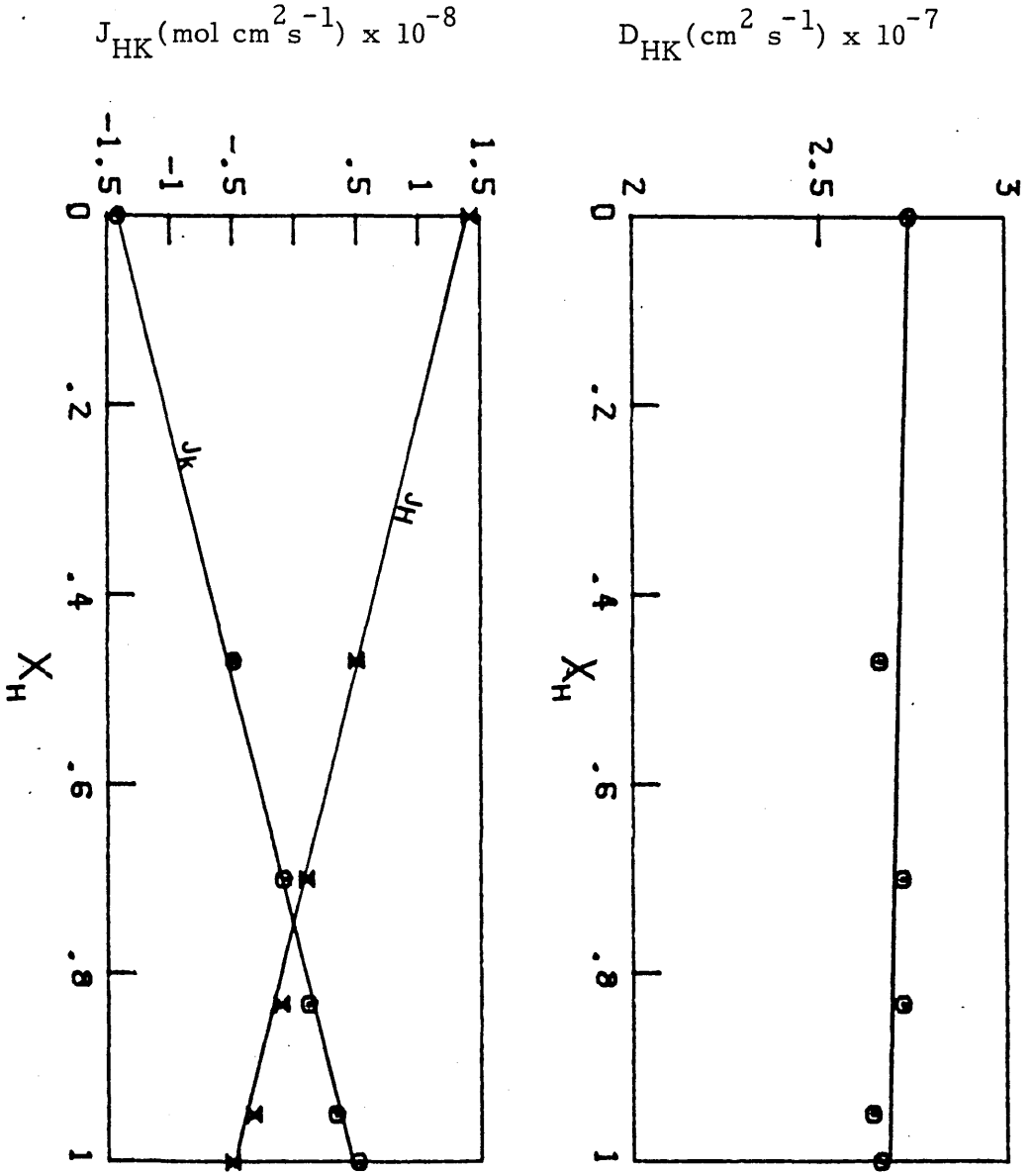
J_{HK}(mol cm^{2}s^{-1}) x 10^{-8}
D_{HK}(cm^2 s^{-1}) x 10^{-7}
-1.5
-1
-.5
.5
1
1.5
2
2.5
3
0
.2
.4
.6
.8
1
X_H
J_K
J_H

Figure (7-9)

A linear relationship observed between electrical conductivity and composition for HCℓ + KCℓ solutions, with total concentration 0.05M, at 25°C.

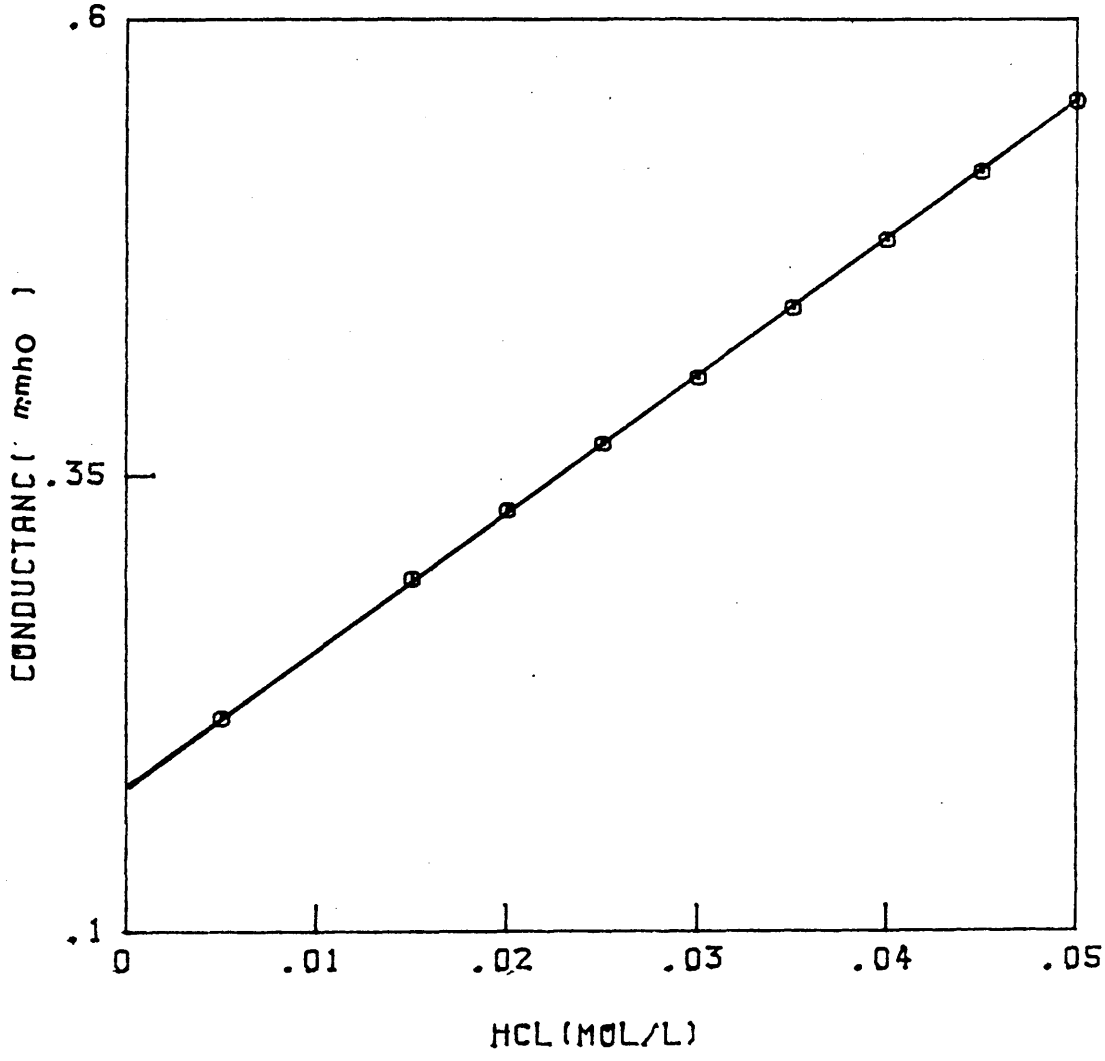
.6
.35
.1
CONDUCTANCE(mmhO)
0
.01
.02
.03
.04
.05
HCL(MOL/L)

Figure (7-10)

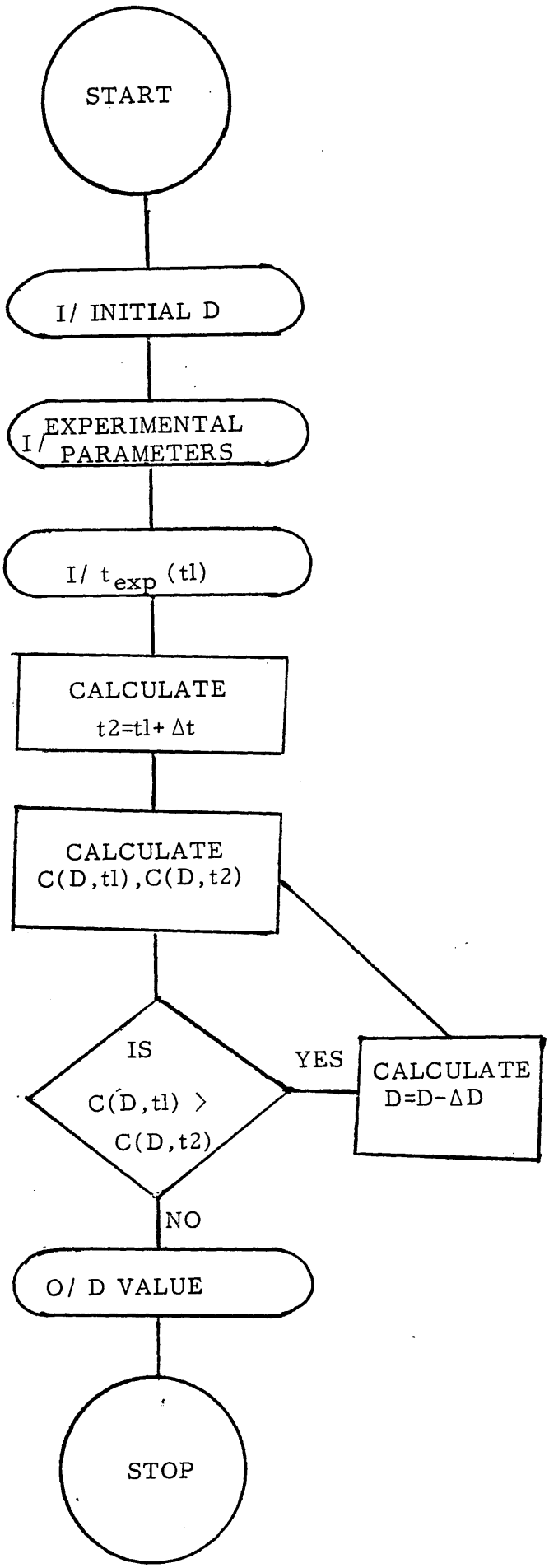
START
I/ INITIAL D
I/ EXPERIMENTAL PARAMETERS
I/ t_{exp} (t1)
CALCULATE
t2=t1+ Δt
CALCULATE
C(D,t1),C(D,t2)
IS
C(D,t1) >
C(D,t2)
YES
CALCULATE
D=D-ΔD
NO
O/ D VALUE
STOP

Figure (7-11)

Sketch of exchange diffusion of H^+/K^+ across Nafion 125 membrane in mixed HCℓ + KCℓ solution of total ionic strength 0.05M ($\bar{X}_K = \bar{X}_H = 0.5$).

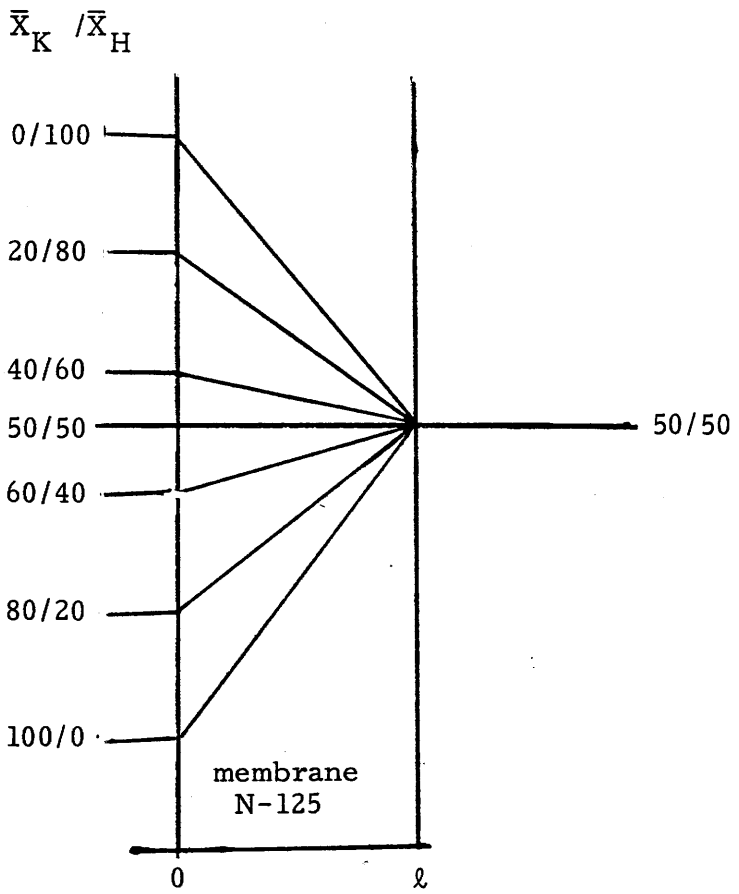

REFERENCES

1. H.A. Daynes, Proc. Roy. Soc. Series A, 97, 286, (1920).
2. R. Paterson and P. Doran, J. Membrane Science, 26, 289, (1986).
3. P. Doran, Ph.D. Thesis, Glasgow University, (1985).
4. R. Paterson and C.R. Gardner, J. Chem. Soc. A, 2254, (1971).
5. H. Ferguson, C.R. Gardner and R. Paterson, J. Chem. Soc. Faraday I, 68, 2021, (1972).
6. C.R. Gardner and R. Paterson, J. Chem. Soc. Faraday I, 68, 2030, (1972).
7. C.R. Gardner, Ph.D. Thesis, Glasgow University, (1970).
8. C. McCallum, Ph.D. Thesis, Glasgow University, (1971).
9. R.G. Cameron, Ph.D. Thesis, Glasgow University, (1976).
10. I. Noureldin, Ph.D. Thesis, Glasgow University, (1983).
11. R. Paterson, in "Biological and Artificial Membranes and the Desalination of Water", Ed. R. Passino. Proc. Pontifical Academy of Sciences Conference, The Vatican (1975), Scripta Varia, 40, 517, (1976) (reprinted by Elsevier).
12. R. Paterson, I.S. Burke and R.G. Cameron, in "Charged Gels and Polymers", Ed. E. Selegny, D. Reidel Publishing Company, Dordrecht-Holland, 1, 157, (1976).
13. J. Crank, The Mathematics of Diffusion, Clarendon Press, Oxford, England, (1959).
14. D.R. Paul and A.T. Di Benedetto, J. Polymer Science, C10, 17, (1965).
15. R.C. Jenkins, P.M. Nelson and L. Sirer, Trans. Faraday Society, 66, 1391 (1970).

16. F.G. Will, J. Electrochem. Soc., 126, 36, (1979).

17. T. Sakai, H. Takenaka and E. Torikai, J. Electrochem. Soc., 133, 88, (1986).

CHAPTER 8

Determination of the Diffusion Coefficient by Concentration Wave Method

8.1 INTRODUCTION

In network thermodynamics, membranes are described in terms of generalised resistors and capacitors (1). These reflect the ability of a membrane both to dissipate power and to store chemical energy internally in each local volume during transport processes. For quantitative modelling, the membrane is subdivided conceptually and mathematically into homogeneous "lumps" or slices, each characterized by its own resistance and capacitance. The accuracy of quantitative modelling of diffusion processes depends upon the degree of reticulation of the lumped model; since the model approaches ever more closely to a true continuum of states as the number of lumps (n) is increased.

As an example, to model a membrane which was exposed on one side to a source of constant effort, SE, (defined by a constant chemical potential of the permeant) and connected to a closed (homogeneous) volume of solution (or gas) on the other (defined by a chemical capacitor, C_l), we may use a bond graph, Fig. (8-1a) or an equivalent circuit, Fig. (8-1b). These alternative representations show a 3-lump model of the membrane. (The bond graph notation, although less familiar, is the more powerful for modelling complex, coupled, transport phenomena (1-3).

For a system which obeys Fick's laws of diffusion it is convenient to use a pseudo-system in which local efforts (properly defined as chemical potentials) may be replaced by concentrations (4,5). It was shown that the chemical resistance, R, for each lump of an n-lump model of a membrane (defined by Fick's law) is given by eqn. (8-1), and the corresponding capacitance, C, is defined by the lump volume,

$$R = \ell/DA \; \alpha \, n \tag{8-1}$$

$$C = \alpha A \ell / n \tag{8-2}$$

In these equations it was assumed that the membrane was regular, of area, A, and thickness ℓ, and had a diffusion coefficient, D, defined by Fick's first law. (The distribution coefficient, α, was introduced (5) to define the concentration of the equilibrium solution as a common effort in all phases).

These networks may be used algorithmically (2,4,5) to compute the system dynamics of a membrane assembly for any experiment or membrane, in which bond graph parameters and initial conditions are defined (4-6). For such simple conditions as described here it is only necessary to know the geometry of the membrane/solution system and the diffusion coefficient and distribution coefficient of the membrane involved (unstirred layers of solution may be treated as additional lumps). These methods are of particular interest for simulation of membrane processes and are easily expanded to deal with multicomponent, coupled transport, including energy transduction (6).

The formal analogy between a network thermodynamic bond graph and an electrical circuit, Fig. (8-1), has led us to re-examine the inverse problem, that of membrane characterisation. With the circuit and bond graph representations clearly in mind, it is obvious that all standard measurements of membrane transport are, in electrical terms, DC methods and typically involve fixed driving forces (the efforts of network theory) and steady state measurements. In particular, the

membrane scientist lacks powerful AC methods used routinely to investigate electrical circuitry. Note that these "DC" models have been used earlier in Chapter 7 to simulate the time-lag behaviour of the membranes during salt diffusion, Fig. (7-3).

Using mathematical models and bond graph simulations, we set out to examine the system dynamics of a simple membrane assembly consisting of a (concentration) source, a membrane, and a collecting vessel, as represented in Fig. (8-1a),when the source of concentration is oscillated with a fixed frequency and amplitude. From the properties of the analogous electrical circuit, Fig. (8-1b), we would expect the membrane to act as an AC filter, reducing the amplitude and causing phase shifts in the emergent waves (detected in the terminal capacitor/collecting volume). In previous work (7), a variety of concentration wave forms, frequencies and amplitudes were tested. From the results it became obvious that, with correct selection of experimental conditions, diffusion coefficients might be obtained directly (and repetitively) from the phase shift of the emergent concentration wave. On the basis of these mathematical models, apparatus was designed and new procedures were devised to perform such experiments in the laboratory. To assist with the design of membrane cells and experimental conditions, computer simulations were made, using a multilumped version of the bond graph, Fig. (8-1a). These predicted the evolutionary path of experiments to a steady state of oscillation (a requirement of the mathematical models) and ensured that cell volumes and other geometric factors in the proposed cell designs would not cause unacceptable deviations from the mathematical predictions, which were limited, at least initially, to infinite collecting volumes, V_c.

In the course of this research we discovered some interesting precedents for the use of forced oscillations, in studies on thermal diffusion, by Ångström (8), Thomson (Lord Kelvin) (9), and more recently in gas diffusion (10).

8.2 Mathematical Models

The membrane is considered to be exposed on one side to forced oscillations in the concentration of the contact solution and to be connected to the other to a closed reservoir or collecting volume, V, whose initial concentration, c^o, is the mean concentration of the ingoing wave. It is assumed also that the membrane is in equilibrium with its contacting solutions at all times, and that (if the membrane is in the form of a clamped sheet) "edge effects" can be neglected (11,12). Fick's laws are assumed with constant diffusion coefficient, D. A further simplification is the assumption that the collecting volume, V, is effectively infinite. In practice this is not a severe limitation. Figure (8-2) shows the concentration in the output volume for the three wave forms of square wave, cosine wave and triangular wave, respectively on the face of the membrane. There is a significant loss of amplitude on the emergent concentration wave while the phase shift does not change.

8.2.1 Cosine Waves

The fundamental responses to a cosine wave were considered initially. The wave form and boundary conditions for a solution of Fick's laws were, eqns. (8-3) and (8-4). In eqn. (8-3) the source of

effort, SE, at any time, t, is defined as the concentration of permeant at the surface of the membrane (x = 0), defined by the cosine function, which oscillates about a mean concentration, c^o, with a frequency of ω rad s^{-1}. Interfacial equilibrium is assumed. With the additional assumption of an infinite homogeneous (stirred) collecting volume, V, its concentration, c_t, is constant and set equal to the mean, c^o, eqn. (8-4). This is obtained at the opposite membrane face (x = ℓ)

$$SE = c = c^o [1 + \cos(\omega t)] \quad \text{at } x = 0 \tag{8-3}$$

and

$$c_t = c^o \quad \text{at } x = \ell \tag{8-4}$$

In this model the quantity of permeant, q_t (mol), transferred into the (infinite) collecting volume, is obtained as a function of time. Once initial transients have decayed, this is given by eqn. (8-5). This was obtained as a solution of Fick's second law of diffusion, by the standard technique of separation of variables (12), under the boundary conditions specified by eqns. (8-3) and (8-4)

$$q_t = B(\omega) \cos[\omega t + \phi(\omega) - \pi/2] + q_o \tag{8-5}$$

where $B(\omega)$ is the amplitude of the emerging wave, defined by eqn. (8-6)

$$B(\omega) = \frac{2^{3/2} A K \alpha c^o D\{2[\cosh(2K\ell) - \cos(2K\ell)]\}^{-\frac{1}{2}}}{\omega} \tag{8-6}$$

and $[\phi(\omega) - \pi/2]$ is the phase change between input and output waves, eqn. (8-7)

$$\phi(\omega) = \tan^{-1}\left\{\frac{-\tan(K\ell)}{\tanh(K\ell)}\right\} + \frac{\pi}{4} \qquad (8\text{-}7)$$

In eqns. (8-6) and (8-7), $K = [\omega/(2D)]^{\frac{1}{2}}$

From eqn. (8-6), it is clear that the phase change of the emergent wave is defined by only three parameters, the frequency of the input wave, the membrane thickness and the diffusion coefficient, eqn. (8-7). The corresponding amplitude, eqn. (8-6) is a more complicated function and depends additionally upon the distribution coefficient of the diffusant, α, and the membrane area, A. These analyses were made under the simplifying assumption that the collecting volume was infinite. Solutions were also obtained for finite systems (7).

Under conditions where the collecting volume, V , is finite and eqns. (8-5), (8-6) and (8-7) remain valid, it is convenient to define the displacements and amplitude of the corresponding concentration waves by dividing eqns. (8-5) and (8-6) by V .

It is clear from eqn. (8-5) that the quantity of permeant or, alternatively its concentration, $c_t = q_t/V$, will oscillate with the same frequency as the forcing wave, eqn. (8-3), but phase shifted by an amount which depends upon the diffusion coefficient and might be used to determine this in test membranes under laboratory conditions.

Bond graph simulations (2,3) were made for a range of common membranes exposed to cosine concentration waves in cells with various

collecting volumes, V , and exposed membrane areas.

The choice of amplitude and frequency for the input concentration wave determines both the phase shift and the amplitude of the emergent wave. For accurate determinations we require that the phase angle $\phi(\omega)$, eqn. (8-7), be large, favouring the application of high frequencies. The amplitude of the emergent wave, $B(\omega)/V$ (expressed as a concentration), is itself frequency dependent, but in the opposite sense. It tends to zero rapidly as frequency is increased. The practical limit to experimental frequency is therefore the sensitivity of the method used for detection of the wave. Since membrane parameters are strongly concentration dependent it is not practical to use large concentration oscillations; once more the most useful application of these methods appeared to be direct and repetitive measurements of diffusion coefficients from the phase shift. For typical membrane conditions large phase shifts were predicted for oscillations with periods in the range 10-1000 sec which were sufficiently long to encourage us to consider generating concentration waves using microcomputer controlled equipment. Experience has shown that practical frequencies are of the order of D/ℓ^2 which is, in turn, equal to the reciprocal of the product RC for a 1-lump bond graph model eqn. (8-1) (2). In free response the relaxation time of the 1-lump membrane $\tau = RC/4 = \ell^2/4D$ (1,5), while breakthrough times for diffusion equal $\ell^2/6D$. It is therefore clear that there is an intrinsic time base for a membrane ($\approx$ RC) and that our choice of frequency should reflect this.

8.2.2 Square Waves

Although performing sinusoidal oscillations in concentration by ingenious use of controlled syringes is feasible, by far the most convenient wave form is the square wave, which may be obtained using sprays, as described below.

A solution for source oscillations in the form of a square wave was similar to those given above. The boundary conditions were as before except that the source, SE, was now a square wave represented by a Fourier series, eqn. (8-8). The corresponding steady state oscillations (also as a summation) are given by eqn. (8-8)

$$SE = c^{o} \{ 1 + \frac{4}{\pi} \sum_{n=1,3,5,\ldots}^{\infty} \frac{(-1)^{(n-1)/2} \cos(n\omega t)}{n} \} \qquad (8\text{-}8)$$

$$q_t = \frac{4}{\pi} \sum_{n=1,3,5\ldots}^{\infty} \frac{B(n\omega)\cos[n\omega t+\phi(n\omega)-\pi/2](-1)^{(n-1)/2}+q_o}{n} \qquad (8\text{-}9)$$

The symbols have the same significance as before but now $\phi(n\omega)$ is the value of $\phi(\omega)$ for the nth contributory wave of eqn. (8-8), and similarly for $B(n\omega)$. The results are shown in Fig. (8-3). Once more an infinite collecting volume, V , was assumed. Since it was shown (7) that the two solutions effectively coincide when $\sqrt{2}DA\alpha K/\omega V \ll 1$. For the test system this function was 0.002 and the change in ϕ, even for a collecting volume of 2 mL, as used in this work, was only 0.09°.

These predictions were verified by bond graph simulations. The calculations were performed using the methods described earlier

for the SE-C model (3,4), but now using the cosine, square, or other wave expressions for SE, as above. Lumped models were constructed according to the membrane and cell parameters of the model to be predicted and resistances and capacitances defined by eqns. (8-1) and (8-2). The state space equations were integrated numerically to simulate the experiment and provide predictions of permeant concentration as a function of time in the collecting volume. It is worth noting that the whole experiment was modelled including the initial period in which transients exist. Additional information as to the outcome of experiments with other wave forms or the time dependent profiles of permeant concentration across the membrane are obtained easily from the same bond graph, as a matter of course.

8.3 On Obtaining the Diffusion Coefficient from the Experimental Phase Shift

The diffusion coefficient cannot be obtained directly from the concentration wave detected in the collecting volume, Fig. (8-4). This is because the equation (such as eqn. (8-10)) which gives concentration in terms of the experimental parameters including D, the diffusion coefficient cannot be inverted to give D for a given concentration. We must therefore solve for D by an iterative process.

The concentration in the infinite volume for a given frequency and diffusion coefficient is

$$c = \mathrm{Re}\left[\frac{(\Theta + 1)\, e^{K\ell_e} e^{iK\ell_e} e^{i\omega t}}{e^{2K\ell_e} e^{2iK\ell_e} + \Theta}\right]$$

where the function Θ is

$$\left(\frac{\frac{\sqrt{2}a'DKe^{-i\pi/4} - 1}{V\omega}}{\frac{1 + \sqrt{2}a'DKe^{-i\pi/4}}{V\omega}} \right)$$

For the case of the square wave the concentration will be a summation of these terms for different values of ω, given explicitly by eqn. (8-10)

$$c = \frac{4}{\pi} \sum \frac{1}{n} \mathrm{Re}\left[\frac{(\Theta(n)+1)e^{K(n)\ell_e} iK(n)\ell_e i(n)\omega t}{e^{2K(n)\ell_e} 2iK(n)\ell + \Theta(n)} \right] \qquad (8\text{-}10)$$

Now the experimental conditions have been chosen so that the infinite volume model holds to a good approximation. This means that the phase of the concentration will depend on α only very weakly and the amplitude will be almost a linear function of α. Thus, though the process given here for finding D for a given concentration at a given time uses the finite volume solution, if α is not known, then it can simply be put equal to 1 and the volume be assumed large. The computer programme used will then find the value of D by using in effect the infinite volume solution. Alternatively, approximate values of α and the real volume may be used (as in fact was done with the experimental results obtained in this chapter).

Basically the program obtains the diffusion coefficient by calculating the concentration for a given value of D at two times: the time at which the peak was observed t_{exp} and a second time slightly greater than t_{exp}. When the concentration for the second time is computed to be greater than that for the first, we have just passed the peak, and the value of D which gives this condition is the true value. D is constantly

stepped down until this happens. (Note the initial value of D must be larger than the true value). The flow chart for the program is given in Fig. (8-5) and full details including the program are given in Appendix A.8.

A first approximation to D can be found by considering only the first term in the square wave summation for the infinite volume analytical solution. We have that

$$\Phi = \tan^{-1}\left[\frac{-1\tan(K\ell)}{\tanh(K\ell)}\right]$$

which is further simplified to

$$\Phi = -K\ell$$

i.e. $$\sqrt{\frac{\omega}{2D}}\,\ell = [(t_{exp}/T)2\pi]-\pi/4$$

where $$\omega t_{exp} = -(\Phi - {}^{\pi}/4).$$

Fig. (8-4) shows how t_{exp} is defined.

8.4 EXPERIMENTAL

In this chapter an alternative means to measure the diffusion coefficient using the same Nafion 125 perfluorosulphonic acid membrane and C_{60} sulphonic acid membrane in heteroionic H^+ / K^+ forms, was tested.

The same equipment and experimental techniques as those developed in Chapter 7 were used. Three sprays were required instead of two, and in the preliminary state the membrane was sprayed with concentrated c^o, equal to that in the filled cell. Once this system was in thermal (and chemical) equilibrium, as indicated by steady temperature and conductivity readings, the experiment was begun by switching between the HCℓ and KCℓ at 0.05M each while the mean concentration of HCℓ + KCℓ in the collecting volume was kept at 0.05M, (HCℓ = KCℓ = 0.025M). A flow chart of the switching program is given in Fig. (8-5).

8.5 RESULTS AND DISCUSSION

The oscillatory method was practicable only because it was possible by using spray techniques to generate square concentration waves at the outer surface of the membrane. The experiments were run using the same equipment and experimental techniques as in Chapter 7.

Nafion 125 and AMF C_{60} membranes were used in heteroionic H^+ / K^+ forms and the same concentration of HCℓ + KCℓ solutions. The total concentration was 0.05M (HCℓ = KCℓ = 0.025M) in the collecting volume, as was used in the first time-lag experiments. The outerside of the membrane was sprayed with 0.05M HCℓ and 0.05M KCℓ, alternated to generate square waves. Using a simple computer program to switch

on and off solenoid valves on air-lines, Fig. (8-5), it was possible to spray alternately with one solution and then another as needed.

In the theoretical section (8.2), both sinusoidal (cosine) waves and square waves are discussed, the latter although requiring a simpler mathematical analysis were rejected for practical purposes. It is simply a matter of the complexity of any system which might be devised and its probable slowness. With square waves all reasonable frequencies might be encompassed and changed by simple modification of one line of the computer instructions.

The method is attractive in that it is repetitive and so in a single experiment many phase-shift (see section (8.3)) measurements can be made and for each a diffusion coefficient calculated, Figs.(8-4), (8-6) and (8-7). The method of calculating the diffusion coefficient from experimental results is given in Appendix A.8. These estimates may be compared with diffusion coefficients obtained from the time-lag method, Tables (8-2) and (8-3). Alternatively the phase change may be calculated, Fig. (8-4) by inserting into eqn. (8-10) the diffusion coefficient from the time-lag method, Table (7-2) which can then be compared with that which may be obtained from the oscillating experiments (7).

Since eqn. (8-10) cannot be transformed to an explicit expression for D, the diffusion coefficient was obtained by method of successive approximations, (7). An approximate value of the diffusion coefficient, D*, was obtained from ϕ^* taken from square wave experiment.

ϕ^* was obtained by measuring the time-shift, t_{exp} from the mid-point of square wave to the next peak of output wave Fig. (8-4), such that

$$\phi^* - \frac{\pi}{2} = 2\pi\, t_{exp}/\tau$$

Since we require only an approximate starting value for D* we may neglect the tanh(Kℓ) term, eqn. (8-7), so that $\phi^* \approx - K\ell + \pi/4$, or rearranging,

$$D^* = \omega \ell^2/2(2\pi\, t_{exp}/\tau - \pi/4)^2$$

With these approximations, D* is always larger than D, the true diffusion coefficient.

Choosing a time t_{max}, when the output wave is at a maximum, the corresponding concentration, $c_t = q_t/V$, was calculated using eqn. (8-9). Since D* is greater than D, the guessed value of D* was stepped down progressively to produce a series of c_t. The experimental diffusion coefficient was taken as the value of D* which reproduced the maximum in c_t.

The mathematical analysis (as for the time-lag also) is based on an 'infinite' collecting volume. In practice the quantities of salt diffused or ions exchanged are measured by changes in the concentration or composition of the solution in the collecting volume. For the time-lag method the collecting volume, although only 2 mL in volume, was to all intents and purposes an effective 'infinite' volume in terms of theory. For a square wave oscillator, a steady state of oscillation in the collecting volume was detected, once more using conductivity electrodes. To test the method, an experiment was simulated using network thermodynamic methods, discussed elsewhere (2,4,5) using data available for salt

diffusion through Visking dialysis membrane, Table (7-2), Figs. (8-2) and (8-3). In Fig. (8-2) concentration waves for cosine, triangular and square waves with equal amplitudes and frequencies are compared. It can be seen that there is little shift in the waves and that the square wave provides the largest amplitude output. Calculations also showed that there was no significant error due to the infinite bath (7) assumption used in the mathematical analysis for a 2 mL collecting volume.

The experiments were conducted at different frequencies to ensure that oscillatory method would work over a range of frequencies, but it was noted that the amplitude of the output waves, into a cell of 2 mL capacity is approximately 1/500 of the input concentration step. The amplitude of emergent wave became much reduced as the frequency was increased and the detection methods had to be very sensitive. Here, as previously discussed, conductivity measurements were used and particular care was needed to prevent temperature fluctuations. A temperature change of 1°C will, in general, cause a 1% change in conductivity for most dilute salt solutions. Techniques to minimise such effects were devised earlier, Chapter 7.

From eqn. (8-6) it is clear that the peak to peak shift (t_{exp}) between input and output waves is a function of the period, T, of the input wave. The amplitude of emergent wave becomes much reduced as the period decreases (i.e. frequency increased). That is the case at 150s period. Experience showed that frequencies of the order of D/ℓ^2 which equals the product of membrane resistance R and capacitance C for the membrane treated as a Fickian system by bond graph methods (3,4), and close to the reciprocal of relaxation time, τ, of the membrane (1,5) for which $\tau = \frac{RC}{4} = \frac{\ell^2}{4D}$.

Most experiments were carried out with periods of 300s and 450s and also tests were made at higher frequencies (periods of 150s). Figures (8-6) and (8-7) were obtained at periods 300s and 450s respectively for H^+/K^+ exchange across Nafion 125 perfluorosulphonic acid membrane. Raw data as collected is shown in Table (8-1).

From the experimental shifts (t_{exp}) a set of diffusion coefficients D_{KH} and D_{HK} were obtained, Tables (8-2) and (8-3) (D_{KH} and D_{HK} are respectively the exchange diffusion coefficient in the membrane where K^+ ion in the spray replaces H^+ in the cell and D_{HK} when the H^+ ion in the spray replaces K^+ in the cell, as in Chapter 7, eqn. (7-8)).

It is clear from Figs. (8-6) and (8-7) that it was possible to obtain extremely regular, reproducible waves. The conductivity rises as hydrogen ion enters the collecting volume and potassium ion leaves and falls when the process is reversed. The exchange was shown to be stoichiometric, since at these very low concentrations of electrolyte (0.05M) chloride coions are effectively excluded from the membrane phase.

In these experiments were shown H^+/K^+ exchange across these membranes. The inner solution was 0.025M HCℓ + 0.025M KCℓ ($\bar{X}_H$ / $\bar{X}_K$ = 1 / 3 on the inner membrane surface), while the outer surface was at 0.05M HCℓ and 0.05M KCℓ. Attempts were made to determine diffusion coefficients for a system in which the inner solution was 0.038M HCℓ + 0.012M KCℓ (this gave $\bar{X}_H$ / $\bar{X}_K$ = 50 / 50 on the inner membrane surface) while the spray solutions gave a H^+/K^+ loading on the outer membrane surface in the run $\bar{X}_H/\bar{X}_K$ = 80/20, 20/80, 60/40, and 40/60.

These experiments were performed over several weeks and although all possible care and precautions were exercised, they proved insufficiently reproducible for use here. The main cause was that the concentration of HCℓ in the inner solution was high (0.038M against 0.012M for KCℓ) and correspondingly the sensitivity of the conductimetric method was reduced. Also by 'stepping down' the spray concentrations to 80/20, 60/40 (as above) the emergent waves were again reduced.

These shortcomings led to the use of the time-lag method, being the preferred method in this experiment. The time-lag has been described before the oscillatory method in this thesis for convenience in presenting concepts and theory. In actual fact the oscillatory method was used first. The oscillatory method has several shortcomings but it is quite useful for preliminary explorations of the type reported here. It is however to be recommended for the measurement of diffusion coefficients with thin membranes where alternative, time-lag $\tau = \ell^2/6D$ would be small. It would be of considerable use also if repetitive determinations of diffusion were required, especially if it were suspected or unknown that a larger time-based process such as swelling or conformational change in the polymer occurred during the diffusion processes.

Table (8-1). Sample of Raw Experimental Results

time (s)	conductance (ohm^{-1} cm^{-1})	time (s)	conductance (ohm^{-1} cm^{-1})
6	7.475E-03	183	7.383E-03
9	7.477E-03	186	7.377E-03
12	7.476E-03	190	7.375E-03
16	7.484E-03	198	7.364E-03
19	7.487E-03	201	7.364E-03
22	7.489E-03	205	7.357E-03
25	7.49E-03	208	7.356E-03
28	7.492E-03	211	7.353E-03
31	7.496E-03	214	7.347E-03
40	7.503E-03	217	7.346E-03
43	7.502E-03	220	7.342E-03
46	7.501E-03	223	7.337E-03
49	7.5E-03	232	7.328E-03
52	7.501E-03	235	7.325E-03
55	7.502E-03	238	7.323E-03
58	7.5E-03	241	7.321E-03
61	7.502E-03	244	7.316E-03
70	7.495E-03	247	7.314E-03
73	7.496E-03	251	7.311E-03
76	7.492E-03	254	7.308E-03
79	7.491E-03	262	7.298E-03
83	7.488E-03	266	7.296E-03
86	7.486E-03	269	7.293E-03
89	7.484E-03	272	7.293E-03
92	7.482E-03	275	7.287E-03
95	7.478E-03	278	7.283E-03
104	7.471E-03	281	7.281E-03
107	7.469E-03	284	7.275E-03
110	7.466E-03	293	7.269E-03
113	7.462E-03	296	7.266E-03
116	7.461E-03	299	7.263E-03
119	7.455E-03	302	7.259E-03
122	7.455E-03	305	7.255E-03
126	7.449E-03	308	7.255E-03
129	7.448E-03	312	7.251E-03
137	7.436E-03	315	7.249E-03
140	7.434E-03	318	7.247E-03
144	7.431E-03	326	7.241E-03
147	7.427E-03	330	7.243E-03
150	7.423E-03	333	7.239E-03
153	7.421E-03	336	7.239E-03
156	7.415E-03	339	7.24E-03
159	7.414E-03	342	7.239E-03
168	7.401E-03	345	7.238E-03
171	7.397E-03	348	7.237E-03
174	7.394E-03	357	7.239E-03
177	7.391E-03	360	7.241E-03
180	7.385E-03		

Table (8-1) contd.

time (s)	conductance (ohm^{-1} cm^{-1})	time (s)	conductance (ohm^{-1} cm^{-1})
363	7.241E-03	543	7.347E-03
366	7.241E-03	546	7.351E-03
369	7.241E-03	549	7.353E-03
373	7.242E-03	552	7.356E-03
376	7.241E-03	555	7.361E-03
379	7.243E-03	558	7.358E-03
387	7.25E-03	561	7.363E-03
391	7.25E-03	570	7.368E-03
394	7.252E-03	573	7.373E-03
397	7.252E-03	576	7.373E-03
400	7.255E-03	580	7.378E-03
403	7.257E-03	583	7.381E-03
406	7.258E-03	586	7.385E-03
409	7.259E-03	589	7.385E-03
418	7.265E-03	592	7.389E-03
421	7.264E-03	601	7.392E-03
424	7.268E-03	604	7.396E-03
427	7.271E-03	607	7.397E-03
430	7.272E-03	610	7.399E-03
433	7.273E-03	613	7.4E-03
437	7.275E-03	616	7.405E-03
440	7.276E-03	619	7.405E-03
448	7.279E-03	622	7.407E-03
452	7.286E-03	631	7.408E-03
455	7.29E-03	634	7.414E-03
458	7.29E-03	637	7.417E-03
461	7.29E-03	641	7.415E-03
464	7.294E-03	644	7.415E-03
467	7.298E-03	647	7.411E-03
470	7.296E-03	650	7.418E-03
479	7.304E-03	653	7.42E-03
482	7.305E-03	662	7.42E-03
485	7.308E-03	665	7.421E-03
488	7.31E-03	668	7.421E-03
491	7.312E-03	671	7.421E-03
494	7.314E-03	674	7.42E-03
498	7.319E-03	677	7.421E-03
501	7.319E-03	680	7.423E-03
509	7.324E-03	683	7.421E-03
512	7.327E-03	692	7.417E-03
516	7.327E-03	695	7.416E-03
519	7.329E-03	698	7.414E-03
522	7.332E-03	701	7.414E-03
525	7.335E-03	705	7.415E-03
528	7.336E-03	708	7.408E-03
531	7.339E-03	711	7.408E-03
540	7.346E-03	714	7.405E-03
		723	7.399E-03

Table (8-2)

Comparison of experimental results obtained from time-lag method and oscillatory method of Nafion 125 perfluorosulphonic acid membranes with a thickness = 0.0141 cm, and area = 0.771 cm^2. The diffusants were 0.05M KCℓ and 0.05M HCℓ against HCℓ + KCℓ (HCℓ=KCℓ=0.025) solution in the output volume, with a total concentration = 0.05M.

No. of Exp.	Methods	Periods T (s)	Time-shift t^*_{exp} (s)	Diffusion Coefficient D_{KH} $cm^2s^{-1}10^7$	Time-shift t_{exp} (s)	Diffusion Coefficient D_{HK} $cm^2s^{-1}x10^7$
1	oscillatory	300	56.7	5.06	50.3	5.70
2		300	56.3	5.10	50.6	5.67
3		300	68.8	4.17	47.6	6.03
4		300	56.4	5.09	-	-
5		300	59.5	4.82	-	-
6		450	64.4	4.45	47.1	5.70
7		450	59.7	4.81	53.3	5.39
8		450	57.5	4.99	51.6	5.56
9		450	-	-	51.4	5.58
			average	4.81±0.33		5.66±0.20
	time-lag		τ^{**} (s)	D_{KH} $cm^2s^{-1}x10^7$	τ (s)	D_{HK} $cm^2s^{-1}x10^7$
1			60	5.52	50	6.63
2			62	5.34	51	6.50
3			64	5.18	52	6.41
4			59	5.62	-	-
			average	5.42±0.20		6.51±0.11

*Fig. (8-4)

**Chapter 7, eqn. (7-2)

Table (8-3)

Comparison of experimental results obtained from the time-lag and oscillatory methods on C_{60} sulphonic acid membranes with thickness = 0.031 cm, and area = 0.771 cm^2. The diffusants were 0.05M KCℓ and 0.05M HCℓ against (0.025M HCℓ + 0.025M KCℓ) solution in the output volume, with total concentration = 0.05M

No. of exp.	Methods	Periods T (s)	Time-lag t_{exp} (s)	Diffusion Coefficient D_{KH} $cm^2s^{-1}x10^6$	Time-lag t_{exp} (s)	Diffusion Coefficient D_{HK} $cm^2s^{-1}x10^6$
1	oscillatory	300	68.9	1.94	50.3	2.14
2		300	68.3	1.96	51.0	2.12
3		300	61.2	2.19	58.0	1.86
4		300	56.3	2.38	57.5	1.88
5		300	68.3	1.96	58.0	1.86
6		300	63.3	2.11	63.3	1.70
7		450	62.81	2.13	54.8	1.94
8		450	61.59	2.17	48.2	2.23
9		450	64.25	2.08	56.2	1.92
			average	2.10±0.14		1.96±0.17
	time-lag		τ (s)	D_{KH} $cm^2s^{-1}x10^6$	τ (s)	D_{HK} $cm^2s^{-1}x10^6$
1			62	2.58	51	3.14
2			64	2.50	48	3.34
3			62	2.58	49	3.27
4			-	-	50	3.20
			average	2.55±0.05		3.24±0.09

Figures (8-1a) and (8-1b)

Fig. 1 (a) - a bond graph representation of 3-lump model of a membrane exposed to a source of effort, SE (either constant or oscillating) on one side and connected to a reservoir or collecting volume on the other, represented by the terminal capicitor, C_t .

Fig. 1 (b) - the equivalent circuit representation of the same membrane system.

Fig 8-1a

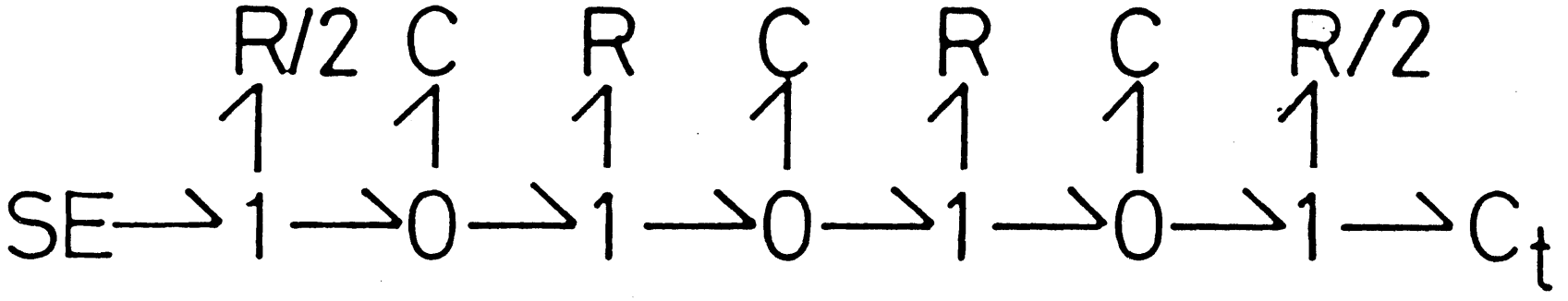

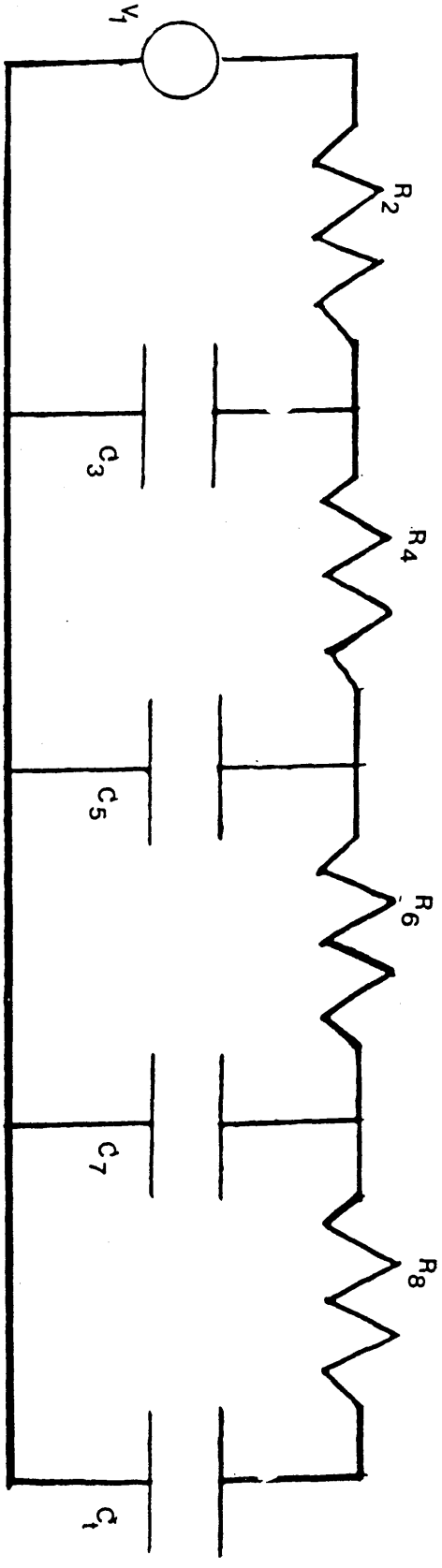

Fig 8-1b

Figure (8-2)

A plot of amplitude Q(t) of solute collected as function of time for a series of regular concentration waves input. It shows the effect of input concentration wave form on the concentration in the collecting volume. Using Visking dialysis membrane the diffusant was 0.05M NaCℓ.

The data used was taken from Table (7-2).

The solid dotted line represents the concentration when the input signal is square wave; the broken line is for cosine input wave, and the solid line is for the case of triangular input wave(7).

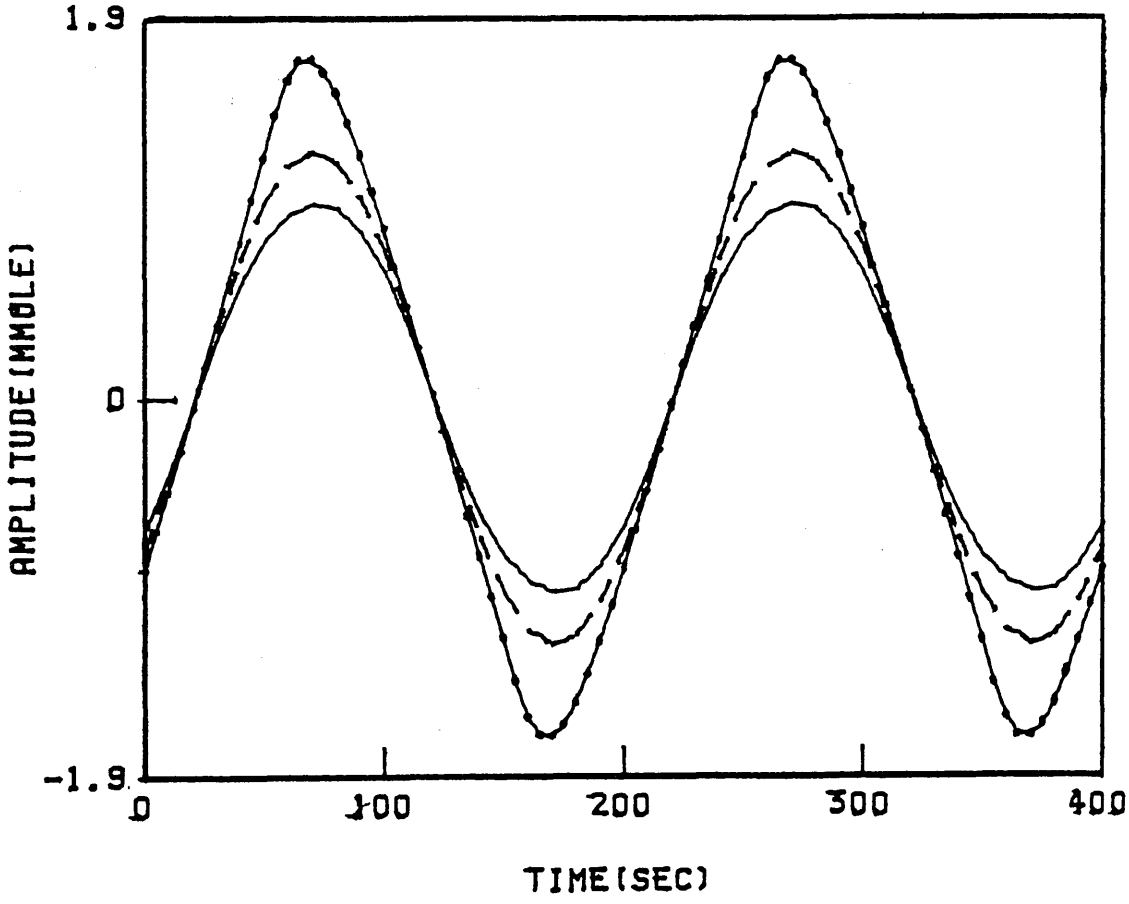
1.9
0
-1.9
AMPLITUDE(MMOLE)
0
100
200
300
400
TIME(SEC)

Figure (8-3)

Concentration waves in the collecting volume, generated by square wave source, using a 20-lump bond graph, as in Fig. (8-1a), using Visking dialysis membrane.

Membrane parameters: $D = 2.95 \times 10^{-6}$ cm^2 s^{-1}, $\ell = 0.0195$ cm, $A = 0.771$ cm^2, $\alpha = 0.75$, $T = 200$s and $c^o = 0.05$M NaCℓ (membrane parameters taken from time-lag experiment, Table (7-2)).

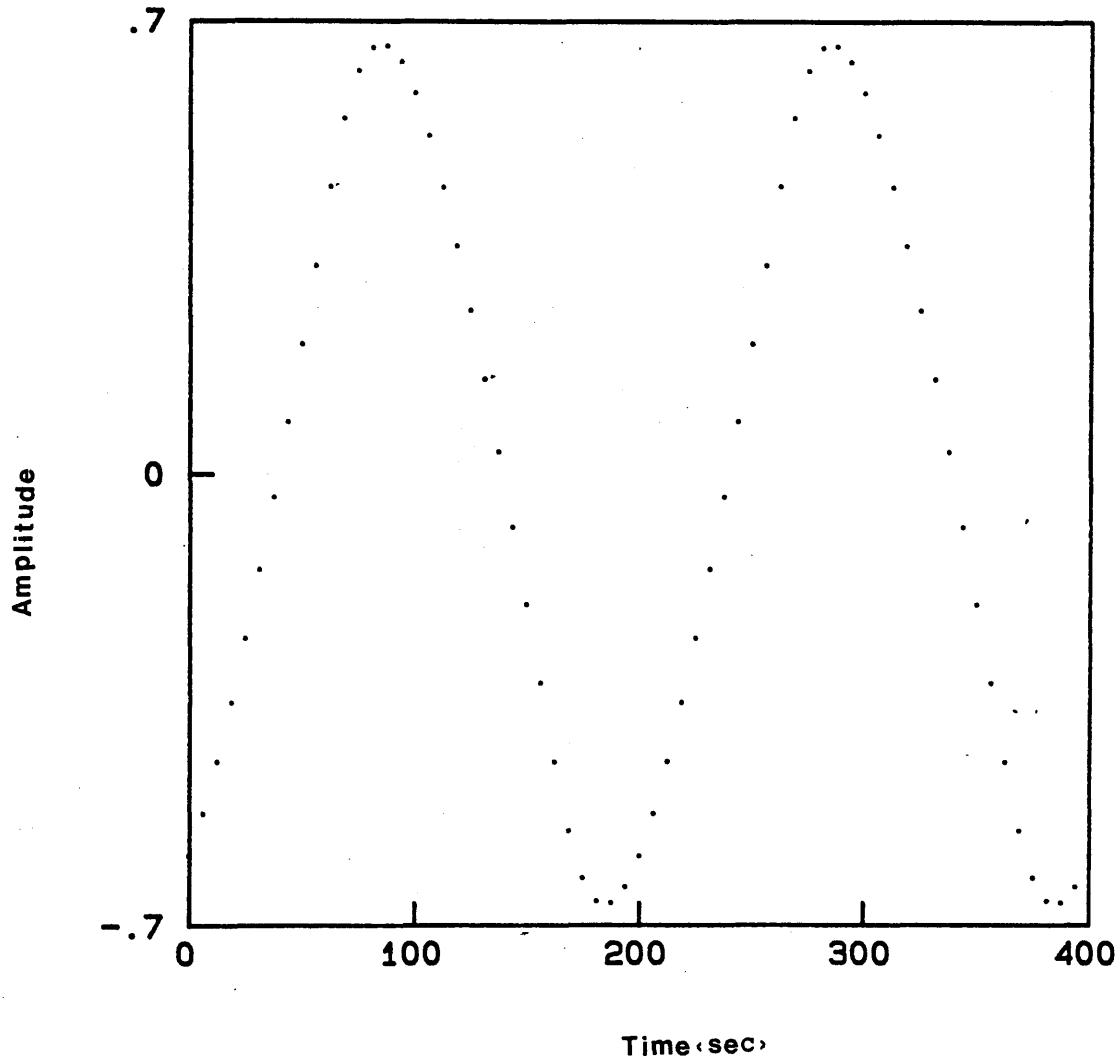
.7
0
-.7
Amplitude
0
100
200
300
400
Time‹sec›

Figure (8-4)

Demonstration of phase shift in the output wave when compared to its corresponding square wave input. The phase shift is shown and marked as t_{exp} and $\omega t_{exp} = -(\phi - \frac{\pi}{4})$. For clarity the wave amplitudes are not to scale.

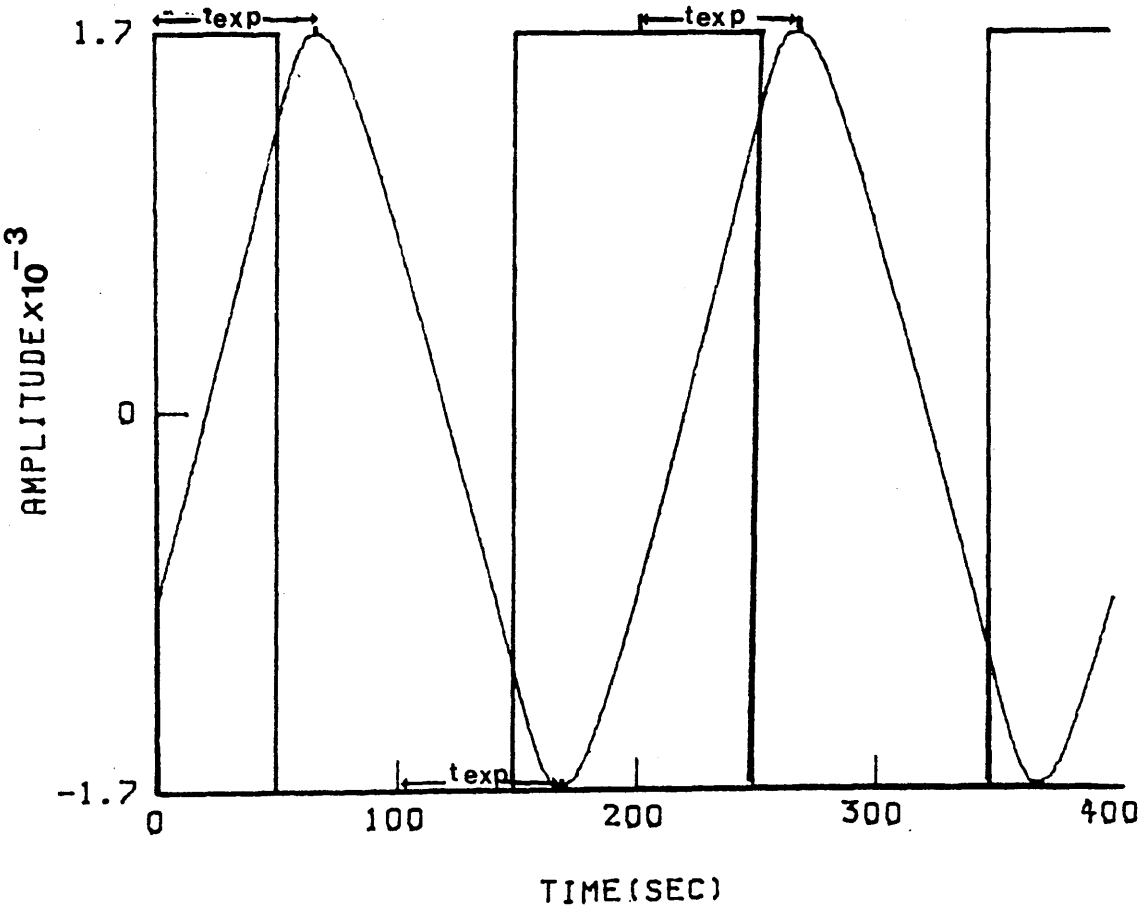
texp
texp
texp
1.7
0
-1.7
AMPLITUDE x10^-3
0
100
200
300
400
TIME(SEC)

Figure (8-5)

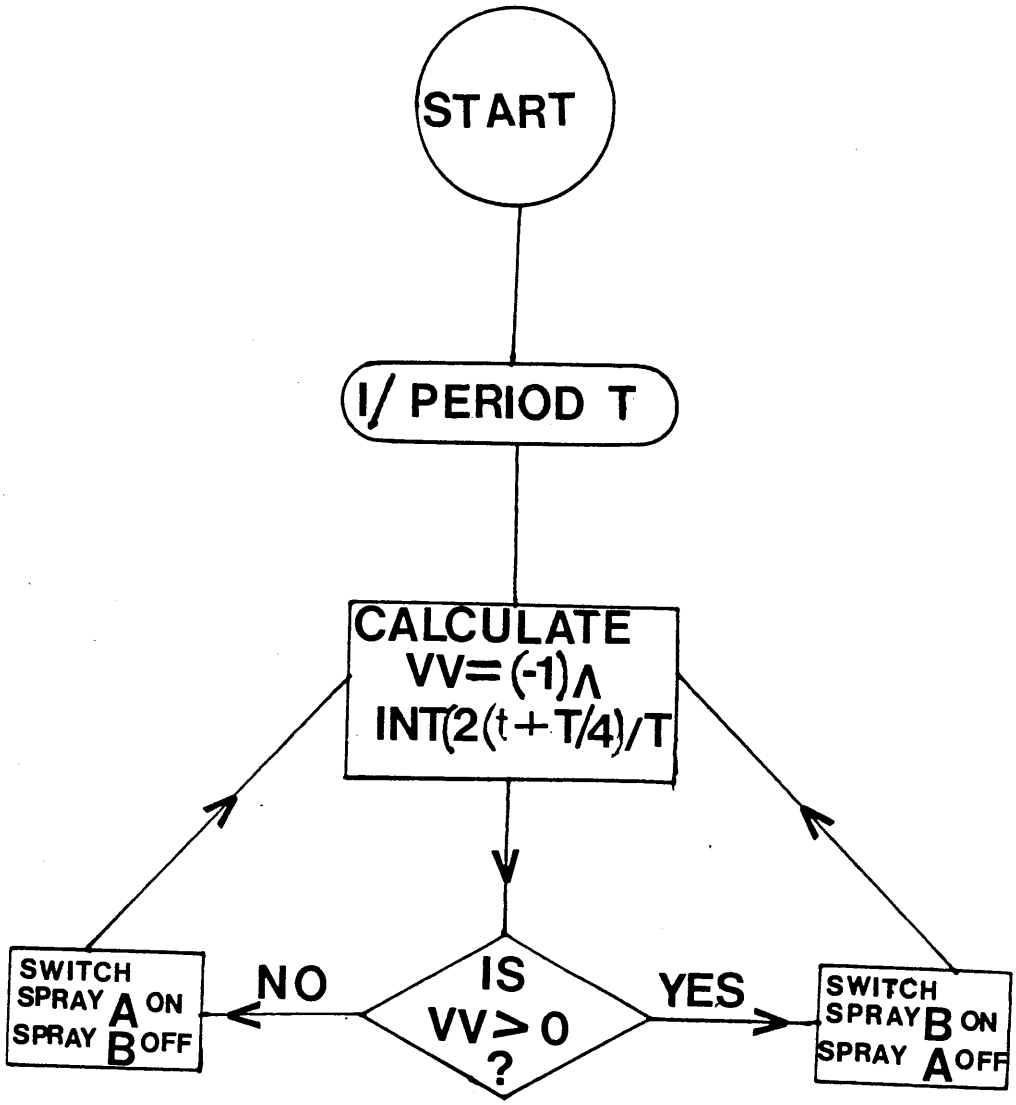
START
I/ PERIOD T
CALCULATE
VV=(-1)^
INT(2(t+T/4)/T
IS
VV>0
?
NO
YES
SWITCH
SPRAY A ON
SPRAY B OFF
SWITCH
SPRAY B ON
SPRAY A OFF

Figures (8-6) and (8-7)

Electrical conductivity against time showing oscillatory concentrations. The membrane was Nafion 125 (perfluorosulphonic acid). The data were collected for two periods - 300s Fig(8-6) and 450s Fig(8-7) . The diffusants were 0.05M HCℓ and 0.05M KCℓ, and the equilibrium composition of the solution in the collecting volume is 0.025M HCℓ + 0.025M KCℓ.

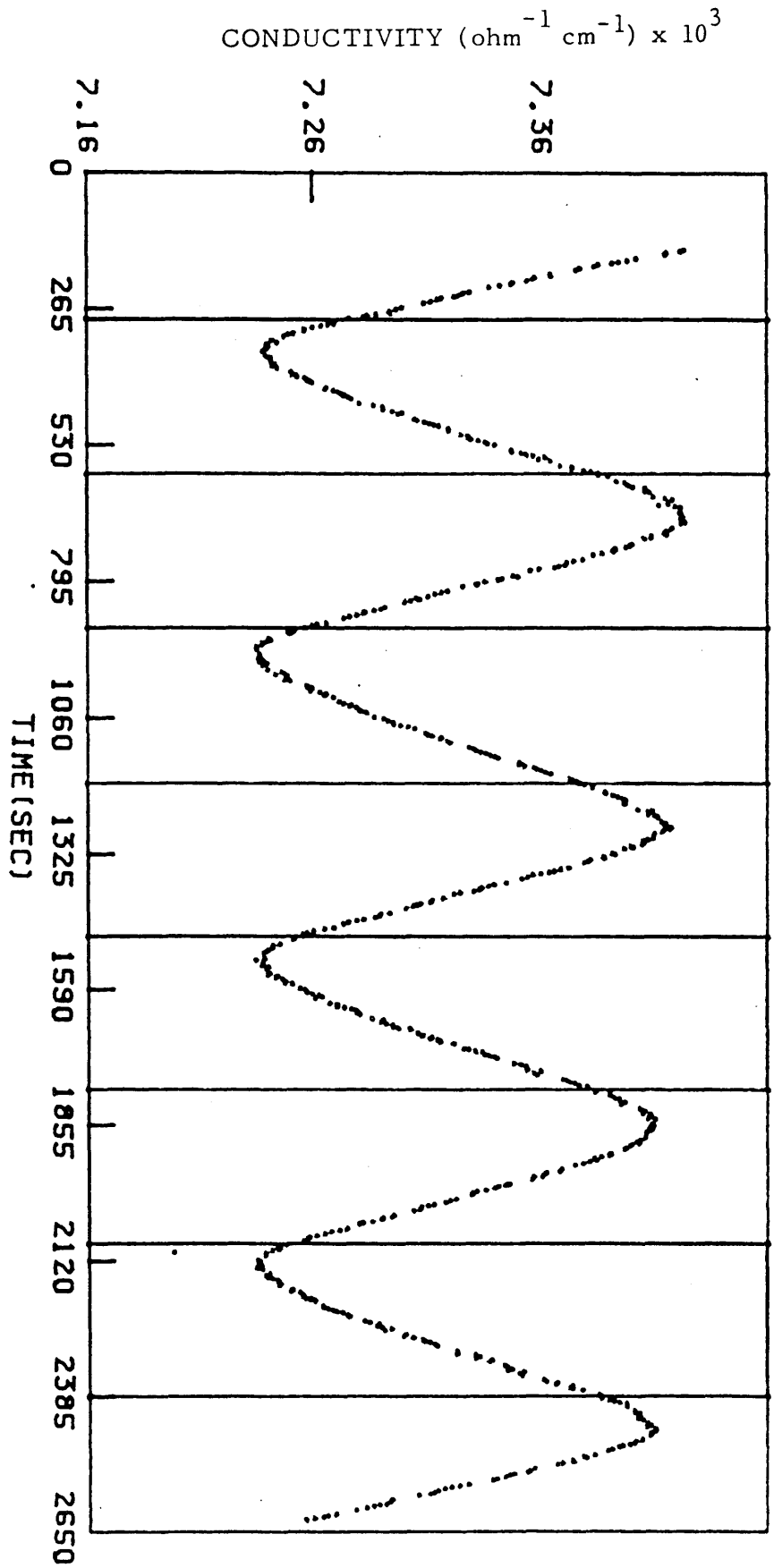
CONDUCTIVITY (ohm^{-1} cm^{-1}) x 10^3
7.16
7.26
7.36
0
265
530
795
1060
1325
1590
1855
2120
2385
2650
TIME (SEC)

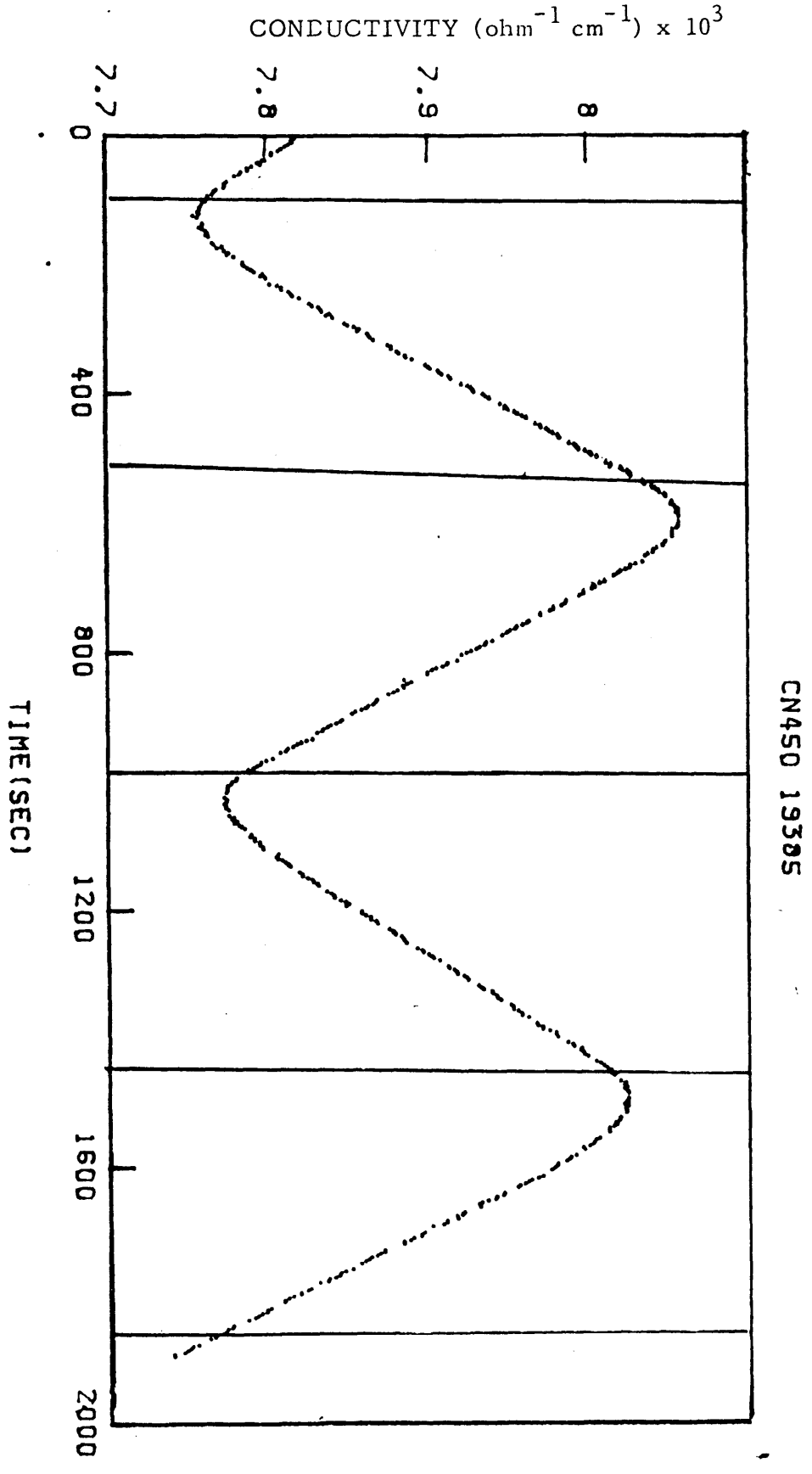
CONDUCTIVITY (ohm^{-1} cm^{-1}) x 10^3
7.7
7.8
7.9
8
0
400
800
1200
1600
2000
TIME(SEC)
CN450 19385

REFERENCES

1. G. Oster, A.S. Perelson and A. Katchalsky, Q. Rev. Biophys., 1, 6 (1973).
2. D. Darnopp and R. Rosenberg, Systems Dynamics: A Unified Approach, Wiley-Interscience, New York, N.Y. (1975).
3. R. Paterson, Network Thermodynamics, in: E.E. Bittar (Ed.), Membrane Structure and Function, John Wiley, New York, N.Y., Vol. 1, p.2 (1980).
4. R. Paterson and Lutfullah, in: Ion Exchange Technology, (Eds. D. Naden and M. Streat), Ellis Horwood, Chichester, p.242 (1984). (Proceedings of Soc. Chem. Ind. Conference, "IEX '84", Cambridge, England).
5. R. Paterson and Lutfullah, J. Membrane Sci., 23, 59 (1985).
6. R. Paterson, Lutfullah and P. Doran, in preparation.
7. P. Doran, Ph.D. Thesis, University of Glasgow (1985).
8. A.J. Ångström, Ann. Phys. Leipzig, 513, 114 (1861).
9. W.W. Thomson (Lord Kelvin), Trans. R. Soc. Edinburgh, 405, 22 (1861).
10. K. Evnochides and E.J. Henley, J. Polym. Sci., A-2, 8, 1987 (1970).
11. R.M. Barrer, J.A. Barrie and M.G. Rogers, Trans. Faraday Soc., 58, 2473 (1962).
12. H.S. Carslaw and J.C. Jaeger, Conduction of Heat in Solids, 2nd Edn., Clarendon Press, Oxford, p.68 (1984).

APPENDIX A.7.1

```
2000  REM  TO SWITCH SPRAY A ON A
     ND SPRAY B OFF
2010  POKE A,1: POKE A,4
2020  GOTO 250
3000  REM  TO SWITCH SPRAY B ON A
     ND SPRAY A OFF
3010  POKE A,2: POKE A,3
3020  GOTO 250
4990  REM  CLOCK SUBROUTINES FIRS
     T SET UP INITIAL CONDITIONS
     IE SET TIMER TO T=0 BY POKIN
     G CORRECT LOCATIONS
5000  FOR X = 32672 TO 32687
5010  POKE (X),0
5020  NEXT X
5030  POKE 32683,227
5040  POKE 32678,0
5050  POKE 32677,191
5060  POKE 32686,32
5070  POKE 32680,255
5080  POKE 32681,255
5090  REM  THIS PART OF SUBROUTIN
     E READS TIME
5100 AA =  PEEK (32680)
5110  PEEK (32680)
5120 C = (AA * 256) + B
5130 C = 65535 - C
5140 C =  INT (C / 1.021190)
5150 C = C / 10
5160 CR = (C * .045855 / 100)
5170 C1 = C + TD - (( INT (CR * 1
     0 + .5)) / 10)
5180  PRINT C1: REM  C1 IS THE TI
     ME IN SECONDS
5190  RETURN
```

APPENDIX A.7.2

```
10 DIMTT(700)
20 PRINT"DO YOU WANT READ OR WRITE "
30 INPUT"'1'READ '2'WRITE";RE
40 IFRE=1THEN530
50 IFRE=2THEN590
60 IF0>RE>2THEN20
70 NU=3
80 PRINT"STEP TIME=";NU
90 IFRE=1THEN63999
100 J=1
110 TI$="000000"
120 OPEN5,5
130 OPEN8,85
140 PRINT#5,"!"
150 GOTO370
160 FORN=1TO1500:NEXT
170 PRINT#5,"M"
180 FORZZ=1TO700:NEXT
190 B=PEEK(59427)AND128
200 INPUT#5,A$
210 IFST=0THEN220:GOTO160
220 B=PEEK(59427)AND128
230 INPUT#5,B$
240 G$=RIGHT$(B$,10)
250 G=VAL(G$)
270 INPUT#8,C$
280 M$=RIGHT$(C$,13)
290 M=VAL(M$)
310 C=-10.7866+58.3474*M-21.9288*M↑2
320 T=INT((C*100)+.5)/100
322 PRINTTAB(3);G;TAB(10);TT(I);T;I
325 PRINT#6,G
330 PRINT#6,TT(I)
340 PRINT#6,T
350 PRINT#6,I
370 I=I+1
380 Q$=MID$(TI$,1,2)
390 Q=(VAL(Q$))*3600
400 W$=MID$(TI$,3,2)
410 W=(VAL(W$))*60
420 E$=MID$(TI$,5,2)
430 E=VAL(E$)
440 TT(I)=E+W+Q
450 IM=TT(I)-TT(I-1)
460 IFIM=>NU THEN160
470 GETG$:IFG$<>""THEN500
480 I=I-1
490 GOTO370
500 UU=500
510 PRINT#6,UU
520 CLOSE6
530 OPEN6,1,0
540 INPUT#6,G$,TT$,T$,I
550 PRINT,G$,TT$,T$,I
560 XX=XX+1
570 IFXX=7000THEN520
580 GOTO540
590 OPEN6,1,1
600 GOTO70
```

APPENDIX A.7.3

```
10 PRINT"□"
30 FORI=1TO150:NEXTI
90 PRINT"□"
95 PRINT"INPUT THE # OF DATA PAIRS TO"
97 PRINT
100 INPUT"BE LOADED FROM TAPE FILE";N
105 DIMX(N):DIMY(N):DIMZ(N)
107 PRINT:PRINT"LOADING FILE DO NOT DISTURB !!!"
110 OPEN6,1
120 FOR I=1 TON
130 INPUT#6,A$
140 INPUT#6,B$
150 INPUT#6,C$
160 INPUT#6,D$
190 X(I)=VAL(B$)
210 Y(I)=VAL(A$)-1.16346E-4*(VAL(C$)-25)
211 Y=Y(I)
212 Z(I)=INT((Y*1E6)-.5)/1E6
215 PRINTX(I),Z(I)
220 IF I=N THEN 250
230 NEXT I
250 CLOSE6
251 PRINT"□":PRINT:PRINT
253 OPEN1,4,31:PRINT#1,"CHANGE";CHR$(5)
254 CLOSE1
255 OPEN4,5
256 T$="S"
265 PRINT#4,N
270 FOR I=1 TO N
280 PRINT#4,X(I)
285 PRINT#4,Z(I)
290 IF I=N THEN 350
300 NEXT I
350 CLOSE4
400 END
READY.
```

APPENDIX A.7.4

```
300  HOME
305  PRINT : PRINT : PRINT
310  PRINT "THIS PROGRAM REQUIRES
      THAT THE S.S.C"
312  PRINT "IS IN SLOT 5. IF THIS
      IS NOT THE "
313  PRINT "CASE THEN TURN OFF TH
     E POWER AND"
314  PRINT "INSTALL THE S.S.C  .
      "
315  PRINT : PRINT : PRINT : PRINT

316  PRINT "ALL DATA IS SAVED TO
     DRIVE 2  "
317  PRINT : PRINT "UNDER THE PRE
     SENT SYSTEM SO MAKE"
318  PRINT : PRINT "SURE A DATA F
     ILE DISK IS IN"
319  PRINT : PRINT "DRIVE 2 OR TH
     E SYSTEM WILL CRASH"
350 D$ =  CHR$ (4)
400  PRINT D$;"PR#5"
402  PRINT  CHR$ (1);"E D"
410  PRINT  CHR$ (1);"F E"
420  PRINT D$;"PR#0"
430  PRINT D$;"IN#5"
450  INPUT N
460  DIM X(N): DIM Y(N)
470  FOR I = 1 TO N
480  INPUT X(I): INPUT Y(I)
495  NEXT I
690  PRINT D$;"IN#0"
700  PRINT D$;"PR#5"
702  PRINT  CHR$ (1);"R": PRINT I
     $;"PR#0"
710  HOME
730  INPUT "FILE NAME";NM$
740  PRINT D$;"OPEN";NM$;",D2"
750  PRINT D$;"DELETE";NM$
760  PRINT D$;"OPEN";NM$
770  PRINT D$;"WRITE";NM$
780  PRINT N
790  FOR I = 1 TO N
800  PRINT X(I): PRINT Y(I)
810  NEXT I
820  PRINT D$;"CLOSE";NM$
830  HOME
900  PRINT D$;"RUN";"TRANS#2";",D
     1"
910  END
```

APPENDIX A.7.5

```
60  REM
62  DIM X1(350),Y1(350),X(200,4),
    Y(200,4)
65  DIM N(4),C(180,3),W(200,4)
70  PRINT "DO YOU WANT THE RESULT
    S TO BE:-"
90  PRINT "         1-LINEAR FIT"
100  PRINT "          2-PLOTTING"
110  GET A: IF A <  = 0 OR A > 3 THEN
    70
120  ON A GOTO 155,1890
130  REM
140  REM ***COUNT FILE POINTS***
150  REM
155  HOME
160  INPUT "TIME AT START OF FIT#
    1=";T1
165  PRINT
170  INPUT "FINAL TIME OF FIT#1 (
    =T SPRAY)=";T0
175  PRINT
180  INPUT "INITIAL TIME FOR FIT#
    2=";T2
183  PRINT
185  INPUT "FINAL TIME FOR FIT#2=
    ";T3
187  PRINT
190  INPUT "MEMBRANE'S THICKNESS=
    ";L
210 D$ =  CHR$ (4)
220  PRINT : INPUT "FILE NAME?";F
    $
230  PRINT D$;"OPEN";F$;",D2"
240  PRINT D$;"READ";F$
250  INPUT N
260  FOR I = 1 TO N
270  INPUT X1(I): INPUT Y1(I)
275  PRINT I; TAB( 5);X1(I); TAB(
    12);Y1(I)
280  IF X1(I) =  < T1 THEN HH = I

290  IF X1(I) =  < T0 THEN N1 = I

300  IF X1(I) =  < T2 THEN VV = I

310  IF X1(I) =  < T3 THEN KK = I

320  NEXT
340  PRINT D$;"CLOSE";F$: GOTO 41
    0
350  REM
360  REM ***LINEAR FIT***
370  REM
400 D$ =  CHR$ (4)
410  HOME : VTAB 10
415 NP = 2
420  PRINT "NO. OF PLOTS?";NP
430  FOR I = 1 TO NP: PRINT
440  PRINT "FILE NAME";I;
```

```
445 F$(I) = F$
446  PRINT F$(I): PRINT
450  NEXT
460 JJ = 1
465  PRINT
470  PRINT D$;"OPEN";F$(JJ);",D2"

480  PRINT D$;"READ";F$(JJ)
490  INPUT NN:NN(J) = NN
493 RR = NN - KK
495 N2 = NN - RR
500 N1 = N1 - HH
510 N = N2 - VV
520  IF JJ = 2 THEN 540
530  IF N1 < 120 THEN 550
540  GOTO 590
550 N = N1
560 MM = HH * 2
570  FOR LL = 1 TO MM: INPUT DUM:
      NEXT
580  GOTO 610
590 CC = VV * 2
600  FOR LL = 1 TO CC: INPUT DUM:
      NEXT
610  PRINT "NO OF POINTS";N
620  FOR I = 1 TO N
630  INPUT X(I,JJ): INPUT Y(I,JJ)
     :W(I,JJ) = 1
640  PRINT X(I,JJ),Y(I,JJ)
650  NEXT
660  PRINT D$;"CLOSE";F$(JJ)
670  DEF  FN A(B) =  INT (B * 1E6
      + .5) / 1E6
680 M = 1
690  PRINT "DEGREE OF FIT REQUIRE
     D=";M
700  HOME
710  PRINT : PRINT "WAIT FOR THE
     RESULTS"
720  FOR I = 1 TO N:C(I,1) = 1: NEXT

730 M1 = M + 1
740  FOR J = 2 TO M1: FOR I = 1 TO
     N
750 C(I,J) = C(I,J - 1) * X(I,JJ)
     : NEXT : NEXT
760  FOR I = 1 TO M1: FOR J = 1 TO
     M1
770 A(I,J) = 0: FOR K = 1 TO N
780 A(I,J) = A(I,J) + C(K,I) * C(
     K,J) * W(K,JJ): NEXT : NEXT
     : NEXT
790  FOR I = 1 TO M1:B(I,1) = 0: FOR
     K = 1 TO N
800 B(I,1) = B(I,1) + C(K,I) * Y(
     K,JJ) * W(K,JJ): NEXT : NEXT

810  FOR J = 1 TO M1:KA(J,3) = 0:
      NEXT
```

```
820  FOR I = 1 TO M1:XM = 0: FOR
     J = 1 TO M1
830  IF KA(J,3) - 1 = 0 THEN 880
840  FOR K = 1 TO M1: IF KA(J,3) -
     1 = 0 THEN 870
850  IF XM -  ABS (A(J,K)) >  = 0
      THEN 870
860 IR = J:IC = K:XM =  ABS (A(J,
     K))
870  NEXT K
880  NEXT J
890 KA(IC,3) = KA(IC,3) + 1:KA(IC
     ,1) = IR:KA(I,2) = IC: IF IR
      - IC = 0 THEN 920
900  FOR IJ = 1 TO M1:DM = A(IR,I
     J):A(IR,IJ) = A(IC,IJ)
910 A(IC,IJ) = DM: NEXT IJ
920 P = A(IC,IC):A(IC,IC) = 1
930  FOR IJ = 1 TO M1:A(IC,IJ) =
     A(IC,IJ) / P: NEXT IJ
940  FOR IK = 1 TO M1: IF IK - IC
      = 0 THEN 980
950 Z = A(IK,IC):A(IK,IC) = 0
960  FOR IJ = 1 TO M1:A(IK,IJ) =
     A(IK,IJ) - A(IC,IJ) * Z
970  NEXT IJ
980  NEXT IK
990  NEXT I
1000  FOR I = 1 TO M1:K = M1 + 1 -
     I
1010  IF KA(K,1) - KA(K,2) = 0 GOTO
     1050
1020 IR = KA(K,1):IC = KA(K,2)
1030  FOR IJ = 1 TO M1:DM = A(IJ,
     IR):A(IJ,IR) = A(IJ,IC):A(IJ
     ,IC) = DM
1040  NEXT IJ
1050  NEXT I
1060  PRINT
1070  FOR I = 1 TO M1:C(I,1) = 0:
      FOR K = 1 TO M1
1080 C(I,1) = C(I,1) + A(I,K) * B
     (K,1): NEXT : NEXT
1090  IF PR = 1 THEN  PR# 1
1100  PRINT "COEFFICIENTS OF POLY
     NOMIAL"
1110  PRINT : PRINT : FOR I = 1 TO
     M1: PRINT "A"I - 1;"= "C(I,1
     ): NEXT
1120  PRINT
1130 PA(JJ,0) = C(1,1):PA(JJ,1) =
     C(2,1)
1140  PRINT "DO YOU WANT TO SEE T
     HE RESULTS"
1150  INPUT "(Y/N)?";R$
1160  IF R$ = "Y" THEN 1180
1170  IF R$ = "N" THEN 1290
1180  PRINT "X"; TAB( 8);"W";
1190  PRINT  TAB( 15);"Y"; TAB( 2
     0);
```

```
1200  PRINT "Y(CAL.)"; TAB( 31);"
      %DEV"
1210  FOR I = 1 TO N:YC = 0: FOR
      J = 1 TO M1:YC = YC + C(J,1)
       * X(I,JJ) ↑ (J - 1)
1220 YC =  FN A(YC):X(I,JJ) =  FN
      A(X(I,JJ))
1230 Y(I,JJ) =  FN A(Y(I,JJ)):W(I
      ,JJ) =  FN A(W(I,JJ))
1240  NEXT
1250 PE =  ABS (Y(I,JJ) - YC) / Y
      (I,JJ) * 100:PE =  INT (PE *
      100 + .5) / 100
1260  PRINT X(I,JJ); TAB( 8);W(I,
      JJ);
1270  PRINT  TAB( 10);Y(I,JJ); TAB(
      20);YC
1280  PRINT  TAB( 30);PE: NEXT
1290 JJ = JJ + 1
1300  IF JJ > 2 THEN 1320
1310  GOTO 470
1320 TX = (PA(1,0) - PA(2,0)) / (
      PA(2,1) - PA(1,1))
1330 TX =  INT (TX * 1000 + .5) /
      1000
1340 TY = (PA(1,0) * PA(2,1) - PA
      (2,0) * PA(1,1)) / (PA(2,1) -
      PA(1,1))
1350 TY =  INT (TY * 1E6 + .5) /
      1E6
1360 M = PA(2,1)
1370 M =  INT (M * 1E10 + .5) / 1
      E10
1380  PRINT : PRINT "TX=";TX: PRINT
      : PRINT "TY=";TY: PRINT : PRINT
      "TO=";TO
1390 T = TX - TO
1400 T =  INT (T * 1000 + .5) / 1
      000
1410  PRINT : PRINT "TIME LAG=";T

1420 D = L ↑ 2 / (6 * T)
1430 D =  INT (D * 1E12 + .5) / 1
      E12
1440  PRINT : PRINT "DIFFUSION CO
      EFICIENT=";D
1450  PRINT : PRINT "PERMEABILITY
      =";M
1460  PRINT : INPUT "DO YOU WANT
      LINEAR FIT AGAIN?";C$
1470  IF C$ = "Y" THEN 70
1480  IF C$ = "N" THEN 1490
1490  PRINT : INPUT "DO YOU WANT
      TO SAVE RESULTS?";A$
1500  IF A$ = "Y" THEN 1530
1510  IF A$ = "N" THEN 1630
1520  CHR$ (4)
1530  PRINT "FILE NAME";
1535  PRINT F$",A"JJ
1540  PRINT D$;"OPEN";F$",A"JJ;",
      D2"
```

```
1542  PRINT D$;"DELETE";F$",A"JJ
1545  PRINT D$;"OPEN";F$",A"JJ;",
                D2"
1550  PRINT D$;"WRITE";F$",A"JJ
1560  PRINT T
1570  PRINT M
1580  PRINT D
1590  PRINT D$;"CLOSE";F$",A"JJ
1600  REM
1610  REM ***X-Y CO-ORDINATES***
1620  REM
1625  PRINT "INPUT X-VALUES TO DR
      AW LINES"
1626  PRINT "FOR FIT#1 & FIT#2"
1630  FOR JJ = 1 TO 2
1640  FOR S = 1 TO 2
1650  PRINT : PRINT "XX";S;
1660  INPUT XX(S): NEXT
1670 S = S - 1
1680  FOR E = 1 TO S
1690 YY(E) = XX(E) * PA(JJ,1) + P
      A(JJ,0)
1700  PRINT XX(E): PRINT YY(E)
1710  NEXT
1770 D$ =  CHR$ (4)
1780 E = E - 1
1790 NN = E
1795  PRINT "FILE NAME";
1800  PRINT F$",A"JJ
1810  PRINT D$;"OPEN";F$",A"JJ;",
      D2"
1812  PRINT D$;"DELETE";F$",A"JJ
1815  PRINT D$;"OPEN";F$",A"JJ;",
      D2"
1820  PRINT D$;"WRITE";F$",A"JJ
1830  PRINT NN: FOR I = 1 TO NN: PRINT
      XX(I): PRINT YY(I): NEXT
1840  PRINT D$;"CLOSE";F$",A"JJ
1845  NEXT JJ
1850  INPUT "ANY OTHER FILE TO WR
      ITE(Y/N)?";A$
1860  IF A$ = "Y" THEN 1630
1870  IF A$ = "N" THEN 70
1880  REM
1890  REM ***PLOTTING***
1900  REM
1905  DIM X(260,4),Y(260,4),N(4)
1910 SN = 3: REM  SIZE OF CHARACT
      ERS
1920 MK = 1: REM   POINT SYMBOLS

1930 ZK = 4: REM  MARK SIZE
1940 DR = 1: REM  POINTS TO BE JO
      INED
1950 DR = 0: REM  POINTS DO NOT B
      E JOINED
1960 BR = 1: REM PITCH OF BROKEN
      LINE
1970  LIST 1540
1980 BD = 1: REM  DRAW BORDER
1990 BD = 0: REM  NO BORDER TO BE
       DRAWN
```

```
2000 PM = 2000: REM  LIMIT TOP LI
     NE
2010 LM = 250: REM  LIMIT BOTTOM
     LINE
2020 GL = 40: REM  LENGTH OF GRAT
     ICS
2030 SU = 50: REM  SPACE BETWEEN
     TOP TITLE AND MARGINE LINE
2040 SX = 150: REM  SPACES BETWEE
     N X-Y TITLES AND AXES LINES
2050 CS = 3: REM  SIZE OF NUMERIC
     AL NUMBERS ON X-Y CO-ORDINAT
     ES
2060 TL = 25: REM  LENGTH OF TITL
     ES
2070 X0 = 350:XM = 1850
2080 Y0 = 300:YM = 1500
2090 D$ =  CHR$ (4)
2110  REM
2120  REM  *** TITLES ***
2130  REM
2140  GOSUB 2660: INPUT "TITLES F
     OR THE GRAPH (Y/N) ? ";B$
2150  IF B$ = "N" THEN 2390
2160  IF B$ = "Y" THEN 2180
2170  IF B$ <  > "Y" OR B$ <  > "
     N" THEN 2140
2180  GOSUB 2660
2190  PRINT "TITLE FOR TOP MARGIN
     "
2200  PRINT : INPUT "? ";T$
2210  IF T$ = "" OR  LEN (T$) > T
     L THEN 2180
2220  GOSUB 2660: PRINT "TITLE FO
     R X-AXIS "
2230  PRINT : INPUT "? ";X$
2240  IF X$ = "" OR  LEN (X$) > T
     L THEN 2220
2250  GOSUB 2660: PRINT "TITLE FO
     R Y-AXIS"
2260  PRINT : INPUT "? ";Y$
2270  IF Y$ = "" OR  LEN (Y$) > T
     L THEN 2250
2280  GOSUB 2660: PRINT "SIZE OF
     CHARACTERS(0-15)"
2290  PRINT : PRINT "SUITABLE SIZ
     E=3)"
2300  INPUT "YOUR CHOICE?";TS
2310  IF SN < 0 OR SN > 15 THEN 2
     280
2320 TP = 1
2330 PP = 1
2340  IF J = 1 THEN DR = 0
2350  IF J =  > 2 THEN DR = 1
2360  REM
2370  REM  *** CO-ORDINATES ***
2380  REM
2390  GOSUB 2660: PRINT "MATHEMAT
     ICAL CO-ORDINATES"
2400  PRINT : PRINT "XMIN,XMAX,YM
     IN,YMAX"
```

```
2410  PRINT : INPUT "ENTER ? ";XS
     ,XB,YS,YB
2420  REM
2430  REM  *** X-Y SEGMENTS ***
2440  REM
2450  GOSUB 2660: INPUT "GRATICUL
     ES (Y/N) ? ";B$
2460  IF B$ = "N" THEN 2520
2470  IF B$ = "Y" THEN 2490
2480  GOTO 2530
2490 AX = 1
2500  PRINT : INPUT "NO OF GRATIC
     S ON X-AXIS ? ";GX
2510  PRINT : INPUT "NO OF GRATIC
     S ON Y-AXIS ? ";GY
2520  HOME : VTAB 5
2530  INPUT "NO OF PLOTS";NP
2540  FOR I = 1 TO NP: PRINT
2550  PRINT "FILE NAME";I;
2560  INPUT "?";NM$(I): NEXT
2570 J = 1
2580  PRINT D$;"OPEN";NM$(J);",D2
     "
2590  PRINT D$;"READ";NM$(J)
2600  INPUT N:N(J) = N
2610  FOR I = 1 TO N
2620  INPUT X(I,J): INPUT Y(I,J)
2630  NEXT
2640  PRINT D$;"CLOSE";NM$(J)
2650  GOTO 2700
2660  HOME : VTAB 10: RETURN
2670  REM
2680  REM  *** SCALING ***
2690  REM
2700  PRINT : PRINT "X
       Y"
2710  FOR I = 1 TO N: PRINT X(I,J
     ),Y(I,J): NEXT
2720 J = J + 1
2730  IF J <  = NP THEN 2580
2740  FOR J = 1 TO NP
2750 N = N(J)
2760 DX = XM - X0:DY = YM - Y0
2770  FOR I = 1 TO N
2780 XQ = (X(I,J) - XS) / (XB - X
     S)
2790 YQ = (Y(I,J) - YS) / (YB - Y
     S)
2800 X(I,J) = X0 + DX * XQ
2810 Y(I,J) = Y0 + DY * YQ
2820  NEXT
2830  IF DR = 0 THEN 2840
2840  IF MK = 0 THEN 2950
2850  REM
2860  REM  *** MARK POINTS ****
2870  REM
2880  FOR I = 1 TO N
2890 XZ = X(I,J):YZ = Y(I,J): GOSUB
     4120
2900  GOSUB 4180: NEXT
2910  IF DR = 0 THEN 2990
```

```
2920  REM
2930  REM  *** DRAW CURVE ****
2940  REM
2950 N = N - 1
2960  FOR I = 1 TO N
2970 XZ = X(I,J):YZ = Y(I,J): GOSUB
     4130
2980  NEXT
2990 BR = 0: GOSUB 4150
3000 DR = 1
3010  NEXT
3020  REM
3030  REM  *** DRAW BORDER ***
3040  REM
3050 BD = 0
3060 XZ = X0:YZ = Y0: GOSUB 4120
3070 YZ = YM: GOSUB 4130
3080 XZ = XM: GOSUB 4130
3090 YZ = Y0: GOSUB 4130
3100 XZ = X0: GOSUB 4130
3110  IF AX = 0 THEN 3470
3120  REM
3130  REM  *** DRAW SEGMENTS ***
3140  REM
3150 JX = DX / GX
3160 JY = DY / GY
3170  FOR I = X0 + JX TO XM - JX STEP
     JX
3180 YZ = Y0:XZ = I: GOSUB 4120
3190 YZ = Y0 + GL: GOSUB 4130: NEXT

3200  FOR I = X0 + JX TO XM - JX STEP
     JX
3210 YZ = YM:XZ = I: GOSUB 4120
3220 YZ = YM - GL: GOSUB 4130: NEXT

3230  FOR I = Y0 + JY TO YM - JY STEP
     JY
3240 XZ = X0:YZ = I: GOSUB 4120
3250 XZ = X0 + GL: GOSUB 4130: NEXT

3260  FOR I = Y0 + JY TO YM - JY STEP
     JY
3270 XZ = XM:YZ = I: GOSUB 4120
3280 XZ = XM - GL: GOSUB 4130: NEXT

3290  REM
3300  REM  *** WRITE SCALES ***
3310  REM
3320 SN = CS:GR = 0: GOSUB 4170: GOSUB
     4190
3330 UN = (CS + 1) * 7
3340 WX = (XB - XS) / GX:WY = (YB
      - YS) / GY
3350 KK = XS
3360  FOR I = X0 TO XM STEP JX
3370 A$ =  STR$ (KK):LN =  LEN (A
     $) * UN
3380 YZ = Y0 - 50:XZ = I - LN / 2
```

```
3390  GOSUB 4120: GOSUB 4140
3400 KK = KK + WX: NEXT
3410 KK = YS
3420  FOR I = Y0 TO YM STEP JY
3430 A$ =  STR$ (KK):LN =  LEN (A
     $) * UN + 20
3440 XZ = X0 - LN:YZ = I - 10: GOSUB
     4120
3450  GOSUB 4140
3460 KK = KK + WY: NEXT
3470  IF TP = 0 THEN 4040
3480  REM
3490  REM  *** WRITE TITLES ***
3500  REM
3510 SN = TS: GOSUB 4170
3520 UN = 7 * ( SN + 1 )
3530 A$ = T$:LN = ( LEN ( A$) * UN
     ) / 2
3540 XZ = X0 + DX / 2 - LN:YZ = Y
     M + SU
3550  GOSUB 4120: GOSUB 4140
3560 A$ = X$:LN = ( LEN ( A$) * UN
     ) / 2
3570 XZ = X0 + DX / 2 - LN:YZ = Y
     0 - SX
3580  GOSUB 4120: GOSUB 4140
3590 A$ = Y$:LN =  LEN ( A$)
3600  IF LN > 2 THEN QR = 1
3610 LN = ( LN * UN ) / 2
3620 XZ = X0 - SX:YZ = Y0 + DY /
     2 - LN
3630  GOSUB 4190: GOSUB 4120: GOSUB
     4140
3640  IF PP = 0 THEN 4040
3650  REM
3660  REM ***WRITE DETAILS***
3670  REM
3680  PRINT : INPUT "DO YOU WANT
     MORE DETAILS(Y/N)?";A$
3690  IF A$ = "Y" THEN 3710
3700  IF A$ = "N" THEN 3940
3710 D$ =  CHR$ ( 4 )
3720  PRINT : INPUT "FILE NAME?";
     B$
3730  PRINT D$;"OPEN";B$;",D2"
3740  PRINT D$;"READ ";B$
3750  INPUT T
3760  INPUT M
3770  INPUT D
3780  PRINT T,M,D
3790  PRINT D$;"CLOSE";B$
3800  GOSUB 4170
3810 A$ =  STR$ ( T )
3820 A$ = "TIME LAG=" + A$:LA =  LEN
     ( A$ )
3830 XZ = X0 + DX + LA + 10:YZ =
     Y0 + DY - 200
3840  GOSUB 4120: GOSUB 4140
3850 A$ =  STR$ ( M )
```

```
3860 A$ = "PERMEAB.=" + A$:LB =  LEN
     (A$)
3870 XZ = X0 + DX + LB + 10:YZ =
     Y0 + DY - 300
3880  GOSUB 4120: GOSUB 4140
3890 A$ =  STR$ (D)
3900 A$ = "D=" + A$:LC =  LEN (A$
     )
3910 XZ = X0 + DX + LC + 10:YZ =
     Y0 + DY - 400
3920  GOSUB 4120: GOSUB 4140
3930  HOME : VTAB 10
3940  INPUT "INITIAL TIME=";XX
3950 XE = (XX - XS) / (XB - XS)
3960  PRINT : INPUT "DO YOU WANT
     THE TIME AT THE '1'BOTTOM OR
     '2'TOP?";S
3970  IF S = 1 GOTO 3990
3980  IF S = 2 GOTO 4020
3990 YZ = Y0:XZ = X0 + DX * XE: GOSUB
     4120
4000 YZ = Y0 + 160: GOSUB 4130
4010  GOSUB 4200: GOTO 4060
4020 YZ = YM:XZ = X0 + DX * XE: GOSUB
     4120
4030 YZ = YM - 160: GOSUB 4130
4040  GOSUB 4200
4050  HOME : VTAB 10
4060  PRINT : INPUT "DO YOU WANT
     MORE PLOT(Y/N)?";A$
4070  IF A$ = "Y" THEN 2140
4080  IF A$ = "N" THEN 70
4090  IF A$ <  > "Y" OR A$ <  > "
     N" THEN 4100
4100  END
4110  REM   *** DIGI-PLOT ROUTINE
     S             ***
4120  PR# 1: PRINT D$;"M" INT (XZ
     );",";  INT (YZ): GOTO 4210
4130  PR# 1: PRINT D$;"D" INT (XZ
     );",";  INT (YZ): GOTO 4210
4140  PR# 1: PRINT D$;"P";A$: GOTO
     4210
4150  PR# 1: PRINT D$;"L";BR: GOTO
     4210
4160  PR# 1: PRINT D$;"B";BN: GOTO
     4210
4170  PR# 1: PRINT D$;"S";SN: GOTO
     4210
4180  PR# 1: PRINT D$;"N";MK: GOTO
     4210
4190  PR# 1: PRINT D$;"Q";QR: GOTO
     4210
4200  PR# 1: PRINT D$;"H": PR# 0
4210  PR# 0: RETURN
```

APPENDIX A.7.6

The analysis may be made using the method of Laplace transforms (1) but for the purposes of comparison with the infinite volume method this treatment is based upon the use of non-orthogonal sine series.

The boundary conditions are

at $x = 0$, $c = c^o$, for $t \geqslant 0$

at $x = \ell$, $(\alpha AD/V)(\delta c/\delta x) = (\delta c/\delta t)$

where V is the finite volume of the collecting vessel.

In this treatment the concentration step is taken as being from zero to c^o. (It is easily modified to deal with steps from non-zero concentration). For a finite volume the time invariant state is equilibrium when the concentration in the collecting volume will be c^o. Assuming Fick's second law the concentration in the collecting volume, c, is given by eqn. A.7.6.1.

$$c = c^o + \sum_{n=0,1,2}^{\infty} A_n \sin(\lambda_n \ell)\exp(-\lambda_n^2 Dt) \qquad \text{A.7.6.1}$$

in which λ_n is the root of the transcendental equation:

$$\lambda_n \sin(\lambda_n \ell) = p\cos(\lambda_n \ell) \qquad \text{A.7.6.2}$$

where $p = \alpha A/V$.

Since the initial concentration is zero, t = 0, we have that

$$\sum_{n=0,1,2\ldots}^{\infty} A_n \sin(\lambda_n x) = -c^o \qquad \text{for } x = 0 \text{ to } \ell$$

Using this method of Peek (2) the values of A_n were found to be:

$$A_n = \frac{-2c^o(p^2 + \lambda_n^2)}{\lambda_n(\ell\lambda_n^2 + \ell p^2 + p)} \qquad n=0,1,2\ldots \qquad (A.7.6.3)$$

From eqns. (A.7.6.1) and (A.7.6.3) the concentration in the collecting vessel now becomes eqn. (A.7.6.4)

$$c = c^o - c^o \sum_{n=0,1,2\ldots}^{\infty} \frac{2(p^2+\lambda_n^2)\sin(\lambda_n \ell)\exp(-\lambda_n^2 Dt)}{(\ell\lambda_n^2 + \ell p^2 + p)\,\lambda_n} \qquad (A.7.6.4)$$

As the experiment proceeds and time increases, terms in λ_n, with $n \geqslant 1$, will rapidly decay.

In order to employ the linear extrapolation procedures of the infinite volume solution, it is necessary to obtain the limiting conditions in which the differences between these two are acceptably small.

The first, eqn. (7-4), required $\alpha A\ell/V = p\ell \ll 1$. Under this condition terms with orders greater than unity in $p\ell$ may be neglected. Eqn. (A.7.6.2) may be rewritten as:

$$\lambda_o \ell \tan(\lambda_o \ell) = p\ell$$

and expanded as a Maclaurin series:

$$\lambda_o \ell(\lambda_o \ell + (\lambda_o \ell)^3/3 + 2(\lambda_o \ell)^5/15 + \ldots) = p\ell$$

Rearranging, to express $(\lambda_o \ell)^2$ as a polynomial in $p\ell$, using standard formulae for reversion of a series,

$$(\lambda_o \ell)^2 = (p\ell - p^2\ell^2/3 + \text{higher terms})$$

and using the binomial theorem eqn.(A.7.6.5) is obtained.

$$\lambda_n \ell = (p\ell)^{1/2}(1 - p\ell/6) \qquad \text{(A.7.6.5)}$$

giving

$$\sin(\lambda_o \ell)/\lambda_o = \ell(1 - p\ell/6)$$

Substitution in eqn. (A.7.6.1) gives eqn. (A.7.6.6)

$$c = c^o - c^o \left(\frac{2(p^2+[p\ell-p^2\ell^2/3]/\ell^2)\ell\{1-p\ell/6\}\exp(-\lambda_o^2 Dt)}{2p(1 + p\ell/3)}\right) \qquad \text{(A.7.6.6)}$$

For conditions where $\lambda_o^2 Dt \ll 1$, $\exp(-\lambda_o^2 Dt) \cong 1-pDt/\ell$, (which gives the second limiting condition, eqn. (7-7).

On substitution in eqn. (A.7.6.6) this approximation gives eqn. (A.7.6.7) after some rearrangement.

$$c = c^o[pD/(\ell)](t - \ell^2/6D)$$

or

$$c = [AD\alpha c^o/(V\ell)](t - \ell^2/6D) \qquad \text{(A.7.6.7)}$$

Eqn. (A.7.6.7) is identical to the steady state relationship, eqn. (7-2) since $Q(t)/V = c$, the concentration of permeant in the collecting vessel, volume, V.

REFERENCES

1. H.S. Carlaw and J.C. Jaeger, in "Conduction of Heat in Solids", Clarendon Press, Oxford, England, (1959).

2. R.L. Peek, Ann. Math. 2, 30, 265 (1929).

Appendix 8.1

Program for Calculating the Diffusion Coefficient from Experimental Results

The program works by starting with a diffusion coefficient which is larger than the value in agreement with the experimental results. It inserts this value along with the time t_1 at which experimentally the peak was observed into the equation for the concentration of the finite volume. This equation is from section 2.3.[1]

$$\mathrm{Re}\{[\frac{\theta\, e^{K(1+i)\ell}}{e^{2K\ell}e^{2iK\ell} + \theta} + \frac{e^{K\ell}e^{iK\ell}}{e^{2K\ell}e^{2iK\ell} + \theta}]e^{i\omega t}\}$$

where $(\frac{\sqrt{2}\, a'D\, Ke^{-i\pi/4}}{V_1\omega} - 1)$

$$\theta = \frac{}{(1 + \frac{\sqrt{2}\, Da'Ke^{-i\pi/4}}{V_1\omega})}$$

and the other symbols have their usual meaning.

It then does the same for a new time $t_2 = t_1 + \Delta t$ and compares the two. If the initial D input is larger than the true value of D then $C(D,t_1)$ will be greater than $C(D,t_2)$, i.e. we are in the region

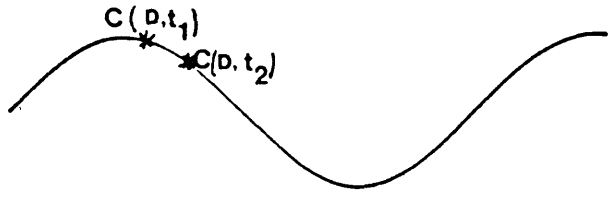

D is then decreased by a small amount and the process repeated until

$C(D,t_1)$ is less than $C(D,t_2)$ at this point the value of D will be the value that conforms to the experimental value. This gives the correct value of D to within the step value at which D is decreased each time and this is made as small as accuracy requires. The difference between t_1 and t_2 is also very small 10^{-2}s.

During the running of the program the following will be asked for.

The Diffusion Coefficient: This is an estimate and must be greater than the real value ($cm^2 s^{-1}$).

The Frequency: This is $2\pi/T$ where T is the period of the oscillations (rad s^{-1}).

The Volume

The Area — Put = 1 if not known

The Distribution Coefficient

The Thickness: Which is the thickness of the membrane (in cm).

The Time: This is t_{exp} as defined in Chapter 8, Figure (8-4).

A first approximation to D can be obtained by using

$$\frac{\omega}{2D}\ell = \left(\frac{t_{exp}}{T} \times 2\pi\right) - \frac{\pi}{4}$$

$$D_{approx} = \frac{\omega \ell^2}{2} / \left(\frac{t_{exp}}{T} \times 2\pi - \frac{\pi}{4}\right)^2$$

A listing of the actual program is given on the next page.

1. P. Doran, Ph.D. Thesis, Glasgow University, 1985.